Influence of Laser Diode Nonlinearities on Fibre Optic Systems Supporting Direct-Sequence Code Division Multiple Access Signals

Thesis Submitted in Candidature for the Degree of

Doctor of Philosophy

March 1999

Serge Geslin

Department of Electronic and Electrical Engineering

University College London

London

United Kingdom

Statement of Originality

The work presented in this thesis was carried out by the candidate. It has not been presented previously for any degree, nor it is at present under consideration by any other degree awarding body.

Candidate:

Serge Geslin

Director of Studies:

Professor John J. O'Reilly

Statement of Availability

I hereby give consent for my thesis, if accepted, to be available for photocopying and for inter-library loan, and for the title and summary to be made available to outside organisations.

Candidate:

Serge Geslin

Acknowledgments

I am very grateful to Professor John J. O'Reilly for taking me as his student and for his advice and motivation throughout the course of this study. I would also like to thank him for his support and guidance during the final preparation of this thesis.

I am very thankful to my friends Assaad Borjak and Luis Moura for their help, encouragement and continuous support and Sen Lin Zhang for useful discussions and his expert assistance with SPW.

Special thanks go to Professor Jean Le Bihan from the Ecole Nationale d'Ingenieurs de Brest for his encouragement and belief.

I want also to express my gratitude to all my friends that contributed to make my stay in london so enjoyable.

I am indebted to the European Communaute for the financial support given during the initial phase of my work through the Human and Capital Mobility Program.

Finally, to my parents and sisters for their love, encouragement and patience.

Summary

This thesis is concerned with the study of the impact of Laser Diode nonlinearities on Direct-Sequence Code Division Multiple Access (CDMA) based fibre-radio systems.

CDMA is a promising technique for radio access for future cellular mobile and personal communication systems. The aim of the third generation systems is the integration of all mobile systems into one universal system. In this context, the use of fibre-optic feeders as the remoting infrastructure in microcellular networks has been proposed for CDMA systems.

The presence of a nonlinear device, such as a laser diode, in such systems leads to the generation of intermodulation products, which consequently affect the system performance and ultimately restrain the maximum number of users the system can serve. In the case of a pure CDMA system, the laser diode nonlinearities are well described by a third-order polynomial without memory. This method enables the assessment of the implication of unequal power transmission of mobile users using the derived bit-error-rate.

Finally, in order to increase the system capacity, a hybrid SubCarrier Multiplexing (SCM)/CDMA system is proposed. The Volterra series method of nonlinear system theory is then presented and applied to SCM systems to investigate the performance of different system configurations.

Contents

List of Figures

List of Tables

Chapter 1

Introduction

Code Division Multiple Access (CDMA) has been investigated over the past 15 years for applications in optical fibre networks. Recently, there has been considerable interest in using Spread Spectrum (SS) CDMA technology for microcellular mobile radio systems. It is well known that CDMA has the advantages of the large user capacity, the effective utilization of the frequency and immunity to multipath fading over other multiple access techniques. For the same reasons, it is effective to use SS/CDMA transmission over optical fibre between base stations and control station [1]. However, the use of Laser Diode in such a system leads to the generation of intermodulation products, which consequently affect a system performance and ultimately restrain the maximum number of users that the system can serve. Many theoretical investigations and experiments have been done for the study of this effect in the case of frequency-division multiple access system [2, 3]. In this thesis, we examine the effect of Laser Diode nonlinearity in CDMA systems for different system configurations.

1.1 Thesis Organisation

Following this introductory chapter, we present an overview of the different standards used in wireless communications. We then present the new generation of wireless communications based on fibre-radio technologies. Finally, we described the multiple access methods employed in the various standards.

In chapter 3 we focus our attention on the Spread Spectrum technology and its applications. We pay particular attention to direct sequence technique and its derivative CDMA. A Fibre Optic(FO)-CDMA system has been implemented using Alta's Signal Processing Worksystem (SPW) simulation framework. Properties of a CDMA network have been emphasised by various simulations.

The impact of Laser Diode nonlinearity on the system performance is addressed in chapter 4. This effect is modeled by a memoryless third-order polynomial. The expressionsof the intermodulation terms for a CDMA system with unequal power transmission are derived. The performance of the system is evaluated using the derived bit-error-rate (BER) and a comparison between the ideal case and the practical case is provided.

In chapter 5 we present the theory to model the laser nonlinearity in the case of Subcarrier Multiplexing CDMA systems. This analysis, based on Volterra functional series, is first presented and then applied to the studied system.

The results of chapter 5 are applied in chapter 6 to study two important SCM/CDMA systems namely: Wireless Local Loop and Mobile Radio systems.

Finally, chapter 7 concludes the thesis, summarising the main achievements and identifying areas where further research may be appropriate.

1.2 Contributions

The research reported here has sought to provide a detailed and comprehensive assessment of the performance of CDMA fibre optic systems, emphasis being placed on the implications of laser nonlinearities. The main contributions of this thesis may be summarised as follows:

- Development of a simulation platform on Alta's SPW framework for study of CDMA optical network. This model allows the simulation of different system configurations in order to analyse the properties of CDMA system.
- Development of analytic expressions for laser diode nonlinearity for FO-CDMA system taking into account unequal power.
- Extension of the volterra series analysis for SCM/CDMA systems to calculate the third-order intermodulation products.
- Development of "software tools" implemented in Matlab and Mathematica for systems simulation.

Some of the contributions made during the course of this research have led to the following publications:

- S. Geslin, S. L. Zhang, and J. J. O'Reilly, "Simulation Tools for Study of CDMA Optical Networks", Proc. of the European Conference on Networks & Optical Communications 1996 (NOC'96), pp. 149-156, Heidelberg, Germany, 25-28 June 1996.
- S. Geslin, S. L. Zhang, and J. J. O'Reilly, "How the Choice of the Spreading Code Sequence in Direct Sequence CDMA Influence the Laser Nonlinearity", Di-

gest of the Communications Research Symposium, pp. 73-76, University College London, 29-30 July 1996.

- S. Geslin, J. Le Bihan, and J. J. O'Reilly, "Modelisation et Simulation d'un Reseau Optique CDMA", Journees Doctorales Informatique & Reseaux, pp. 8-8/8-12, Ecole Nationale Superieure des Telecommunications, Paris, 11-13 Sep. 1996.

- S. Geslin, A. Borjak, and J. J. O'Reilly, " The impact of imperfect power control on direct-sequence CDMA in optical transmission", IEE colloquium on CDMA Techniques and Applications for Third Generation Mobile Systems, pp. 13/1-13/5, London, 19 May 1997.

- S. Geslin, A. Borjak, L. Moura, and J. J. O'Reilly, "The Implication Of Nonlinear Effect On DS/CDMA With Imperfect Power Control In Optical Transmission", 1997 IEEE-MTT-S International Microwave Symposium Digest, June 8-13, Volume III, pp. 1763-1766.

- S. Geslin, A. Borjak, and J. J. O'Reilly, "The Effect of Laser Diode Nonlinearity Direct-Sequence Code Division Multiple Access with Imperfect Power Control", Proc. of the European Conference on Networks & Optical Communications 1997 (NOC'97), pp. 164-167, Antwerp, Belgium, 17-20 June 1997.

- Serge Geslin, Assaad Borjak, and John J. O'Reilly, "The Effect of Nonlinearity on QPSK Based Direct-Sequence Code Division Multiple Access in Optical Transmission", TRS'97 Conference Proceedings, pp. 76-79, University College

London, 21-22 July 1997,

Chapter 2

Towards the Development of Third Generation Mobile Communications Systems

2.1 Introduction

This century has seen the development of a public wireline network that allows reliable and affordable communication of voice and low-rate data around the globe. There is also a multiplicity of specialised wired networks optimised for purposes such as the local communication of high-speed data. The goal of wireless communication is to allow the user access to the capabilities of the global network at any time without regard to location and mobility. In other terms, the vision of future telecommunications is "information at any time, at any place, in any form" [4]. This requires the provision of universal service access and mobility support, including both personal and terminal mobility. Therefore, emerging third-generation mobile telecommunications systems play an important role, since they should provide universal access to a wide range of basic and supplementary telecommunications services supported by fixed networks for example, Public Switched Telephone Network (PSTN), Integrated Services Digital Network (ISDN), and Broadband ISDN (B-ISDN) and to other services specific to mobile users.

A variety of services (e.g. paging, cellular) based on wireless communications already exist today. Personal Communication Services (PCS), a family of communications services supporting personal handset and service mobility, represents the next generation of personal services which rely on wireless communication technology. In particular, these systems aim for the integration of all mobile radio applications (cordless, cellular, and paging systems, including mobile satellite systems) into one universal system.

This chapter starts by presenting an overview of the current state of wireless communications with descriptions of first and second generation mobile communications systems. Then, we discuss the challenge facing the development of the so-called third generation mobile systems.

2.2 First Generation Mobile Communications Systems

The first generation mobile communications systems were introduced in the late 1970's and early 1980's in analog form to provide local mobile speech services. These were further extended to nationwide coverage in a number of countries. The user had to subscribe to a single operator and hence user mobility was limited to the coverage of the operator's network. Various standard systems were developed and deployed worldwide: AMPS (Advanced Mobile Phone Service) in the United States, NTT (Nippon Telephone and Telegraph) system in Japan, TACS (Total Access Communications System) in the United Kingdom, NMT (Nordic Mobile Telephones) in European countries, and so on.

Fast user growth was observed, penetrating up to 10% of the calls in North America, Western Europe, and Japan. The access technique used was Frequency Division Multiple Access (FDMA). Capacity and quality were the major problems in the first-generation systems, as well as being incompatible systems.

2.2.1 Analog Cellular Systems: AMPS and ETACS

In the late 1970s, AT&T Bell Laboratories developed the first U.S. cellular telephone system called AMPS [5]. AMPS was first deployed in late 1983 in the urban and suburban areas of Chicago by Ameritech. In 1983, a total of 40 MHz of spectrum in the 800 MHz band was allocated by the Federal Communications Commission for AMPS. In 1989, as the demand for cellular telephone services increased, the Federal Communications Commission allocated an additional 10 MHz (called the extended spectrum) for cellular telecommunications. The first AMPS cellular system used large cells and omni-directional base station antennas to minimise initial equipment needs, and the system was deployed in Chicago to cover approximately 2100 square miles. The AMPS system uses a 7-cell reuse pattern with provisions for sectoring and cell splitting to increase capacity when needed. AMPS is used throughout the world and is particularly popular in the U.S., South America, Australia, and China.

In Europe, several first-generation systems similar to AMPS have been deployed, including TACS in the United Kingdom, Italy, Spain, Austria and Ireland; NMT in many countries; C-450 in Germany and Portugal; Radiocom 2000 in France; and RTMS (Radio Telephone Mobile System) in Italy. The European Total Access Communication System (ETACS) was developed in the mid 1980s, and is virtually identical to AMPS, except that it is scaled to fit in 25 kHz (as opposed to 30 kHz) channels used throughout Europe. Another difference between ETACS and AMPS is how the telephone number of each subscriber (called the mobile identification or MIN) is formatted, due to the need to accommodate different country codes throughout Europe and area codes in the U.S.

2.2.2 First-Generation Analog Cordless

Since 1984, analog cordless telephones in the United States have operated on ten frequency pairs in the bands 46.6-47.0 MHz (base transmit) and 49.6-50.0 MHz (handset transmit). Prior to 1984, five of the 49 MHz frequencies were paired with five frequencies near 1.6 MHz, an arrangement that proved less than satisfactory due to the imbalance in the performance of the two links and the limited number of channels. The first cordless telephones were imported to Europe from the Far East and the United States. In most of Europe, such equipment was illegal but was sold in large quantities "for export only". In the United Kingdom, a standard very similar to the one originally used in the United States was introduced (MPT 1322) to offer an alternative to illegal imports [6]. This standard (sometimes referred to as "CT0"), allowed for eight channel pairs near 1.7 MHz (base unit transmit) and 47.5 MHz (handset transmit), and most units could access only one or two channel pairs. A similar standardisation approach was adopted in France.

In the rest of Europe, the reaction to the demand for cordless communication was to develop the analog cordless standard known as CEPT/CT1 (Conférence Européenne des Postes et Télécommunications/ Cordless Telephone) [7]. This cordless standard provides for forty 25 kHz duplex channel pairs in the bands 914-915/959-960 MHz (80 pairs are allocated for CT1+ in the bands 885-887/930-932 MHz, which do not overlap with the GSM allocation) and form a Dynamic Channel Assignment scheme, whereby one of the 40 (or 80) duplex frequency pairs is selected at the beginning of each call. In Japan, there are 89 duplex channels near 254 MHz (handset transmit) and 380 MHz (base transmit) allocated to analog cordless telephones using FM. The channel spacing is 12.5 kHz and the allowed transmit power is 10 mW.

2.3 First to Second Generation Systems

Following the very great success of mobile cellular networks, based on analogue transmission, in penetrating the business market there was a clear need to introduce new solutions based on the transmission of digitised voice or data in order to improve the quality and range of services offered and to create a more efficient use of the allocated spectrum. With remarkable foresight the European nations worked together to produce the pan-European Global System for Mobile (GSM) standard, based on FDMA/TDMA principles, which is now achieving sales worldwide. In the U.S., the need to introduce more efficient digital networks was also perceived but, with a different commercial and regulatory regime, several competing solutions have been developed including the first commercial Code Division Multiple Access (CDMA) systems proposed alongside the more usual FDMA/TDMA approaches. In particular the Qualcomm solution, based on a narrow spread bandwidth of 1.23 MHz, has been specifically targeted at mobile cellular operation. A U.S. interim standard, IS-95, has been written around the Qualcomm system. The cellular world moves rapidly and the availability of new spectrum in the 2 GHz region, plus technology improvements leading to the genuine pocket phone, have led to the European PCN (Personal Communication Network) (or DCS1800, now re-named GSM 1800) and the U.S. PCS concepts with market penetration expanding rapidly in both the consumer and business sectors.

In the cordless world, the development of new digital technologies gave birth to Personal Handyphone System (PHS, formerly PHP) in Japan, Digital Enhanced Cordless Telephone (DECT) in Europe, and Personal Access Communication Services (PACS) in North America. These may increase the call penetration depth up to 30% and introduce many new services. Although the second generation and its supplement will cover local, national, and international services, it will still have one major drawback in terms of universal service facility.

2.3.1 Digital Cellular Systems

The Pan-European GSM System and GSM 1800

Global System for Mobile (GSM) is a second generation cellular system standard that was developed to solve the fragmentation problems of the first cellular systems in Europe. GSM is the world's first cellular system to specify digital modulation and network level architectures and services. Before GSM, European countries used different cellular standards throughout the continent, and it was impossible for a customer to use a single subscriber unit throughout Europe.

GSM was originally developed to serve as a pan-European cellular service and promised a wide range of network services through the use of ISDN. GSM's success has exceeded the expectations of virtually everyone, and it is now the world's most popular standard for new cellular radio and personal communications equipment throughout the world. GSM was first introduced into the European market in 1991. By the end of 1993, several non-European countries in South America, Asia, and Australia had adopted GSM and the technically equivalent offshoot, GSM 1800, which supports PCS in the 1.8 GHz to 2.0 GHz radio bands recently created by governments throughout the world. It is predicted that by the year 2000, there will be between 20 and 50 million GSM subscribers worldwide [8, 9].

IS-54 in North America

The first generation analog AMPS system was not designed to support the current demand for capacity in large cities. Cellular systems which use digital modulation techniques (called digital cellular) offer large improvements in capacity and system performance [10].

After extensive research and comparison by major cellular manufacturers in the late 1980s, the United States Digital Cellular System (USDC) was developed to support more users in a fixed spectrum allocation. USDC is a time division multiple access (TDMA) system which supports three full-rate users or six half-rate users on each AMPS channel. Thus, USDC offers as much as six times the capacity of AMPS. The USDC standard uses the same 45 MHz FDD scheme as AMPS. The dual mode USDC/AMPS system was standardised as Interim Standard 54 (IS-54) by the Electronic Industries Association and Telecommunication Industry Association (EIA/TIA) in 1990.

CDMA Digital Cellular Standard: IS-95

A U.S. digital cellular system based on Code Division Multiple Access (CDMA) technique which promised increased capacity [11] was standardized as Interim Standard 95 (IS-95) by the U.S. Telecommunications Industry Association (TIA). Like IS-54, the IS-95 system is designed to be compatible with the existing U.S. analog cellular system (AMPS) frequency band, hence mobiles and base stations can be economically produced for dual mode operation. IS-95 allows each user within a cell to use the same radio channel, and users in adjacent cells also use the same radio channel, since this is a direct sequence spread spectrum CDMA system. CDMA completely eliminates the need for frequency planning within a market.

To facilitate graceful transition from AMPS to CDMA, each IS-95 channel occupies 1.25 MHz of spectrum on each-way link, or 10% of the available cellular spectrum for a U.S. cellular provider. Unlike other cellular standards, the user data rate (but not the channel chip rate) changes in real-time, depending on the voice activity and requirements in the network. Also, IS-95 uses a different modulation and spreading technique for the forward and reverse links. On the forward link, the base station simultaneously transmits the user data for all mobiles in the cell by using a different spreading sequence for each mobile. A pilot code is also transmitted simultaneously and at a higher power level, thereby allowing all mobiles to use coherent carrier detection while estimating the channel conditions. On the reverse link, all mobiles respond in an asynchronous fashion and have ideally a constant signal level due to power control applied by the base station.

2.3.2 Digital Cordless

Two second generation cordless telephone standards have been developed in Europe for domestic and office applications, as well as for public telepoint services and radio local loop. The first of the standards was CT2. This was followed by the ETSI DECT standard which addressed the same markets while offering a higher capacity and greater functionality. In Japan, PHS has been developed.

CT2 Common Air Interface

CT2 is the second generation of cordless telephones introduced in Great Britain in 1989 [12]. The CT2 system is designed for use in both domestic and office environments. It is used to provide telepoint services which allow a subscriber to use CT2 handsets at a public point (a public telephone booth or a lamp post) to access the PSTN.

CT2 is a digital version of the first generation, analog, cordless telephones. When compared with analog cordless phones, CT2 offers good speech quality, is more resistant to interference, noise, and fading, and like other personal telephones, uses a compact handset with built-in antenna. The digital transmission improves security. Calls may only be made after entering a PIN, thereby rendering handsets useless to unauthorised users.

The CT2 standard defines how the Cordless Fixed Part (CFP) and the Cordless Portable Part (CPP) communicate through a radio link. The CFP corresponds to a base station and the CPP corresponds to a subscriber unit. The frequencies allocated to CT2 in Europe and Hong Kong are in the 864.10 MHz to 868.10 MHz band. Within this frequency range, forty Frequency Division Duplexing (FDD) channels have been assigned, each with 100 kHz bandwidth.

Digital Enhanced Cordless Telephone

The Digital Enhanced Cordless Telephone (DECT) is a universal cordless telephone standard developed by the European Telecommunications Standards Institute (ETSI). It is the first pan-European standard for cordless telephones and was finalized in July 1992.

DECT provides a cordless communications framework for high traffic density, short range telecommunications, and covers a broad range of applications and environments. DECT offers excellent quality and services for voice and data applications. The main function of DECT is to provide local mobility to portable users in an in-building Private Branch exchange (PBX). The DECT standard supports telepoint services as well. DECT is configured around an open standard (OSI) which makes it possible to interconnect wide area fixed or mobile networks, such as ISDN or GSM, to a portable subscriber population. DECT provides low power radio access between portable parts and fixed base stations at a range of up to a few hundred metres.

Personal Handy Phone System

In 1989, the Japanese Ministry of Posts and Telecommunications set up a group to define the requirements for the introduction of Personal Handy Phone System (PHPS) for digital cordless telephonic applications. The PHPS standard was finally published in March 1983. Voice and data services have been defined, including circuit and packet data transmission with a maximum bit rate of 128 kb/s. Around 20 supplementary services are also specified (e.g. automatic call back, call forwarding, calling number identification) and the protocol incorporates expansion capabilities for additional features.

For residential use, both incoming and outgoing calls are possible and in addition, two terminals may communicate directly (without going through the base station) if they are close enough. The PHPS standard benefits from a frequency allocation of 77 carriers in the 1900 MHz band. The air interface is based on TDMA/TDD access method with eight time slots per frame and allows four bidirectional communications per 300 kHz wide carrier.

2.4 Third Generation Wireless Networks

With the current rapid growth of technology, it can now emphatically be said that the objective of today's communication engineers to achieve a Future Wireless Personal Communication (FWPC) system, which was yesterday's myth (before 1970) will be tomorrow's reality (beyond 2000).

These third generation wireless systems will evolve from mature second generation systems. The aim of the third generation wireless networks is to provide a single set of standards that can meet a wide range of wireless applications and provide universal access throughout the world. In third generation wireless systems, the distinctions between cordless telephones and cellular telephones will disappear, and a universal personal communicator (a personal handset) will provide access to a variety of voice, data and video communication services, will operate in varied region (dense or sparsely populated regions), and will serve both stationary users and vehicular users travelling at high speeds [14]. Third generation systems will use the Broadband Integrated Services Digital Networks (B-ISDN) to provide access to information networks, such as the Internet and other public and private databases.

Thus, FWPC systems will convert the already shrinking world into a global village. An FWPC, defined as being the ultimate goal of today's communication engineers, will provide communication services from any person to any person in any place at any time without any delay in any form through any medium by using one pocket-sized unit at minimum cost with acceptable quality and security through the use of a personal telecommunication reference number.

The IMT-2000 (International Mobile Telecommunications beyond the year 2000), previously known as FPLMTS (Future Public Land Mobile Telecommunication System) will set the scope for the third generation wireless systems and will consolidate a range of terminal mobility services under a single global standard. The IMT-2000 standard is intended to ensure interoperability across different wireless environments (cellular mobile, cordless telephony, satellite mobile services) and mobility on a global scale.

In Europe, the objectives of the research and development of FWPC systems are focused in three technological platforms [13]: Universal Mobile Telecommunication Systems (UMTSs), Mobile Broadband Systems (MBSs), and Wireless Local Area Networks (WLAN).

2.4.1 PCS Definition

The terms Personal Communication System (PCS) or Personal Communication Network (PCN) are used to imply emerging third generation wireless systems for hand-held devices. The definition of PCS has evolved over time. Some of the earlier definitions have been as follows:

- An extension and integration of current and emerging wired and wireless telecommunications network capabilities allowing, ultimately, communication with persons.
- A wide array of personal communications services: cellular, cordless phones, paging, wireless private branch exchange (PBXs), WLANs, and so on.

The current definition of PCS can be found in the American National Standards Institute (ANSI) approved standard, "Personal Communications Terminology" (ANSI T1.702-1995), and reads as follows: "A set of capabilities that allows some combination of terminal mobility, personal mobility, and service profile management". PCS is a new concept which will expand the horizon of wireless communications beyond the limitations of current cellular systems to enable communication with a person, at any time, at any place, and in any form [15]. The enabling concepts for providing universal personal communications include terminal mobility provided by wireless access, personal mobility based on personal numbers, and service portability through management of user service profiles. Because of the inherent nature of mobility associated with personal communications, wireless communications and PCS have now become almost inseparable concepts.

Today, personal communication services are provided by a range of first and second generation networks and technologies. The terms first and second generation refer to the underlying technology being either analogue or digital, as in Figure 2.1. A

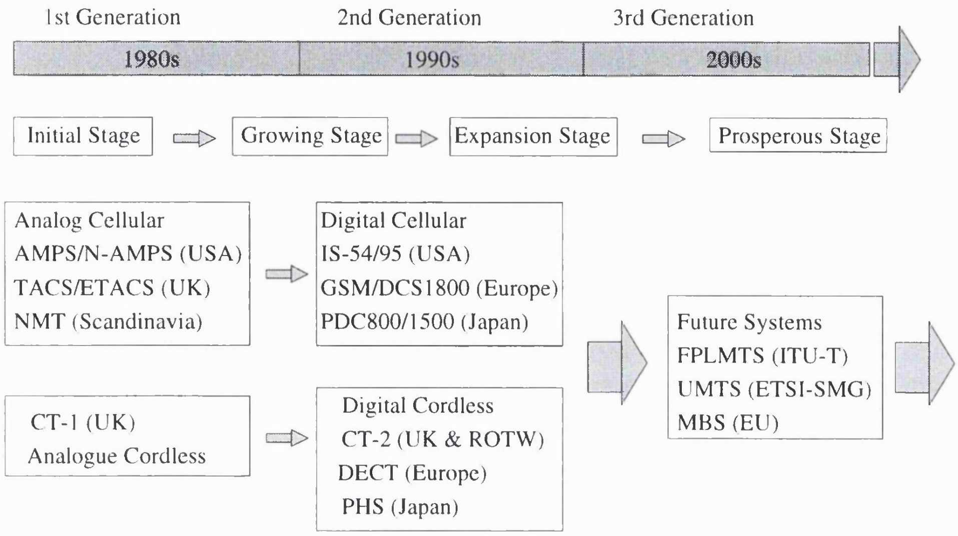

Figure 2.1: Evolution of wireless networks

key characteristic foreseen for the third generation is that of bringing together all the attributes of personal communications into a single unified system. First generation cellular systems are usually national or regional standards, e.g. AMPS in the U.S., TACS in the UK. This has restricted the market for each system, and has tended to limit the scope for users to take their mobiles outside their home networks.

GSM addressed this problem by standardising the radio and network interfaces, imposing rigorous type approval of mobile equipment, and requiring GSM operators to establish technical and commercial roaming agreements. As a result, subscribers can use the GSM system when abroad, provided their home network has a roaming agreement with the local GSM operator.

2.4.2 UMTS: The Cellular Concept

Europe is taking a leading position in the definition of third generation mobile since it is expected that mobile and personal communications will become a key driver for growth and innovation in the next millennium as well as being a necessary building block of the Wireless Information Society. UMTS moves mobile and personal communications forward from second generation systems that are delivering mass market low-cost digital telecommunications services. UMTS is the third generation mobile standard that links mobile personal communications users into networked broadband multimedia, information-technology and telecommunications services and applications for Europe and the global society [16]. Movement towards this new opportunity will be driven by new applications, liberalisation, social demand, seamless mobile and fixed network access, operating environments, implementation and timing. UMTS's technology must encourage this movement by naturally fostering innovation and competition. One major distinction of UMTS relative to second generation systems is the hierarchical cell structure designed for gradated support of a wide range of multimedia broadband services within the various cell layers by use of advanced transmission and protocol techniques, as indicated in Figure 2.2. Second-generation systems are mainly based on a single-layer cell structure employing frequency reuse within adjacent cells in such a way that each single cell is capable of managing its own radio zone and radio circuit control within the mobile network, including functions such as traffic management and handover procedures. The traffic supported in each cell is fixed because of frequency limitations and little flexibility of radio transmission mainly optimised for voice and low rate data transmission. Increasing traffic leads to costly cellular reconfigurations such as cell splitting and cell sectorisation. The multilayer cell structure in UMTS aims to overcome these problems by overlaying, discontinuously, pico- and microcells over the macro-cell structure with wide area coverage. The various cells shown in Figure 2.2 differ mainly in terms of size, channel, and propagation characteristics. As a consequence, the above differences result in a different set of services and mobility features being supported by each cell.

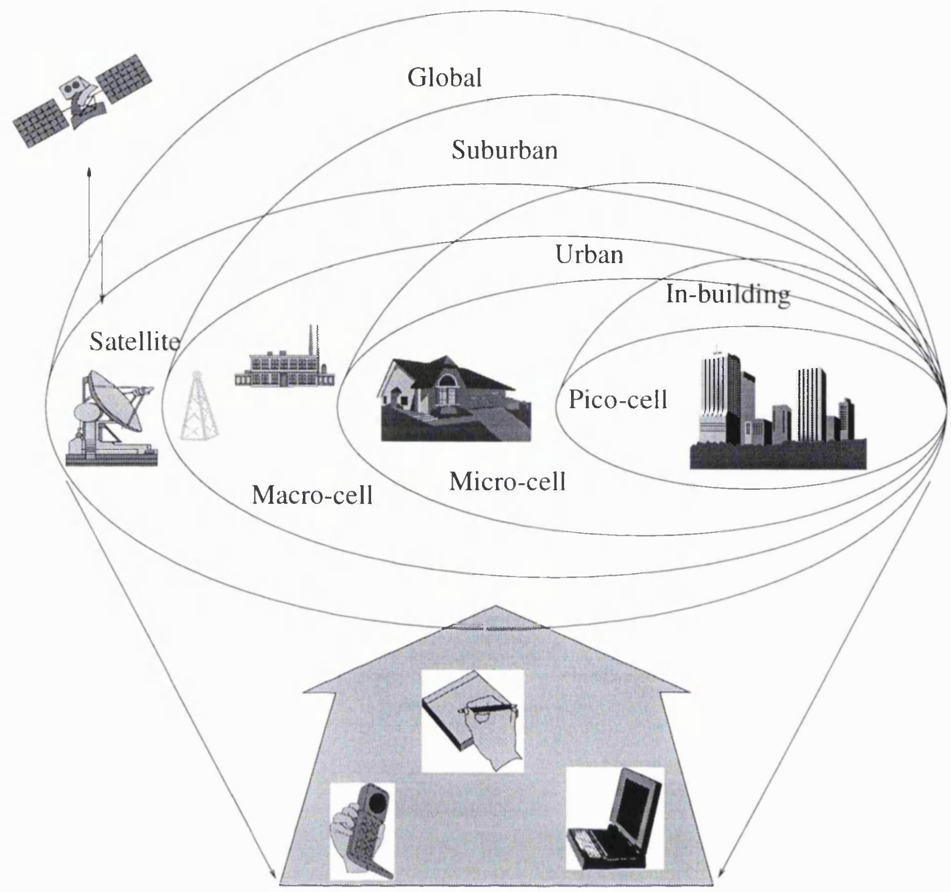

Figure 2.2: Hierarchical Cell Structure

The radio-cell architecture consists of

- mega-cells using satellites for remote areas,
- macro-cells for wide area (ubiquitous) coverage,
- micro-cells supporting high density urban areas,
- pico-cells for indoor use.

Due to low mobility support and smaller delay spread in picocells, high bit rates and traffic density can be supported with low complexity as opposed to lower bit rates and traffic load in macrocells, supporting high mobility and resistance against higher delay spread by robust transmission techniques.

2.4.3 Mobile Broadband Systems

The realisation of the B-ISDN based on optical fibres, the increasing demand for high data rate transmission and the requirement for mobility lead to the concept of Mobile Broadband Systems (MBS) [17, 18, 19]. MBS was in fact a European project as part of the RACE programme. With high data rate exchange up to about 100 Mbit/s, MBS would "fill the gap" between the fixed B-ISDN and UMTS as it is shown in Figure 2.3. The MBS will use Asynchronous Transfer Mode (ATM).

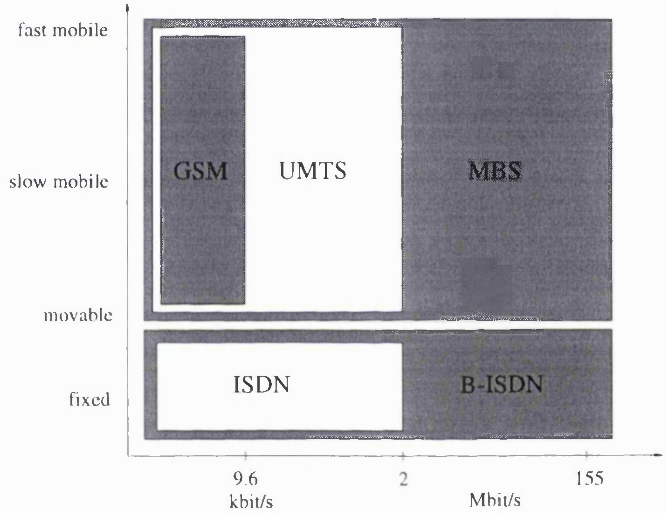

Figure 2.3: Required data rate for different systems

It will typically support services above 2 Mbit/s but lower rate could also be used as for UMTS. Applications of the MBS depend on the quality of service available. There will be a transmission from point-to-point links to point-to-multipoint links. The MBS project has proposed the use of two wavebands, the 60 GHz band for very small cells (picocells) and the 40 GHz band for larger cells. Figure 2.4 shows the proposals.

MBS is investigated for microcellular networks for which at least 40 frequency channels transmitting 34 Mbit/s each must be made available with a typical cell radius of 100 m. A channel spacing of 50 MHz therefore leads to a spectrum requirement around 2 GHz [18].

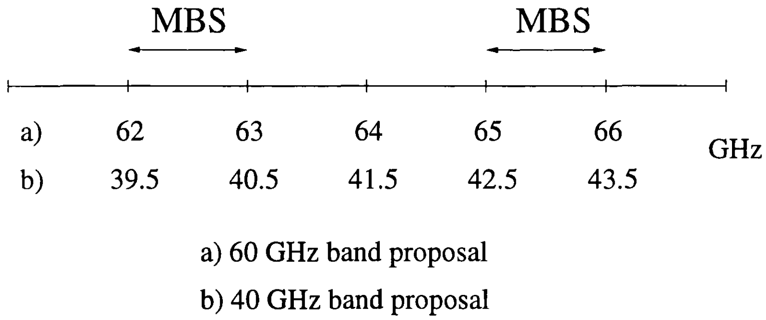

Figure 2.4: Proposed MBS frequency allocations

2.4.4 Wireless Local Area Networks

Proliferation of portable and laptop computers, wide acceptance of mobility, and potential cost savings in avoiding the wiring or rewiring of buildings are driving forces for broadband wireless access for in-building environments. Consequently, third generation mobile systems must incorporate an integrated Wireless Local Area Network (WLAN) capability to maintain "universality". Application areas include mobile systems for offices, industrial automation, financial services, medical and hospital systems, and education and training, with network connection for portable computers and personal digital assistants as well as ad hoc networking.

In creating a high-rate (up to 155 Mbit/s) local data communication link, significant research is required to identify reliable system and associated air interface. Important issues include frequency allocation and selection, choice of bandwidth efficient coding schemes, specification of medium access procedures, definition of link control protocols as well as connectivity aspects related to connection to other wired or wireless communications networks. In brief, the WLAN R&D activities seek for solutions that recognise application, environment, cost, performance, networking and system architecture requirements.

2.5 Wireless Communications Based on Fibre-Radio Technologies

Wireless communications have become a significant area of growth within the last few years [20, 21]. There is a diverse range of products and services currently on the market, but cellular or personal communications services (PCS) radio networks probably have the highest public profile [22]. These services provide highly mobile, widely accessible two-way voice and data communications links [23].

At the same time, optical fibre networks as the high capacity trunk transmission have favourably progressed. Moreover, wired systems represented by optical fibre communication, and wireless systems including long-haul microwave communication, satellite communication, mobile communication and indoor radio - both of these wired and wireless systems have made remarkable advance and development with highly developed theory and technology.

2.5.1 System Configuration

Future third-generation mobile systems will require the support of an integrated optical network infrastructure, as cell size decreases and narrow-band telephony services migrate from fixed copper wire connections to mobile radio. Therefore, tomorrow's communication networks would employ wireless media in the local area and utilise high-capacity wired media in the metropolitan and wide-area environments. A new transmission medium has been born in which radio waves are carried from base stations (BS) to the central station (CS) by optical fibre and thereafter propagated in the atmosphere. An example of such a network is provided in Figure 2.5. In this system, radio base stations are connected with optical fibres and millimetre waves are used for the radio interface within cells. Therefore, wireless systems and networks will not only

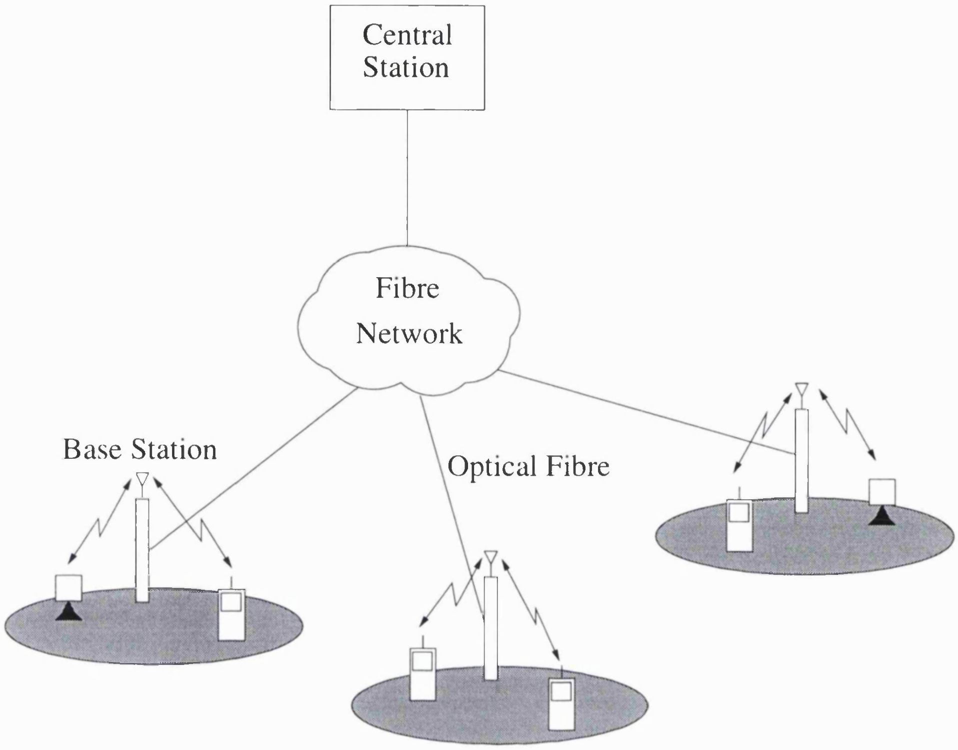

Figure 2.5: Network configuration

provide communication capability between mobile terminals but will also permit these mobile devices to have access to "wired" networks.

In Table 2.1, the different phases of the evolution of wireless communications are summarised.

2.5.2 FRANS project

In Europe, R&D on Third Generation technology falls under the European Community RACE (Research into Advanced Communications in Europe) and ACTS (Advanced Communications Technologies and Services) programmes [24]. The main objective of the RACE programme, in the context of mobile and personal communications, was the

1980s	Deployment of analog cellular systems worldwide
1990s	Digital cellular deployment and dual mode operation of digital systems
2000s	Future Public Land Mobile Telecommunications Systems (FPLMTS) / International Mobile Telecommunications 2000 (IMT-2000) / Universal Mobile Telecommunication Systems (UMTS) to be deployed with multimedia services
2010s	Wireless broadband communications to be available with B-ISDN and ATM networks
2010S+	Radio over fibre (such as fibre optic microcells)

Table 2.1: The different phases of the evolution of wireless communications

development and validation of the necessary key technologies and concepts that would in the future constitute the "building blocks" of the UMTS system. The ACTS programme, while capitalising on the RACE experience, is conceived as a demand-driven R&D program of demonstration trials that will prepare the ground for a European-wide, internationally competitive broadband telecommunications infrastructure that naturally has a mobile communication dimension.

One of the ACTS projects, FRANS (Fibre Radio ATM Networks and Services), is concerned with field trials demonstrating an optically supported millimetre wave radio link as a final drop to provide rapid, flexible deployment of broadband interactive services. It merges existing passive optical networks (PONs) with a photonic technique for generation, modulation and transmission of information bearing millimetre wave signals to a hybrid fibre radio customer access system. Two trials are planned, using different bit rates and based on different multiple access techniques in the uplink.

The two approaches are:

- A 622 Mbit/s downlink with TDMA uplink of 40 Mbit/s aggregate (~2 Mbit/s per user), both with millimetre wave radio part working in the 30 GHz range.

- A 155 Mbit/s downlink with millimetre wave radio interface at ~30 GHz and CDMA uplink (1-5 x 2 Mbit/s per user) with a microwave radio part at ~2.5 GHz (Figure 2.6).

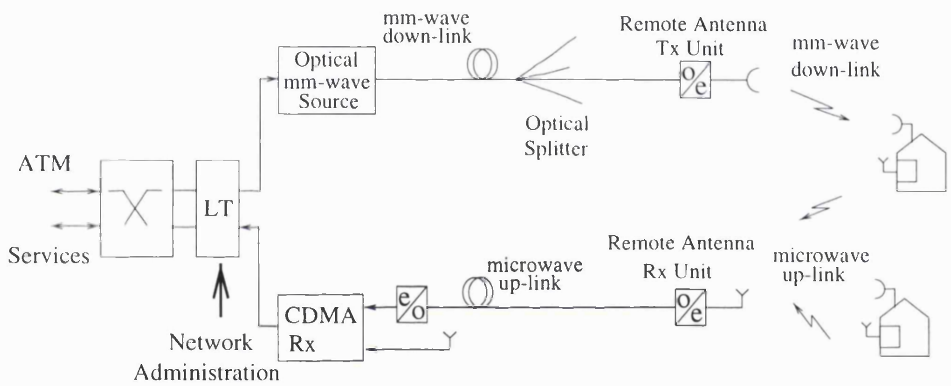

Figure 2.6: Architecture of the 155 Mbit/s multi 2Mbit/s platform

The downlink is based on a principle developed in RACE 2005 (MODAL). Two optical spectral components, separated by the required millimetre wave frequency, are generated and modulated in a central unit and distributed via a PON to antenna sites close to the users, where the two components mix in a PIN photodiode and a modulated millimetre wave signal is generated and radiated. The TDMA uplink uses a different millimetre wave frequency, remote down conversion in the antenna unit and microwave transport over the PON to the central unit. The CDMA uplink uses a microwave carrier frequency transmitted directly to the central unit or over a fibre-optically remoted antenna.

2.6 Multiple Access Techniques for Wireless Communications

2.6.1 Introduction

Multiple access schemes are used to allow many mobiles to share simultaneously a finite amount of radio spectrum. The sharing of the spectrum is required to achieve high capacity by simultaneously allocating the available bandwidth (or the available amount of channels) to multiple users. For high quality communications, this must be done without severe degradation in the performance of the system.

In wireless communications systems, it is often desirable to allow the subscriber to send simultaneously information to the base station while receiving information from the base station. For example, in conventional telephone systems, it is possible to talk and listen simultaneously, and this effect, called duplexing, is generally required in wireless telephone systems. Duplexing may be done using frequency and time domain techniques. Frequency Division Duplexing (FDD) provides two distinct bands of frequencies for every user. The forward band provides traffic from the base station to the mobile, and the reverse band provides traffic from the mobile to the base. In FDD, any duplex channel actually consists of two simplex channels, and a device called a duplexer is used inside each subscriber unit and base station to allow simultaneous radio transmission and reception on the duplex channel pair. The frequency split between the forward and reverse channel is constant throughout the system, regardless of the particular channel being used. Time Division Duplexing (TDD) uses time instead of frequency separation to provide both a forward and reverse link. If the time split between the forward and the reverse time slot is small, then the transmission and reception of data appears simultaneous to the user. TDD allows communication on a single channel (as opposed to requiring two simplex or dedicated channels) and simplifies the subscriber equipment since a duplexer is not required.

2.6.2 Multiple Access Methods

Frequency Division Multiple Access (FDMA), Time Division Multiple Access (TDMA), and Spread Spectrum Multiple Access (SSMA) are the three major access techniques used to share the available bandwidth in a wireless communication system [25].

FDMA was the earliest and is the simplest form of multiple access. With FDMA the available channel bandwidth is subdivided into a number, say N, of frequency non-overlapping subchannels and a subchannel is assigned to each user upon request. FDMA is commonly used in wireline channels to accommodate multiple users for voice and data transmission.

TDMA is another method for creating multiple subchannels for multiple access. In this method, the duration T_f, called the frame duration, is subdivided into, say N, non overlapping subintervals, each of duration, T_f/N. Then each user who wishes to transmit information is assigned to a particular time slot within each frame. TDMA is frequently used in data and digital voice transmission.

With FDMA and TDMA, problems arise when the data from the users accessing the network is bursty in nature. In other words, the information transmissions from a single user are separated by periods of no transmission, where these periods of silence may be greater than the periods of transmission. Such is the case generally with users at various terminals in a computer communications network that contains a central computer. To some extent, this is also the case in mobile cellular communication systems carrying digitised voice, since speech signals typically contain long pauses.

In such an environment where the transmission from the various users is bursty and low-duty cycle, FDMA and TDMA tend to be inefficient because a certain percentage of the available frequency slots or time slots assigned to users do not carry information. Ultimately, an inefficiently designed multiple access system limits the number of simultaneous users of the channel.

An alternative to FDMA and TDMA is to allow more than one user to share a channel or subchannel by use of spread spectrum multiple access technique [26]. This method will be described in detail in the next chapter.

2.7 Summary

In this chapter, an overview has been given of the current state of wireless communications with a presentation of the different standards. The first generation mobile communication systems were introduced at national level, for example NMT in Scandinavia, AMPS in the U.S. and TACS in the UK. These systems use analogue modulation and were specified essentially as separate dedicated systems for paging, cordless phone, mobile terrestrial and mobile satellite communication. In the early 1990s, second generation systems started to be introduced at regional (continental) level, e.g. GSM in Europe, Australasia, India and the Gulf States. These systems use digital modulation techniques.

The next step, now expected for the first decade of the next century, will be the introduction of a global system called UMTS in Europe and FPLMTS in the rest of the world. This system, which will use digital modulation techniques and support bit-rates of up to 2 Mbit/s, is based upon 2 GHz technology and will possibly merge paging, cordless phone, mobile terrestrial and mobile satellite standards into a single, unified standard.

Beyond the year 2000, mobile broadband applications are expected to become more and more important, at least in some environments. As a consequence, bandwidth has been provisionally identified in the 40 to 60 GHz range for a MBS supporting services requiring transmission rates up to 155 Mbit/s.

Furthermore, to respond to the increasing demand for broadband services, in the near future, a new generation of wireless communications based on fibre-radio technologies will be developed. These networks will allow end-to-end connectivity on all-optical paths, removing some of the existing bandwidth limitations.

We have also described the multiple access methods used in wireless systems. In the next chapter, we will present the spread spectrum technique in detail.

Chapter 3

Spread Spectrum Communications Systems

3.1 Introduction

In the last chapter, we described the history of mobile communications and detailed the evolution of the present mobile systems. We stated that CDMA is proving to be a good candidate for future mobile communications. In this chapter, we present the foundation for Spread Spectrum (SS) theory used in CDMA systems.

The use of SS modulation was first introduced in the mid 1950's mainly as a novel form of transmission, overcoming the rigid restrictions in radio bandwidth allocation [27, 28]. Spread spectrum found immediate application in military communications, as a mechanism of transmitting signals in very noisy environments with very high security [29]. However, there are a number of non-military applications that also benefit from the unique characteristics of spread spectrum modulation [30, 31]. For example, it can be used to provide multi-path rejection in a ground-based mobile radio environment [32, 33]. Yet another application is in multiple-access communication in which a number of independent users are required to share a common channel without an external synchronising mechanism; here, for example, we may mention a ground-based mobile radio environment involving mobile vehicles that must communicate with a central station.

This chapter describes first the general concepts of the SS technology with a detailed presentation of the direct sequence technique. Then, different codes used in spread spectrum communication systems are introduced. Finally, using the Signal Processing Worksystem (SPW) simulation framework, simulation results of an implemented Code Division Multiple Access (CDMA) system are presented.

3.2 Fundamentals of Spread Spectrum

3.2.1 Definition

The definition of SS modulation may be stated in two parts:

1. SS is a means of transmission in which the data sequence occupies a bandwidth in excess of the minimum bandwidth necessary to send it.

2. The spectrum spreading is accomplished before transmission through the use of a code that is independent of the data sequence. The same code is used in the receiver (operating in synchronism with the transmitter) to despread the received signal so that the original data sequence may be recovered.

Although standard modulation techniques such as frequency modulation and pulse-code modulation satisfy part 1 of this definition, they are not SS techniques because they do not satisfy part 2 of the definition.

In spread spectrum modulation, the bandwidth expansion does not combat white noise as it does in frequency modulation, pulse position modulation and other wide-band modulation methods. This is because bandwidth expansion is achieved by something that is independent of the message, rather than being uniquely related to the message. Since the SS system is not useful in combating white noise, it must have other properties that make it worth considering. The properties that may be cited are the following:

- Interference suppression, the most important property.
- Energy density reduction.
- Ranging (time delay measurements).

3.2.2 Interference Suppression

There are several types of interference amongst which are:

- Interference from other users. This may be intentional (hostile) or unintentional (other authorised users).
- Interference from an enemy, termed "jamming". Protection against this type of interference is termed "anti-jamming". Usually the jamming power is much larger than any of the users' power.
- Multiple access interference. In multiple access, there are several coordinated users using the same spreading bandwidth (BW), and there is the need to suppress the interference between such users. SS techniques solve this problem.
- Multi-path interference (self-jamming). In this case, the signal is received (at the receiver) via several paths. The signals received from these paths interfere with each other and produce fading and distortion, this is actually self-jamming.

3.2.3 Energy Density Reduction

There are two reasons for this energy density reduction:

- To meet international allocation regulations. For example, in order to assure the secrecy of communications between a satellite and a given received area on the earth (from other areas), we must have the energy density of the signal (from the satellite) to the boundary of this area so small that it can't be received by the neighbouring areas. This means that the signal transmitted by the satellite to any specific area on earth must meet international regulations: spreading the energy of the signal over a very large BW will make the energy density very small and will allow the transmitted power to be increased, thus improving the performance.
- To minimise detectability and preserve privacy. In this case, the signal is frequency spread so that the spread power level is less than the background noise and can't be detected by unauthorised users. However, it can be recovered and received properly at the receiver by authorised users.

3.2.4 Ranging

This property of SS lies in its ability to yield accurate distance information. It is well known that a broadband signal can be resolved in time much more precisely than a narrow-band signal. Thus by transmitting a signal with a large bandwidth, it is possible to measure delay times much more accurately and obtain more accurate range information. This is of importance not only in radar systems, but also in navigation systems.

3.2.5 Spread Spectrum Systems

A SS system in its more general form is illustrated in Figure 3.1. It uses the following

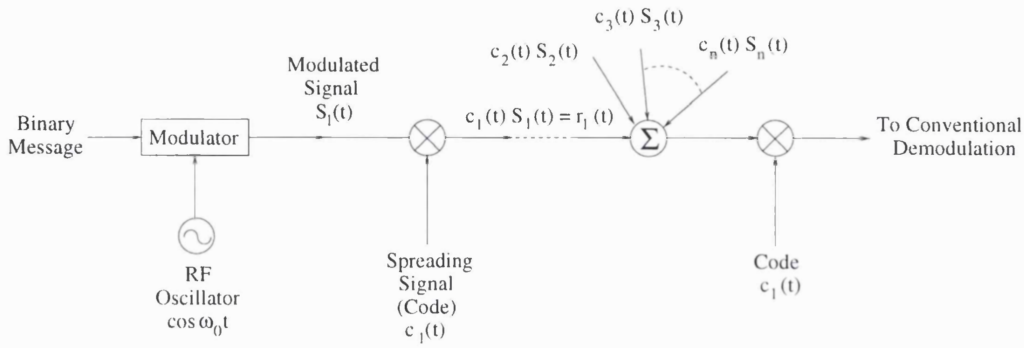

Figure 3.1: Spread Spectrum System

steps:

- First, the carrier $A\cos\omega_0(t)$ is modulated with the message to produce a modulated signal $S_1(t)$ given by $S_1(t) = A_1(t)\cos[\omega_0 t \quad]$. Any type of modulation can be used.

- Second, $S_1(t)$ is multiplied by a "spreading or code function" $c_1(t)$. Usually $c_1(t)$ is kept secret and its use is restricted to the community of authorised users. The resulting signal is $r_1(t)$ given by $r_1(t) = c_1(t)S_1(t)$. Thus, the spectrum of $r_1(t)$ is the convolution of the spectrum of $c_1(t)$ and $S_1(t)$. Then, if $S_1(t)$ is relatively narrow-band compared with the spreading (or code) signal $c_1(t)$, the product $r_1(t)$ will have nearly the bandwidth of $c_1(t)$, that is the spreading bandwidth.

- Third, the spread spectrum signal $r_1(t)$ is transmitted over the channel.

  At the same time, other users do the same, by multiplying their signals $(S_2(t), S_3(t), \cdots, S_n(t))$ by other code functions $(c_2(t), c_3(t), \cdots, c_n(t))$.

  The signal $s_r(t)$ received at the receiver is therefore given by

  $s_r(t) = c_1(t)S_1(t) + c_2(t)S_2(t) + c_3(t)S_3(t) + \cdots + c_n(t)S_n(t)$.

- At the receiver: its first stage multiplies the desired signal (let it be $S_1(t)$) by the corresponding code function $c_1(t)$ giving signal to the demodulator equal to $c_1^2(t)S_1(t) + c_1(t)c_2(t)S_2(t) + c_1(t)c_3(t)S_3(t) + \cdots + c_1(t)c_n(t)S_n(t)$. The code functions $c_1(t), c_2(t), \cdots, c_n(t)$ are orthogonal functions having the property:

$$\int_0^T c_r(t)c_s(t) = \begin{cases} 0 & r \neq s \\ 1 & r = s \end{cases}$$

where T is the signal duration. Therefore the signal at the receiver demodulator output $= S_1(t)$, theoretically, and the desired signal can be extracted perfectly and the unwanted signals rejected.

Figure 3.2 shows, in simple terms, using rectangular spectra, the convolution of the two spectra. The narrow spectrum corresponds to the data message and the wide spectrum corresponding to the PN code. Several encoding and transmission techniques based on

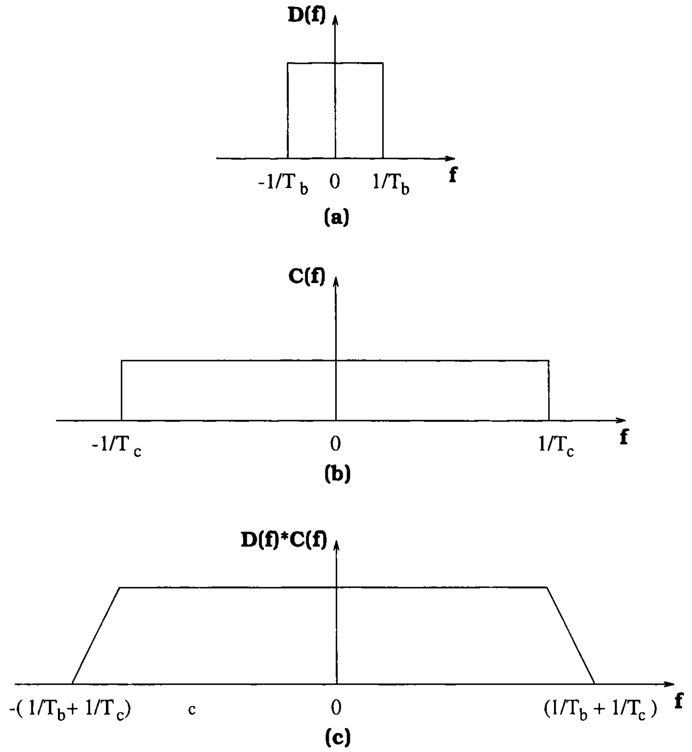

Figure 3.2: Convolution of spectra of the (a) data signal with the (b) PN code signal

SS principles have been developed. Direct Sequence is the one that has been mainly employed for communication purposes, whereas other SS techniques have been used for other purposes such as ranging. A description of the SS techniques is presented next.

3.3 Spread Spectrum Techniques

There are many different types of SS techniques and one way of classifying them is by modulation. The most common modulation techniques employed are the following

- Direct Sequence (Pseudo-noise)
- Frequency hopping
- Time hopping
- Chirp
- Hybrid methods

3.3.1 Direct Sequence (DS) or Pseudo-noise (PN)

In the Direct Sequence (DS) SS technique the message signal is modulo-2 added to a pseudo-noise spreading code which is of a much higher bit rate. The basic method for accomplishing the spreading is shown in Figure 3.3. For discriminating between data bits and code bits, the latter are referred to as "chips". The pseudo-noise (PN) code is selected from a family of such codes with special correlation characteristics (which will be described in detail in section 2.4.3). The code period generally (although not necessarily) is equal to the data bit period.

A crucial parameter that determines the degree of spreading is the ratio of the BW of the signal transmitted to the BW of the information signal $BW_{RF}/BW_{INFO} = R_c/R_{data}$. This ratio is called the Processing Gain (PG) and reflects the degree of

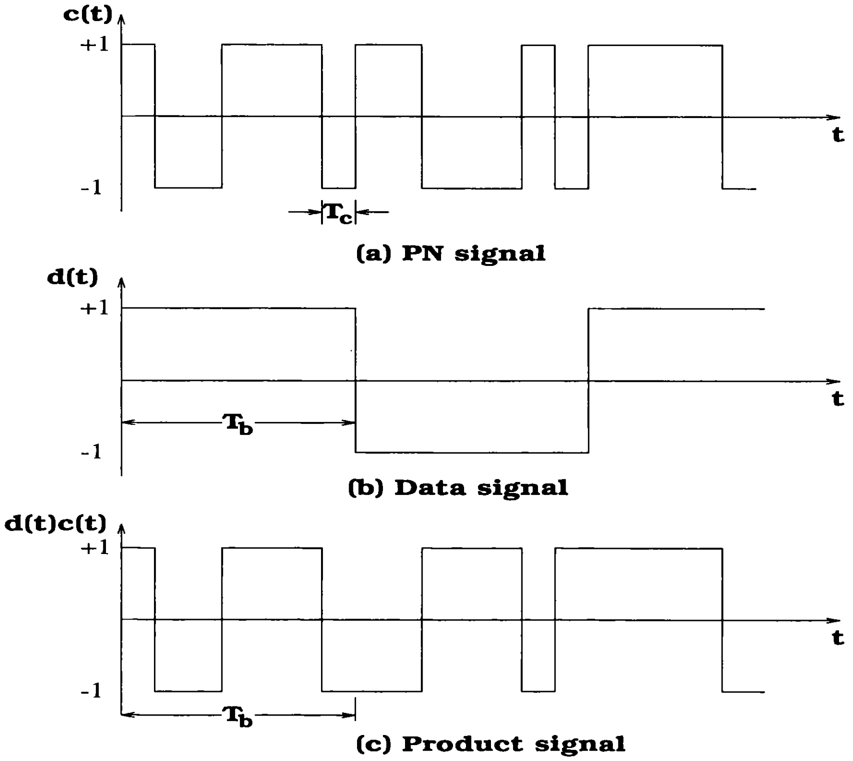

Figure 3.3: Generation of a DS spread-spectrum signal

spreading of the signal power [34]. From the receiver point of view PG expresses the degree of reduction of the received signal power within the original signal BW. Since the power spectral density is very low it is not possible to recover the original message using conventional methods. Message recovery will be achieved by despreading the received signal, as will be demonstrated next. Obviously, for a constant data rate, the faster the code, the higher the processing gain.

At the receiver, signal despreading is achieved by multiplying the received signal which consists of the desired transmitted signal, signals from other co-users and noise, with a local code which has to be a synchronised replica of the code used for encoding the desired transmitted signal.

This multiplication will reproduce the narrowband desired signal while the undesired signals will be further spread in the frequency domain. Mixing with a local oscillator (LO) followed by filtering using a narrowband bandpass filter at the Intermediate

Frequency (IF) (or a lowpass if the LO is of the same frequency as the RF carrier) will reject most of the power of the interfering signals, recovering the original baseband data signal. Figure 3.4 depicts the DS communications link while Figure 3.5 illustrates the reception and despreading operation. Although the main application of SS initially

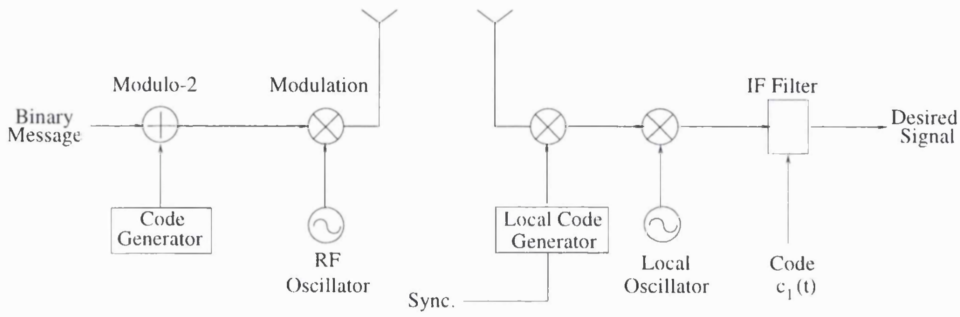

Figure 3.4: A Direct Sequence Communications Link

was to establish a communications link between a transmitter and a receiver in a noisy environment, it became very clear that this technique could be employed in a multiple access communications system, by allocating a particular code to identify each individual user (Code Division Multiplexing). Such networks are named CDMA for Code Division Multiple Access.

The number of users that can be accommodated by the system depends mainly on the cross-correlation properties of the family of codes employed by the users since this determines the amount of unwanted crosstalk that is present at the receiver even after filtering. Therefore the choice of codes with very low crosscorrelation is of great importance for this sort of SS communications systems.

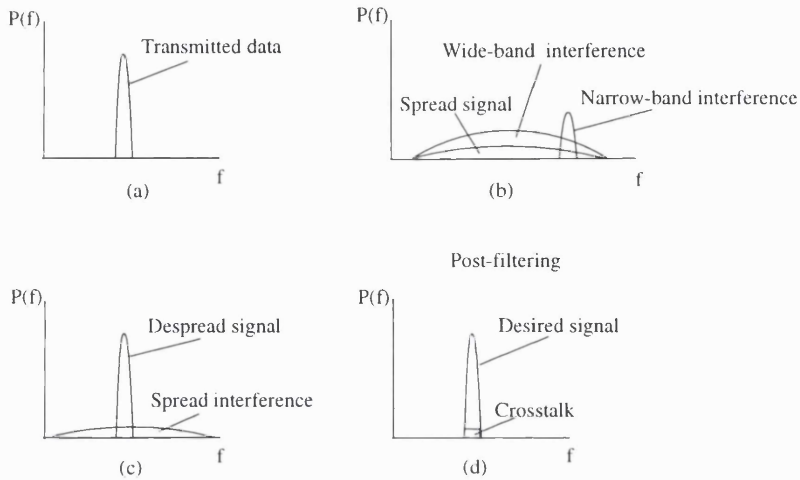

Figure 3.5: Despreading operation: (a) The original message signal, (b) The received signal at each receiver, (c) The received signal after local multiplication. The desired signal is despread, (d) The signal after filtering. The interference outside the message signal BW is rejected.

3.3.2 Other Spread Spectrum Techniques

Several other SS techniques exist although it must be recognised that DS is the main SS technique applied in communications systems. However, it is useful to review the other SS techniques, which can be found in several applications (such as radar- ranging systems) and could also be employed in special cases in communications systems.

Frequency Hopping

In this technique, a Frequency Hopping (FH) carrier is used. The carrier remains at a given frequency for a duration of a chip, and then hops to a new frequency somewhere in the spreading bandwidth for the next chip [35]. This type of signal is illustrated in Figure 3.6. In such a system, the hopping pattern is determined by an independent pseudo-random code. The FH is actually accomplished by means of a frequency synthetiser which in turn is driven by a PN code. It is frequently convenient to categorise FH systems as either "fast hopping" or "slow hopping", since there is a considerable difference in performance for these two types of systems. A fast hopping

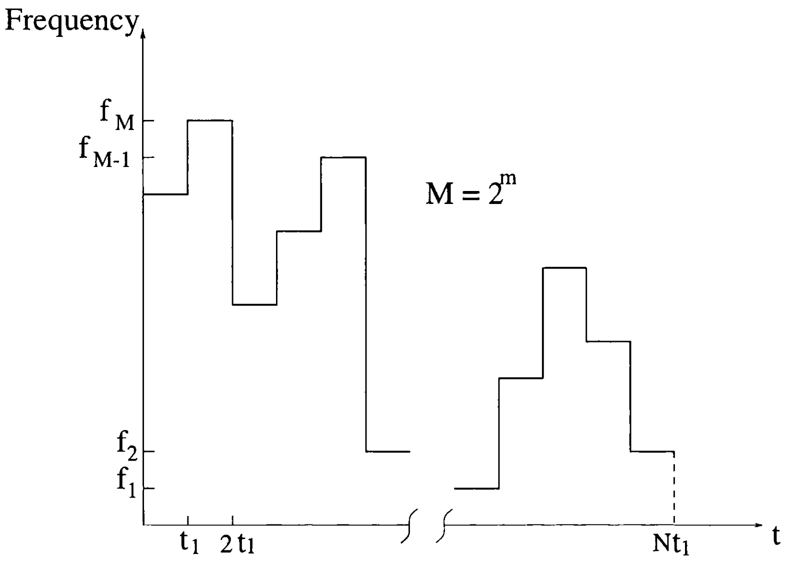

Figure 3.6: Frequency Hopping signal

system is usually considered to be one in which the FH takes place at a rate that is greater than the message bit rate, and then the bandwidth of the transmitted signal is equal to the reciprocal of the hopping duration. In a slow-hopping system, the hop rate is less than the message bit rate and the bandwidth of the transmitted signal is equal to that of the data signal. There is, of course, an intermediate situation in which the hop rate and the message bit rate are of the same order of magnitude.

Time Hopping

In a Time Hopping (TH) case, message signals are transmitted in short pulses whose intervals are again determined by a PN code. Each data bit is divided in N subdivisions. During the duration of a data bit a subdivision is selected randomly by the spreading code so that intervals between successive pulses are varied accordingly. A TH waveform is illustrated in Figure 3.7.

TH is actually very close to the classical pulse position modulation scheme.

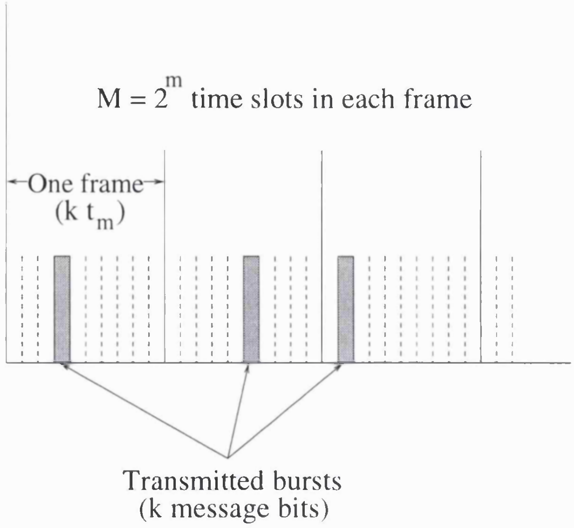

Figure 3.7: Time hopping waveform

Chirp Spread Spectrum

Chirp systems are the only SS systems that do not employ a code sequence to control their output signal spectra. A chirp SS system utilises linear frequency modulation of the carrier to spread the bandwidth. So the frequency of the transmitted pulse is linearly increased from a frequency f_1 to f_2 during the pulse. The relationships between frequency and time are shown in Figure 3.8, in which T is the duration of a given signal waveform and B is the bandwidth over which the frequency is varied. In this case the processing gain is simply BT. It is also possible to use nonlinear frequency modulation, and in some cases this may be desirable. This is a technique that is very common in radar systems but is also used in communication systems especially in hybrid forms.

Hybrid Spread Spectrum Systems

The use of a hybrid system attempts to capitalise upon the advantage of a particular method while avoiding the disadvantages. Many different hybrid combinations are possible. Some of these are:

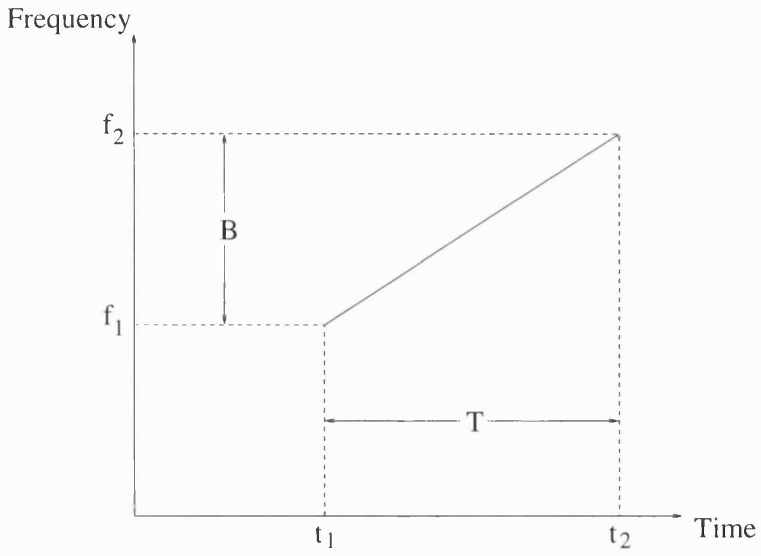

Figure 3.8: Chirp-hopping signal

- PN/FH
- PN/TH
- FH/TH
- PN/FH/TH

To illustrate how a hybrid system might operate, consider the case of a PN/FH hybrid system. This system might use a PN code to spread the signal to an extent limited by either code generator speed or acquisition time. Then FH would be used to increase the frequency spread. The difference between the frequencies in the FH portion of the system would normally be equal to the bandwidth of the PN code modulation. Usually some form of non-coherent message modulation is used because of the FH, and differential phase shift keying is a typical example. Since there are fewer frequencies to be implemented, the frequency synthesiser is simpler for a given overall bandwidth. Thus this system gains some of the advantages of DS systems and of FH systems, and avoids some of the disadvantages of both.

3.4 Codes for Spread Spectrum Systems

The spread spectrum technique is fundamentally based on the idea of encoding the signals to be transmitted. In general, data are (or become) in digital form and the codes used for encoding would be in digital form as well. The design and selection of codes have to follow some special criteria that are derived from the requirements of the communications system. So, a family of codes which will be allocated to a group of users should have the following two properties:

- Each signal in the set is easy to distinguish from a time-shifted version of itself (very high auto-correlation).
- Each signal in the set is easy to distinguish from (a possibly time-shifted version of) every other signal in the set (very low or zero cross-correlation).

Several families of PN codes have been studied mathematically and implemented using shift register technology. A PN sequence is a periodic binary sequence with a noiselike property that is usually generated by means of a feedback shift register, a general block diagram of which is shown in Figure 3.9.

PN code generators are periodic in that the sequence that is produced repeats itself

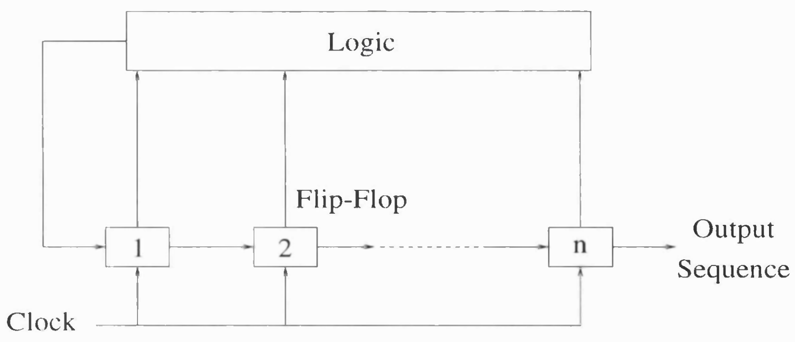

Figure 3.9: Linear PN code generator

after some period of time. When the code is generated by a maximal linear PN code generator, the value of N is $2^n - 1$, where n is the number of stages in the code generator. Each period of the sequence contains 2^{n-1} ones and $2^{n-1} - 1$ zeros. In DS spread spectrum applications the binary sequence with elements {0,1} is mapped into a corresponding sequence of positive and negative pulses according to the relation

$$p_i(t) = (2b_i - 1)p(t - iT)$$

where $p_i(t)$ is the pulse corresponding to the element b_i in the sequence with elements {0,1}. We shall call the equivalent sequence with elements {-1,1} a bipolar sequence, since it results in pulses of positive and negatives amplitudes.

The two more commonly used families are the m-sequences and the Gold codes which are described next.

3.4.1 M-Sequences

Maximal length codes or m-sequences are by definition the longest codes that can be generated by a given linearly shift register or a delay element of a given length. This means that the n stages of the shift register are connected with proper feedback so that they generate codes of the longest possible length, with respect to the number of stages in the shift register. In binary shift register sequence generators, the length of such a sequence is $N = 2^n - 1$ (where n is the number of stages of the shift register).

There are some sets of m-sequences that have certain cross-correlation upper bounds and therefore they could be employed in a multiple access communication scheme. These particular sets are called "preferred" m-sequences [36]. Unfortunately, preferred sets include a very small number of codes. Actually, no more than six sequences can be found in a preferred set. This fact makes m-sequences unsuitable for multiple access systems with many users.

The main m-sequences properties are summarised below:

- Auto-correlation

$$C_a(u,u)(\tau) = \begin{cases} N & for\ \ \tau = 0 \\ 1 & for\ \ \tau = 1,\cdots,N-1 \end{cases}$$

- Cross-correlation For n not a multiple of 4 there are sequences of 3-valued cross-correlation:

  $C_c(u,v)(\tau) = -1$ or $-t(n)$ or $t(n) - 2$ where $t(n) = 1 + 2^{[(n+2)/2]}$

  For n multiple of 4 there are sequences of 4-valued cross-correlation:

  $C_c(u,v)(\tau) = -1 + 2^{(n+2)/2}$ or $-1 + 2^{n/2}$ or -1 or $-1 - 2^{n/2}$

- Period of code $N = 2^n - 1$

- Number of sequences per set Maximal connected sets are limited to 6 sequences

- Number of "1's" in a period is $K = \frac{N}{2} + 1$

As a conclusion, although m-sequences exhibit the desired bounded cross-correlation, they offer only a small number of available sequences and therefore they are unsuitable for multiple access communications systems where a large number of subscribers need to be identified by a particular code.

The modified m-sequence (or m+1 sequence) is another type of code. These codes are generated from the m-sequence by a simple modification in the following way [37]: from an n-stage maximal length shift register the m-sequence is generated with a period $N = 2^n - 1$. The original m-sequence is taken, plus the $N-1$ different shifted versions of this sequence and at the end of each of them we add a "0" or a "1". This is the new family. The cross-correlation of these codes for $\tau = 0$ is 0 and the number of sequences that this family accommodates is equal to the period N of the code. Furthermore this type of code exhibits perfect orthogonality, due to the fact that the number of agreements is now equal to the number of disagreements. So for optical

CDMA systems the proposed m+1 sequences offer the possibility of a greater number of users and at the same time they have very good interference rejection properties. However it must be stressed that this applies to synchronous transmission codes, where a form of synchronisation is maintained among all the transmitters.

3.4.2 Gold codes

Another set of codes derived from m-sequences was proposed by R. Gold in 1967 [38]. They are generated by modulo-2 addition of two preferred m-sequence as is shown in Figure 3.10. Two shift registers are driven by a common clock so that their addition is

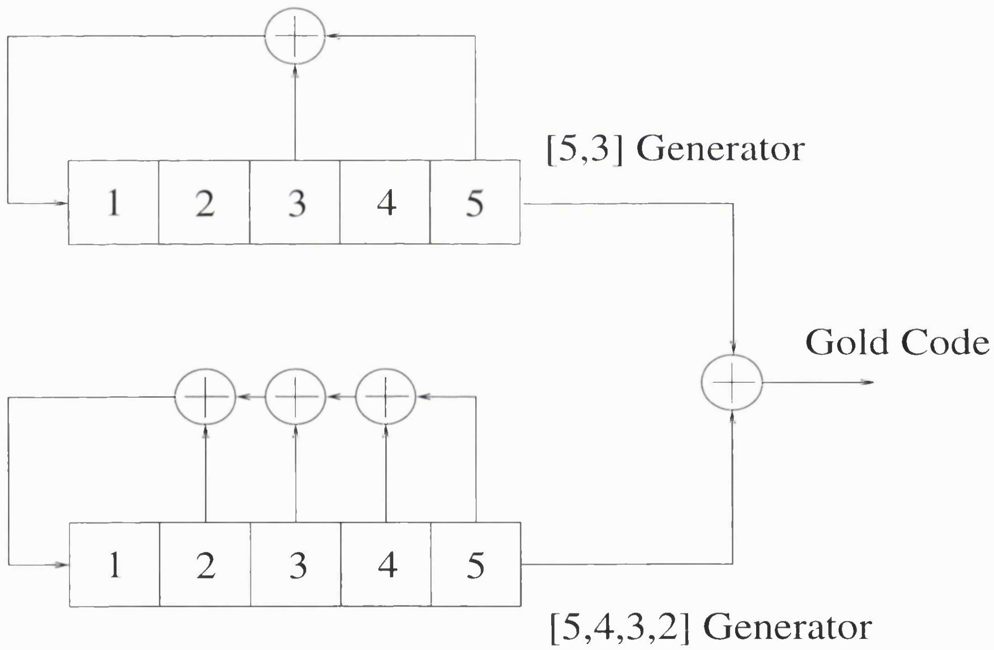

Figure 3.10: A Gold code generator

synchronised for a one by one bit modulo-2 addition. The two m-sequences must have the same period and speed. Since it is modulo-2 addition, the generated Gold code will have the same period, $N = 2^n - 1$, as the two m-sequences, while the number of "1's" in the new code will vary depending on the initial m-sequences and their relative shift.

Gold Codes properties are summarised below:

- Auto-correlation For $\tau = 0, C_a(u,u)(\tau) =$ length of the code N

- Cross-correlation The periodic (synchronous) cross-correlation function takes 3 values depending on whether n is an odd or even number. For n an odd number then

  $C_c(u,v)(\tau) = -1$ for 50% of the shifted code cases

  $C_c(u,v)(\tau) = -1 - 2^{(n+2)/2}$ for 25% of the shifted code cases

  $C_c(u,v)(\tau) = -1 + 2^{(n+2)/2}$ for 25% of the shifted code cases

  For n even and not a multiple of 4, then

  $C_c(u,v)(\tau) = -1$ for 75% of the shifted code cases

  $C_c(u,v)(\tau) = -1 - 2^{(n+2)/2}$ for 12.5% of the shifted code cases

  $C_c(u,v)(\tau) = -1 + 2^{(n+2)/2}$ for 12.5% of the shifted code cases

- Period of code $N = 2^n - 1$

- Number of sequences per set $N + 2$

- Number of "1's" in a period.

  This number K depends on the relative shift of the codes. However, if n is odd then K is well defined as follows:

  $K = 2^{(n-1)}$ for $[2^{(n-1)} + 1]\%$ of cases

  $K = 2^{(n-1)} + 2^{(n-1)/2}$ for $[2^{(n-2)} - 2^{(n-3)/2}]\%$ of cases

  $K = 2^{(n-1)} - 2^{(n-1)/2}$ for $[2^{(n-2)} + 2^{(n-3)/2}]\%$ of cases

Although the cross-correlation properties of Gold codes defined above apply for the case of synchronous transmission, where all the codes are transmitted in fixed time frames, the performance of a system using Gold codes of these correlation values is very close to the corresponding random values in a purely asynchronous transmission case.

Gold codes under bipolar correlation have been demonstrated to be the best among the known codes for asynchronous transmission and therefore have been extensively employed in radio communications as well as in ranging applications.

3.5 Modelling of a Optical Network Supporting CDMA Signals

In recent years, fibre-optic code division multiple access has become an interesting scheme for taking advantage of excess bandwidth in single mode fibres [39]. A typical FO-CDMA communication system is shown in Figure 3.11. In such a system, the

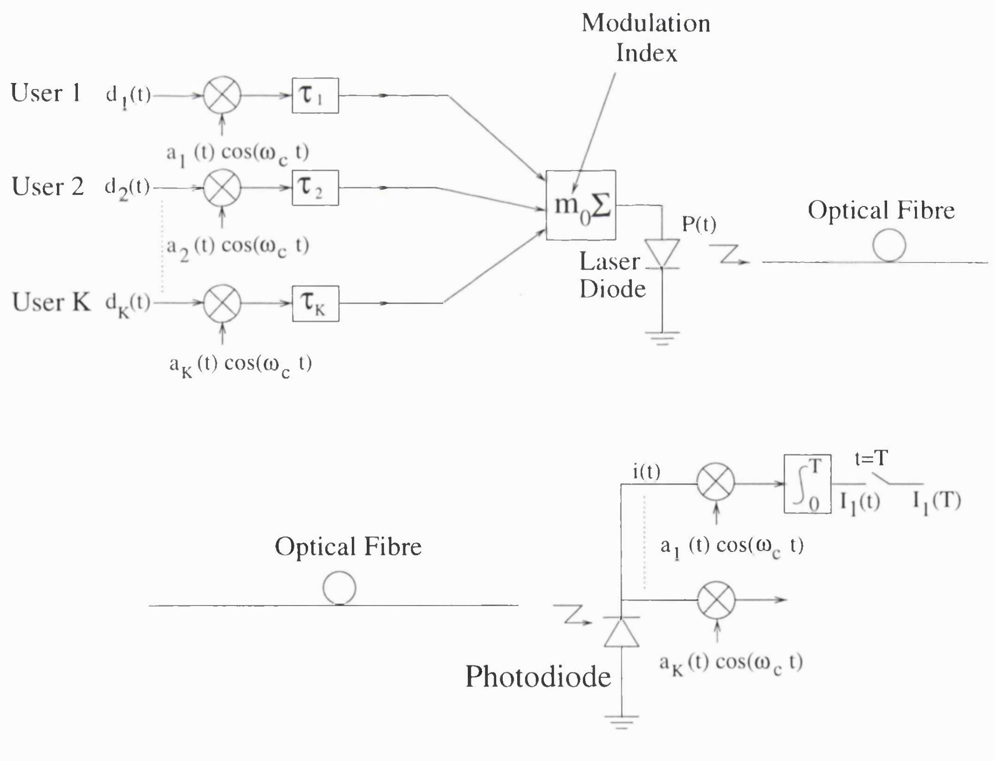

Figure 3.11: Model of CDMA system in optical communication

message signal is multiplied by a PN spreading code which is of a much higher bit rate. The product is used to amplitude modulate a carrier and then the sum of the spread spectrum signals is used to modulate the optical intensity of the LD. The signal is transmitted to the receiver via an optical fibre. At the receiver end, the signal is detected and recovered after despreading, as explained in section 3.3.1.

The modelling of the FO-CDMA system has been implemented using the Signal Processing Worksystem (SPW) by Alta Group. Most of the constituted blocks of the FO-CDMA are blocks provided by the SPW library; the key exception is the laser diode model. In the following section, the SPW platform is described and the Laser Diode model is implemented.

3.6 Signal Processing Worksystem

3.6.1 SPW Description

It was decided to use the Signal Processing Worksystem (SPW) by Alta Group as the modelling platform.

SPW is an integrated framework for developing DSP and communications products. The vast DSP library, graphical design methodology, fast simulator, test and analysis facility and implementation options make SPW an appropriate choice for concept-to-prototype design.

SPW can be used to model and simulate a system, then debug, revise, and resimulate the system until optimal results are obtained.

SPW consists of several modules. The main modules are: Designer/BDE, Signal Calculator, and Signal Flow Simulator.

In the 'block diagram editor' (BDE), a system is constructed as a set of functional blocks connected by wires. Each block is a symbol that represents an operation, and the interconnecting wires symbolise the flow of signals between blocks. These blocks can either be from the BDE library or produced by the user. The Signal Flow Simulator converts the BDE system models into simulation programs. It processes input signals created by the Signal Calculator and then executes the simulation.

In the Signal Calculator, we can create input signals for the simulation and view the result of our simulations. The signal calculator allows us to view the signal as an eye diagram, as a distribution and to perform a Fast Fourier Transform on the signal, among other functions.

3.6.2 Custom-Coded Block

In SPW, we can create our own library blocks called custom-coded blocks (CCBs). A custom-coded block is a signal processing block whose function is specified by a 'C' program written by the user.

The creation of a CCB involves the following steps:

- Create the symbol model in the BDE window. This symbol model contains the input/output ports for the signal processing, function and graphical elements such as boxes, lines and text.

- Create the parameter screen model in another BDE window. The parameter model contains graphical elements (boxes, lines and text), certain mandatory parameters, plus any user-set table block parameters we want to use with the block.

- Link the symbol model to the parameter model by using the LINK command in the BDE window.

- Generate the source code template files by using the Template command in the Prepare Block (PB) sub-window. The PB tool creates two template files, .c and

.h. The .c file contains the source code that implements the block function. The .h file code declares the variable used in the .c program.

- Insert the signal processing source code into the template files. Four parts need to be written according to the mathematical model describing the input-output relation of the component to be modelled by editing the .h and .c file in a text editor window: the 'state structure' part of the .h file and the 'initialize function' part, the 'run output function' part and the 'termination function' part of the .c file.

- Compile the code to create the object file by using the COMPILE command in the PB sub-window.

- Add the block to the standard blocklist (or to a custom block) by using the LINK command in the PB sub-window.

3.7 DFB Laser Modelling

Before implementing our model, we need to describe mathematically our component.

3.7.1 Theoretical Model of DFB Laser

A single-mode laser diode (e.g. a DFB laser diode) can be described by the rate equations for the photon number P and the electron number N [40]

$$\frac{dP(t)}{dt} = GP(t) - \frac{P(t)}{\tau_p} + R_{sp}(t) \tag{3.1}$$

$$\frac{dN(t)}{dt} = \frac{I(t)}{q} - \frac{N(t)}{\tau_n} - GP(t) \tag{3.2}$$

with I the injected current into the active layer, τ_p the photon lifetime, τ_n the electron lifetime and q the electronic charge. The gain G which includes the effects of lateral carrier diffusion is given by

$$G = \Gamma V_g a(\frac{N}{V_a} - N_0)(1 - \frac{\epsilon \Gamma P(t)}{qV_a}) \tag{3.3}$$

and the spontaneous emission rate R_{sp}

$$R_{sp} = \frac{\beta_{sp}\Gamma N}{\tau_n} \tag{3.4}$$

with Γ the optical confinement factor, V_g the group velocity, a the differential gain coefficient, V_a the volume of the active region, N_0 the transparency carrier density and the fraction of spontaneously emission coupled into the lasing mode β_{sp}. The pair of coupled differential equations can be rationalised very easily by the following physical reasoning. Equation 3.1 gives the photon rate, the first term accounts for the stimulated emission, the second term for the photon loss through the cavity and the third term the number of spontaneous generated photon. Equation 3.2 gives the electron rate, the first term indicates that the number of carriers concentrated in the conduction band increases with the injected current, the second term governs the carrier loss due to spontaneous emission and the last term gives the loss due to stimulated emission.

These two equations are simultaneously solved for a current waveform $I(t)$ to generate the following complex electric field output from the laser

$$\bar{E}_{out}(t) = \sqrt{P_l(t)}exp[j\phi(t)] \tag{3.5}$$

where $P_l(t)$ is the laser output power per facet and is related to the photon population by

$$P_l(t) = \frac{P(t)hcV_g\alpha_m}{2\lambda_0} \tag{3.6}$$

where c is the speed of light in vacuum, h is Planck's constant, λ_0 is the lasing wavelength and α_m is given by [41]

$$\alpha_m = \frac{1}{2L} ln\left(\frac{1}{R_1R_2}\right) \tag{3.7}$$

which is the mirror loss and accounts for radiation escaping from the Fabry-Perot cavity because of finite reflectivities R_1 and R_2, with L being the length of the cavity. The derivation of equation 3.6 is intuitively obvious if we denote that $V_g\alpha_m$ is the rate at which photons of energy $h\nu$ escape through the two facets. The phase term, $\phi(t)$ is given by

$$\phi(t) = 2\pi \int_0^t \Delta\nu(t')dt' \tag{3.8}$$

where

$$\Delta\nu(t) = \frac{\alpha}{4\pi}\Gamma V_g a\left(\frac{N(t)}{V_a} - \frac{\bar{N}}{V_a}\right)\left(1 - \frac{P(t)}{V_a}\Gamma\epsilon\right) \tag{3.9}$$

where α is the linewidth enhancement factor and $\bar{N}$ is the average value of the carrier population at the emission reference wavelength.

3.7.2 Creation of DFB Laser CCB

The symbol model adopted for the DFB Laser CCB is shown in Figure 3.12. The implementation of the DFB laser has one input and four outputs; the input is the drive

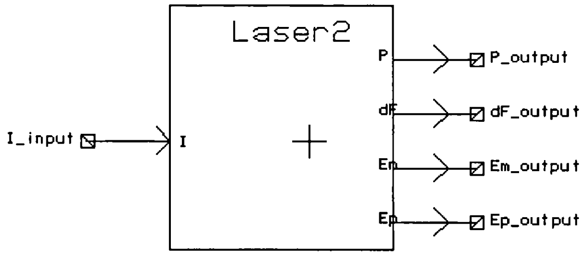

Figure 3.12: Symbol model of laser

current and the outputs are power, electric field magnitude, phase and chirp. The 'initialise function' and 'run output function' parts of .c files are implemented as follows. The 'initialise function' parts contain the 'C' code to calculate the initial variable values. First, the initial variable values $P(t)$ and $N(t)$ are calculated from solving the rate equations at $t = 0$. By setting $t = 0$ in equations 3.1 and 3.2, neglecting the carrier diffusion and rearranging then we can obtain the steady state solution by solving:

$$\begin{aligned} N^2\frac{\Gamma V_g a}{\tau_n V_g}(1-\beta_{sp}\Gamma) + \frac{I}{q}(\frac{1}{q} + \Gamma V_g a N_0) & \\ +N\left(\frac{V_g a N_0 \beta_{sp}\Gamma^2}{\tau_n} - \frac{1}{\tau_n\tau_p} - \frac{\Gamma V_g a N_0}{\tau_n} - \frac{I\Gamma V_g a}{q V_a}\right) &= 0 \end{aligned} \tag{3.10}$$

which is a quadratic equation and we can solve for N, hence we can then obtain P:

$$P = \frac{\beta_{sp}\Gamma\frac{N}{\tau_n}}{\frac{1}{\tau_p} - \Gamma V_g a(\frac{N}{V_a} - N_0)} \tag{3.11}$$

Then, the equations are iterated until steady state values are obtained. The 'run output function' part contains the 'C' code to calculate the photon and electron populations for each sample value. Figure 3.13 shows the parameter model of the DFB Laser CCB. The parameter model defines the feedback type of the CCB, defines the type of each parameter and gives its value. All the parameter values of the DFB Laser can be changed by push-down from the symbol model to the parameter window just before running the simulation of a system.

LASER2 BLOCK PARAMETERS

Feed Through type	ALL_FEED_THROUGH
Initial Value	0.0
I bias	20e-3
I at Ref lambda	35e-3
Wavelength	1550e-9
Line Width Enhancement Factor	5.0
Sampling Frequency	64e11
Active Volume	5.6e-17
Gain Compression Factor	4.5e-23
Optical Confinement Factor	0.4
Carrier Density @ G = 0	1e24
Gain Coefficient	2.5e-20
Spontaneous Emission Factor	3.9e-4
Carrier Lifetime	1e-9
Photon Lifetime	1.4e-12
Group Velocity	74948114.5
Alpha_m	45e2

Figure 3.13: Parameters of laser

3.7.3 Simulation Example of the DFB Laser CCB

In order to validate our Laser model, two simulation examples of the DFB Laser CCB are given. In the first simulation, we apply a step of current on the laser to observe the transient response. Transient phenomena accur because of the time required for the electron and photon populations to come into equilibrium.

In our experiments, the laser current is abruptly increased, say when $t = 0$, from its initial value I_0 to the final value I, which is greater than I_{th}.

Three experiments are carried out to investigate the dependence of the transient response with the bias current I_0. In the three experiments, I_0 is fixed at 10, 15 and 17 mA and I is fixed at 30, 35 and 37 mA respectively. The results are shown in Figure 3.14. When the laser is turned on by increasing the device current from its initial value to the above-threshold value I greater than I_{th}, stimulated recombination is delayed

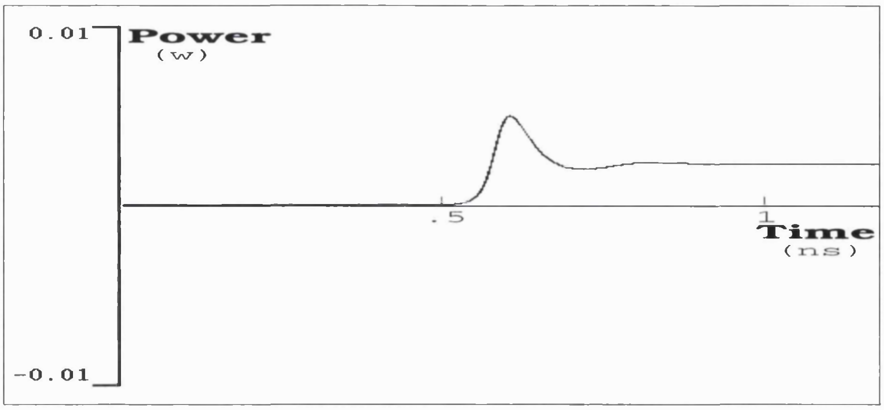

(a)

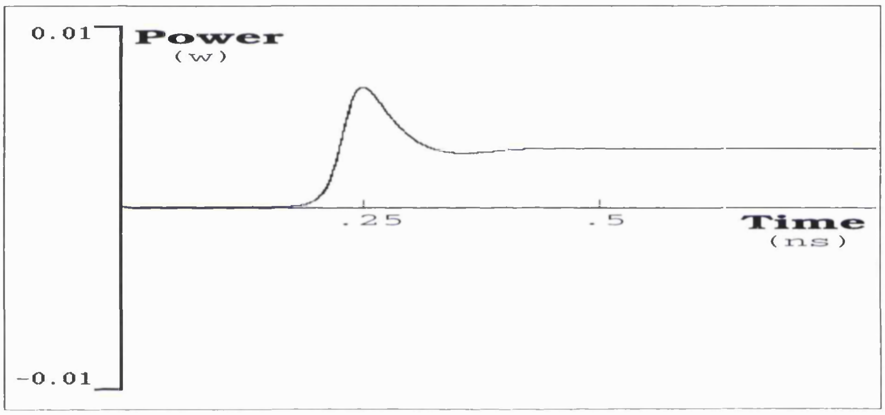

(b)

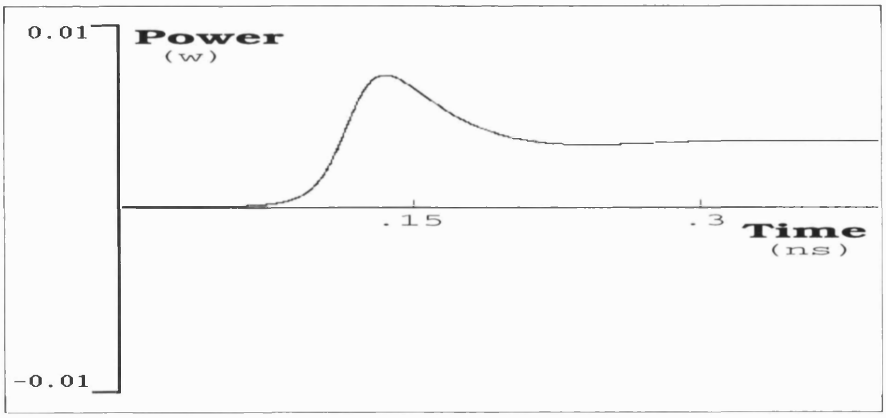

(c)

Figure 3.14: Transient response for I = 30 mA (a), 35 mA (b) and 37 mA (c)

by t_d, the time during which the carrier population rises to its threshold value. In the simple approximation where the recombination rate is constant the result is [42]

$$t_d = \tau_n \ln\left(\frac{I - I_{off}}{I - I_{th}}\right) \tag{3.12}$$

In our simulation, the value of I_{th} is 17.5 mA. The calculation of t_d for $I = 30mA$ gives $t_d = 0.875ns$. The measured value is approximately $0.88ns$. Equation 20 shows that t_d decreases with an increase in the current I. This phenomenon is observed in our simulation.

One of the important advantages of semiconductor laser is that they can be directly modulated, i.e. one can readily obtain short optical pulses useful for optical communication by modulating the device current.

The second simulation considered this case. The DFB Laser is intensity modulated by using a PN sequence generator taken from the standard SPW libraries. Figure 3.15 shows the optical pulses for a DFB Laser modulated by a PN sequence at 1 GHz.

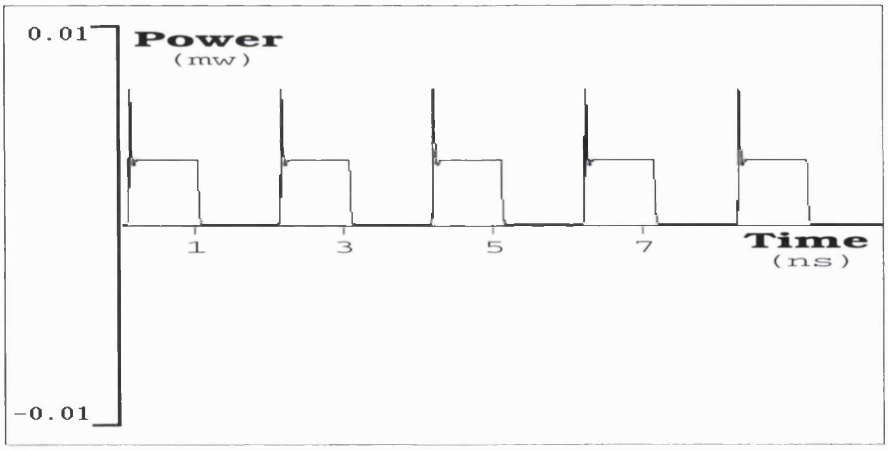

Figure 3.15: Modulation response for DFB Laser at 1 GHz

3.8 Simulation of a FO-CDMA System

In order to simulate our system a modelling platform has been implemented. In the BDE window, we have built a simulation tool including models for most basic components. These component models are either CCBs or symbols and subsystems produced directly in the BDE window by using components of the BDE library. Then, simulation can be carried out directly and the results analysed in the signal calculator window. Various simulations have been undertaken, but for simplicity and explanation reasons we present results for a 7-bit spreading sequence.

3.8.1 Selective Addressing Capability

Simulations have been undertaken using the modelling platform. In these simulations, we use an illustrative 7-bit Gold Code sequence for spreading the data. Every bit "1"is encoded to this sequence of "1s" and "-1" while every bit "-1" is encoded to the complementary sequence.

The first case considered is the case when the reference code is identical to the one used by the transmitter for coding. Figure 3.16 shows the cross-correlation result for transmitting a 1 -1 1 1 -1 1 -1 data sequence. We see that the cross-correlation is positive if a "1" is transmitted and negative for a "-1". In this case, the data are recovered. Next, we consider the case when the reference code is desynchronised by one bit in respect to the code used at the transmitter. Figure 3.17 corresponds to this case. We see that we obtain a positive cross-correlation value for 3 chip times and a negative value for 4 chip times if a bit "1" is transmitted. After integration and threshold decision we get a "-1" and so the data are not recovered. Then, we consider the case when the reference code and the code used at the transmitter are different. The result is shown in Figure 3.18. The cross-correlation takes a positive value during

3 chip times and a negative value during 4 chip times when a bit "1" is transmitted. In this case, the data are not recovered. These three simulations show that a CDMA network offers the possibility of a selective addressing capability, i.e. a user can recover data only if he has a replica of the code used for coding the data.

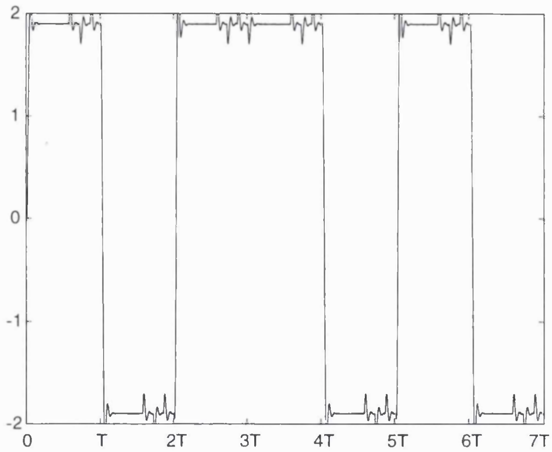

Figure 3.16: The reference code is identical to the one used by the transmitter for coding

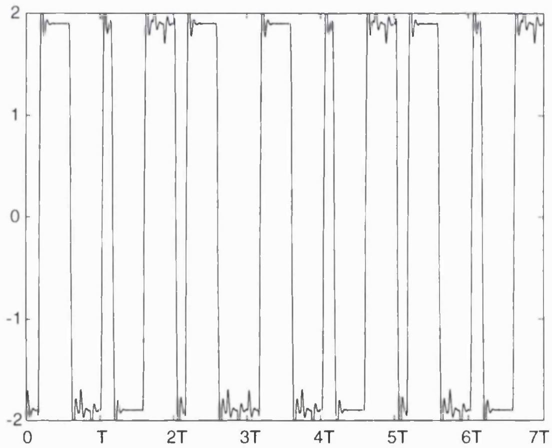

Figure 3.17: The reference code is desynchronised by one chip in respect with the code used at the transmitter

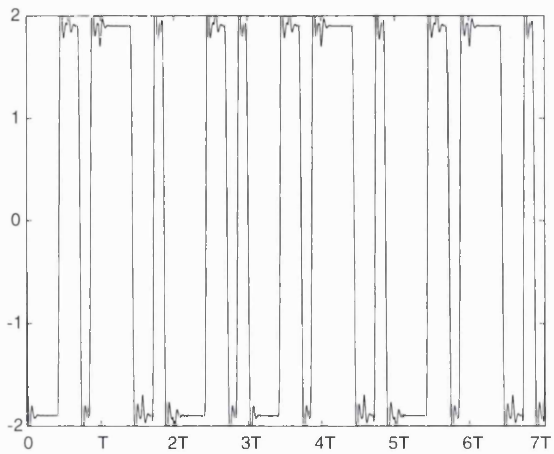

Figure 3.18: The reference code and the code used at the transmitter are different

3.8.2 Multiple Access Capability

Another important property of CDMA systems is that they offer the possibility of multiple access. Three illustrative simulations have been carried out and the results are shown in Figure 3.19, Figure 3.20 and Figure 3.21 for synchronous and asynchronous transmission of three users and for asynchronous transmission of nine users. For the case of three synchronous users, the cross-correlation value takes the positive value, say b, during 4 chips, the positive value $3b$ during 1 chip and the negative value $-b$ during 2 chips if a bit "1" is transmitted. The cross-correlation result is $5b$ which is a positive value and so the data are recovered. For the asynchronous case, the cross-correlation value takes the value b during 4 chips and the value $-b$ during 3 chips. The cross-correlation result is b so the data are recovered too. For nine asynchronous users, we have the value b during 3 chips and the value $-b$ during 4 chips. The cross-correlation result is $-b$ and the data are not recovered. These results are in agreement with the theoretical value of the cross-correlation function. In fact, for n being odd, the periodic (synchronous) cross-correlation function takes 3 values.

In our simulations, we had $n = 3$ and

$C_c(u, v)(\tau) = -1$ for 50% of the shifted code cases

$C_c(u, v)(\tau) = -1 - 2^{(n+2)/2} = -5$ for 25% of the shifted code cases

$C_c(u, v)(\tau) = -1 + 2^{(n+2)/2} = +3$ for 25% of the shifted code cases

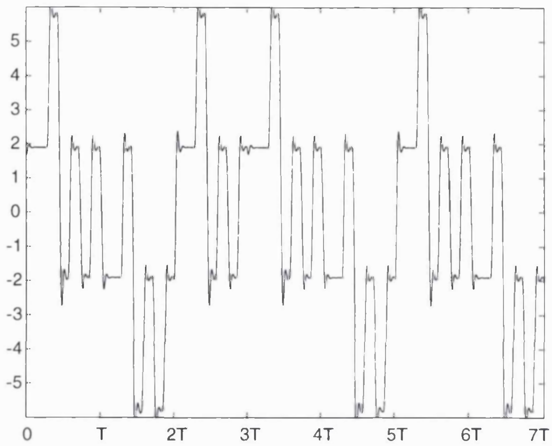

Figure 3.19: Synchronous transmission of three users

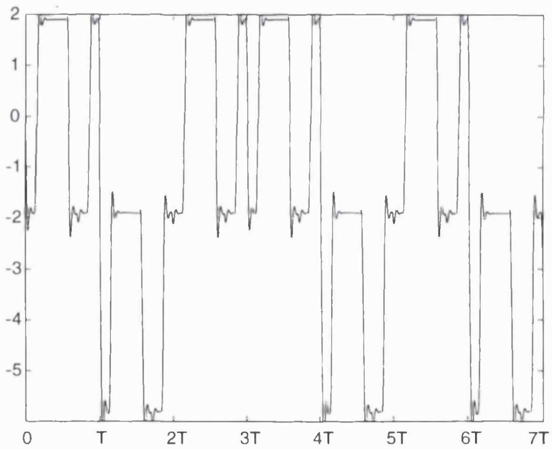

Figure 3.20: Asynchronous transmission of three users

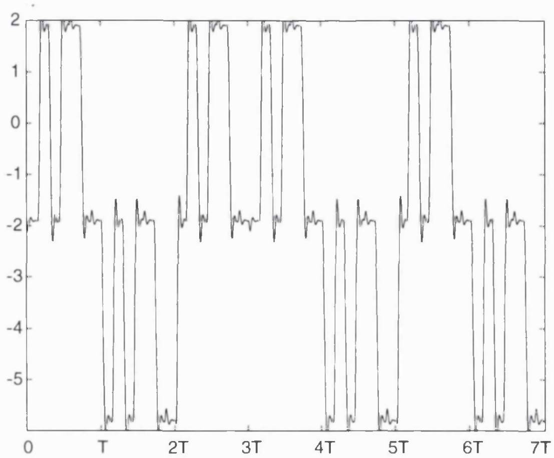

Figure 3.21: Asynchronous transmission of nine users

Although the cross-correlation properties of Gold codes defined above apply for the case of synchronous transmission, where all the codes are transmitted in fixed time frames, the performance of a system using Gold codes of these correlation values is very close to the corresponding random values in a purely asynchronous transmission case. Let us take the case of nine users, as an example. At the receiver, we have eight cross-correlation function taking value -1 for four of them, value -5 for two of them and value 3 for the last two. The autocorrelation value is 7. So, the result is $7-(1*4)-(5*2)+(3*2)=-1$ and corresponds to the simulation value.

3.8.3 Effect of the Spreading Sequence on the Laser-Induced Nonlinearity

In order to study this case, simulations have been carried out for various code sequences and various numbers of users considering the Intermodulation Distortion (IMD) due to LD. The intermodulation to signal ratio versus the modulation index is used to compare system performance.

In Figure 3.22 the IMD to signal ratio for six users and a code sequence length of 127 is shown for m-sequences and m+1 sequences. We see that the difference between the two curves is quite small, which can be explained by the fact that the two families are generated in the same way. However compared with m sequences, m+1 sequences have the advantage of offering a greater number of codes i.e. the possibility to accommodate more users. Figure 3.23 provides the comparison between an m+1 sequence and a Gold code with the same values of parameters. For six users the performance is the same for the m+1 sequences and Gold code.

In Figure 3.24, we increase the number of users to 16 without changing the length of the code sequence. We notice that there is a difference of about 5 dB between the two

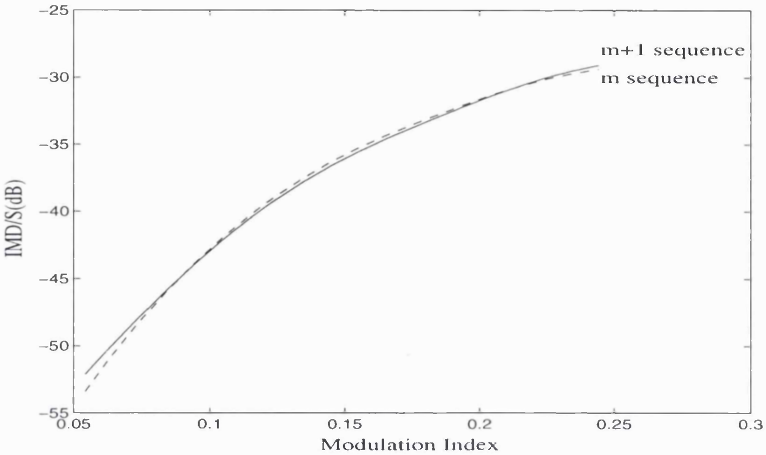

Figure 3.22: Comparison between m-sequence and m+1 sequence for 6 users

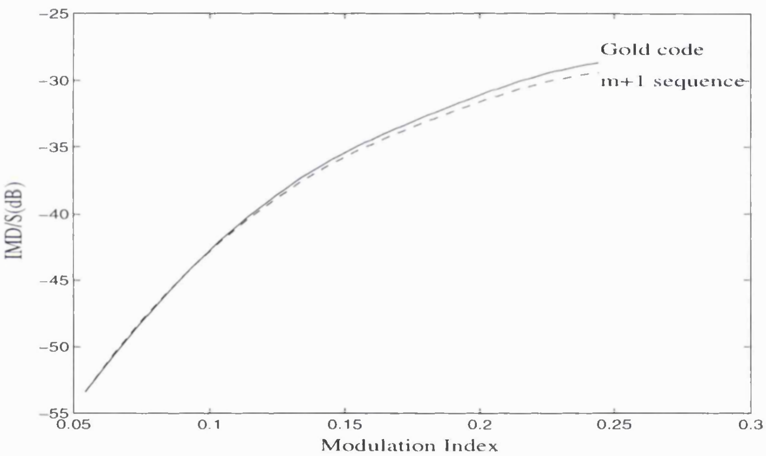

Figure 3.23: Comparison between Gold code and m+1 sequence for 6 users

code sequences and this difference reduces with an increase of the modulation index. From Figure 3.23 and Figure 3.24 we see that the performance of the Gold code is better than the m+1 sequence for a greater number of users. This is because m+1 sequences exhibit high interference rejection properties for synchronous CDMA system but they do not maintain these properties in the case of asynchronous transmission. For example, the 8 chip long m+1 sequences can have cross-correlation as high as 4. Obviously this value is unacceptable for CDMA networks. In contrast, the cross-correlation values of a Gold code in a purely asynchronous transmission case are very

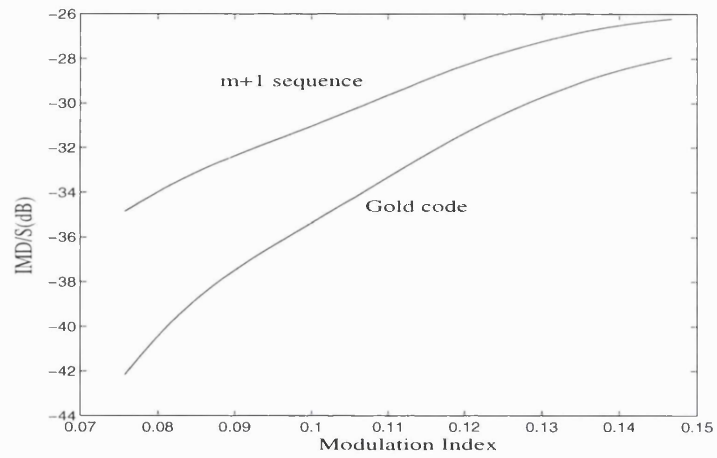

Figure 3.24: Comparison between Gold code and m+1 sequence for 16 users

close to the case of synchronous transmission.

3.9 Summary

In this chapter, a description of the SS technique and its applications has been presented. Among the SS techniques, direct sequence has been explained in more detail as it is the most widely utilised one in practical systems. Moreover, SS/CDMA application for microcellular mobile radio systems has enjoyed increased interest because of its advantages such as potentially large user capacity, effective utilisation of frequency and immunity to multipath fading.

Recently, optical fibre has been widely utilised for the link between a central station and base stations in the mobile radio communication environment. This is because optical fibres provide an inexpensive means of connection and flexible access capability. In addition, it will make possible the delivery of multimedia and broadband services for the mobile/wireless communication systems.

Such a system has been implemented using Alta's SPW simulation framework and simulations have been undertaken to emphasise the properties of CDMA systems such as addressing and multiple access capabilities. In an optical network, the use of a LD produces harmonics and intermodulation terms which will affect the system performance. We have assessed the IMD due to the laser diode for various code sequences. All the results reinforce the fact that Gold code under bipolar correlation are the best amongst the known codes for asynchronous transmission.

In the next chapter, the laser diode nonlinearity model is introduced and this effect is studied for a CDMA network.

Chapter 4

Impact of Laser Nonlinear Effect On Direct Sequence /CDMA Systems: Memoryless Nonlinearity

4.1 Introduction

In the last chapter, we introduced the concept of spread spectrum modulation and the reasons for its use. In particular, we described the use of spread spectrum Code Division Multiple Access (CDMA) transmission over optical fibers for microcellular mobile communications systems. In this system, the mobile asynchronous signals are communicated to the Control Station (CS) by optical communication. The Base Station (BS) is employed as electrical-to-optical converter for the mobiles-to-CS link and as an optical-to-electrical converter for the CS-to-mobiles link. Thus, laser diodes and photodiodes are required for the optical feeder between the CS and the BSs. But the use of a laser diode in such systems leads to the generation of harmonics and/or intermodulation products, which consequently affect the system performance. Moreover, these systems suffer from the near-far problem [43], necessitating the use of power control techniques. These techniques cannot be perfectly accomplished in practical systems, leading to performance deterioration due to the nonoptimal performance of the correlation receiver under these circumstances [44].

In this chapter, the impact of imperfect power control on an asynchronous direct sequence code division multiple access (DS/CDMA) system employing optical transmission and its influence on the bit-error-rate is studied taking into account the nonlinearity of the Laser Diode (LD). This chapter is organised as follows. First, the laser nonlinearity model used is presented. Then, the nonlinear effect on CDMA system is discussed. In section 4.3, the nonlinear effect on CDMA systems with unequal power is derived and the performance of the system is evaluated using the derived bit-error-rate with comparaison between the ideal case and the practical case for both BPSK and QPSK based systems. Finally, the results obtained are compared to those of FDMA systems.

4.2 Laser Diode Nonlinearity

4.2.1 Introduction

Whenever a number of signals pass through a nonlinear device, energy is transferred to frequencies that are sums and differences of the original frequency. For the case of a semiconductor laser, InterModulation Products (IMP) originate from three distinct nonlinear effects [45].

The first source of IMP's is the nonlinearity of the laser power-current curve, which can be caused by leakage current and other effects not included in the laser rate equation solutions. These IMP's can be calculated using a power series expansion of the laser

P-I curve around the bias point. The optical power of second and third-order IMPs relative to the fundamental carrier are then proportional to d^2L/dI^2 and d^3L/dI^3, respectively.

In addition to the static nonlinearity, a semiconductor laser exhibits dynamic nonlinearity that is caused by the interaction of photons and electrons in the laser cavity. This effect is well described by the laser rate equations. Using a small-signal analysis of the laser rate equations, Lau and Yariv [46] first showed that the calculated two-tone third order IMD for a GaAs laser match well with experimental data. Their results were later extended to InGaAsP lasers [47]. Although the closed-form analysis is restricted to two closely spaced microwave carriers, the result shows clearly the frequency-dependent nonlinear characteristics. The analysis shows that the nonlinear distortion becomes larger when the modulating frequencies are closer to the resonance frequency.

Finally, the last source of IMP's is the clipping effect which occurs when the instant driving current swings occasionally below the Laser Diode (LD) threshold current. This last phenomenon commonly occurs when the LD is modulated by a sum of large number of signals, and consequently leads to the generation of IMP's.

Figure 4.1 shows the IMP's for a laser diode modulated by three signals at frequencies f_1, f_2 and f_3. The resulting distortion limits the performance of communication systems [48].

In our system, for the link between the base station and the control station, the sum of all the Spread Spectrum electrical signals is used to modulate the optical intensity of the LD. The nonlinear characteristics of a LD produces intermodulation terms which influence the system performance.

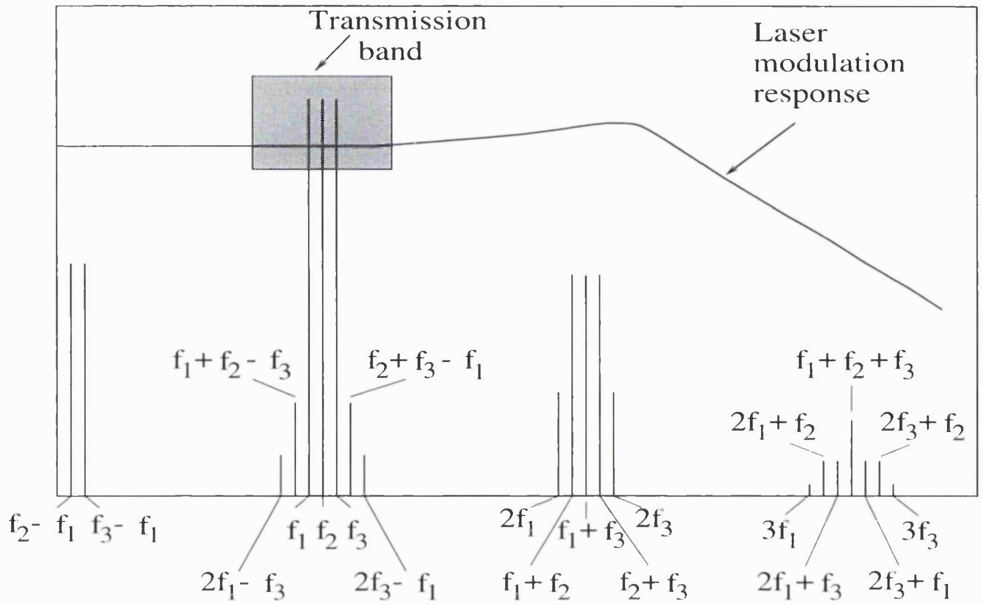

Figure 4.1: Sidebands and harmonics generated by a three-tone modulation of a laser diode

4.2.2 Nonlinearity Without Memory

An important concept in nonlinear theory is the concept of a "memoryless nonlinearity" which occurs when the output signal is an instantaneous function of its input. As a consequence the distortion is frequency independent, as opposed to a nonlinearity with "memory" where the distortion is frequency dependent. For this latter case and when the distortion is weak, the nonlinearity is best represented by a Volterra functional series. This situation can pertain for subcarrier multiplexing (SCM)/ CDMA systems and will be studied in the next chapter.

In our present case, a third-order polynomial without memory is used to represent LD nonlinearity [3]. As shown in [49], a nonlinear LD without memory can be represented by a third-order polynomial as

$$P = A + P_t(S + A_2 S^2 + A_3 S^3) \tag{4.1}$$

where P is the output optical power modulated by the current signal S, P_t the average transmitting optical power, and A, A_2, and A_3 are constants related to the characteristics of the laser diode used. For an ideal laser diode, A_2 (the 2^{nd} order IMD) and A_3 (the 3^{rd} order IMD) are equal to zero. The optical power output is proportional to the modulating signals and can be expressed by

$$P(t) = P_t\Big(1 + m_0 S\Big) \tag{4.2}$$

where m_0 is the modulation index for the case when all the mobile users transmit the same power and is given by

$$m_0 = \frac{\hat{P}}{< P >} \tag{4.3}$$

where $\hat{P}$ is the average output power and $< P >$ is the peak power of the modulating signal. Figure 4.2 shows the ideal power output against current characteristic for a sinusoidal modulation of an injection laser.

For a practical nonlinear LD, A_2 and A_3 in equation (4.1) are not equal to zero; harmonics or intermodulation products, which are combination of the original frequencies, are generated and energy is more or less transferred on them and degrades the system performance. A_2 induces the zero and double frequency components, and A_3 induces the common and triple frequency components. If the transmission band is limited to a single octave, the second-order distortion can be ignored and only one harmonic of the third-order term influences the system performance. Since in the CDMA case only one harmonic of third-order intermodulation term influences the system performance, therefore A_2 is disregarded, reducing equation (4.1) to

$$P(t) = P_t(1 + S + A_3 S^3) \tag{4.4}$$

In the next section, the term induced by the 3^{rd} order intermodulation is derived.

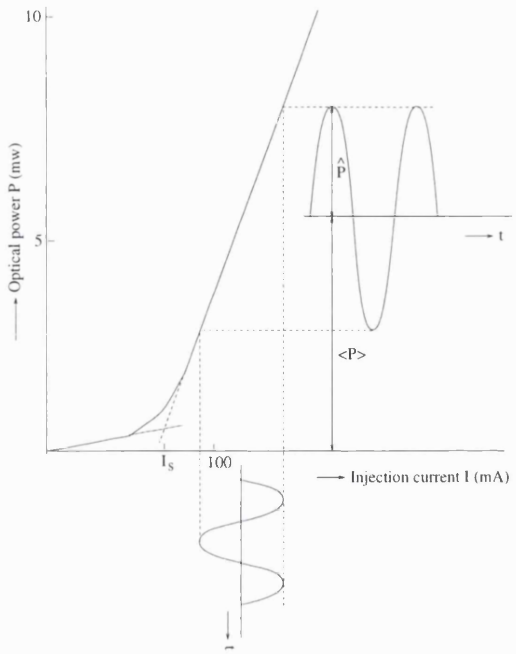

Figure 4.2: Idealized conversion from an electrical sinusoid into an optical sinusoid

4.2.3 Third-Order Intermodulation

We consider a DS/SS multiple access system with Binary Phase Shift Keying (BPSK) signaling (see Figure 4.3). The k^{th} mobile user that transmits data continuously and asynchronously is presented by the SS signal $s_k(t-\tau_k)$ as

$$s_k(t-\tau_k) = d_k(t-\tau_k)a_k(t-\tau_k)\cos(\omega_c t+\phi_k), \qquad (k=1,2,...,K) \tag{4.5}$$

where ω_c is the common center frequency, ϕ_k $(0 \le \phi_k \le 2\pi)$ is the phase of the k^{th} carrier, τ_k $(0 \le \tau_k \le T)$ is the time delay of the k^{th} user, and T is the bit duration. The bit data stream of the k^{th} user is given by

$$d_k(t) = \sum_{\ell=-\infty}^{\infty} d_\ell^{(k)} p_T(t-\ell T); \qquad d_\ell^{(k)} \in \{-1,1\} \tag{4.6}$$

where $d_\ell^{(k)}$ is a bit data value in the interval $[\ell T, (\ell+1)T]$, and

$$p_T(t) = \begin{cases} 1 & 0 \le t \le T \\ 0 & \text{otherwise} \end{cases} \tag{4.7}$$

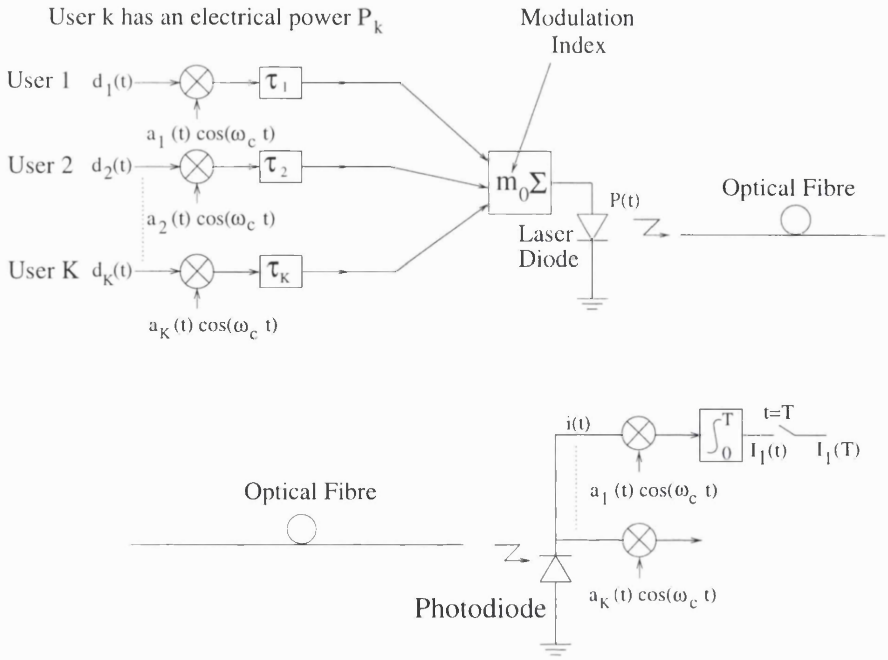

Figure 4.3: BPSK CDMA System Model in Optical Transmission

Each carrier is phase and amplitude coded by a waveform $a_k(t)$ given by

$$a_k(t) \;=\; \sum_{n=-\infty}^{\infty} a_n^{(k)} p_{T_c}(t-nT_c); \qquad a_n^{(k)} \in \{-1,1\} \tag{4.8}$$

where $a_n^{(k)}$ is a periodic binary sequence. Each bit is assumed to be encoded with N chips ($T = NT_c$). When the laser is modulated by a sum of SS signals, the optical power output of the laser is given using Equations (4.5) and (4.4) by

$$P(t) \;=\; P_t\left(1 + m_0\sum_{k=1}^{K} s_k(t-\tau_k) + A_3 m_0^3\Big(\sum_{k=1}^{K} s_k(t-\tau_k)\Big)^3\right) \tag{4.9}$$

Using the following relation

$$\begin{aligned}\left[\sum_{k=1}^{K} x_k\right]^3 \;&=\; \sum_{k=1}^{K} x_k^3 + 3x_1^2\sum_{k=2}^{K} x_k + 3x_1\sum_{k=2}^{K} x_k^2 \\ &\quad +3\sum_{j=2}^{K}\sum_{\substack{k=2\\k\neq j}}^{K} x_j^2 x_k + 3x_1\sum_{j=2}^{K}\sum_{\substack{k=2\\k\neq j}}^{K} x_j x_k + \sum_{i=2}^{K}\sum_{\substack{j=2\\j\neq i}}^{K}\sum_{\substack{k=2\\k\neq i,j}}^{K} x_i x_j x_k \end{aligned} \tag{4.10}$$

and noticing $d_k^2(t-\tau_k) = c_k^2(t-\tau_k) = 1$, the contribution of the third-order at ω_c gives for the different terms of 4.10

$$\frac{3}{4} m_0^3 \sum_{k=1}^{K} d_k(t-\tau_k)a_k(t-\tau_k)\cos(\omega_c t + \phi_k) \tag{4.11}$$

$$\frac{3}{2}m_0^3\sum_{k=2}^{K} d_k(t-\tau_k)a_k(t-\tau_k)\Big[\cos(\omega_c t+\phi_k)+\frac{\cos(\omega_c t+2\phi_1-\phi_k)}{2}\Big] \tag{4.12}$$

$$\frac{3}{2}m_0^3 d_1(t-\tau_1)a_1(t-\tau_1)\sum_{k=2}^{K}\Big[\cos(\omega_c t+\phi_1)+\frac{\cos(\omega_c t+2\phi_k-\phi_1)}{2}\Big] \tag{4.13}$$

$$\frac{3}{2}m_0^3\sum_{j=2}^{K}\sum_{\substack{k=2\\k\neq j}}^{K} d_k(t-\tau_k)a_k(t-\tau_k)\Big[\cos(\omega_c t+\phi_k)+\frac{\cos(\omega_c t+2\phi_j-\phi_k)}{2}\Big] \tag{4.14}$$

$$\frac{3}{4}m_0^3 d_1(t-\tau_1)a_1(t-\tau_1)\sum_{j=2}^{K}\sum_{\substack{k=2\\k\neq j}}^{K} d_j(t-\tau_j)d_k(t-\tau_k)a_j(t-\tau_j)a_k(t-\tau_k)$$
$$\Big[\cos(\omega_c t+\phi_1+\phi_j-\phi_k)+\cos(\omega_c t+\phi_1-\phi_j+\phi_k)+\cos(\omega_c t-\phi_1+\phi_j+\phi_k)\Big] \tag{4.15}$$

$$\frac{1}{4}m_0^3\sum_{i=2}^{K}\sum_{\substack{j=2\\j\neq i}}^{K}\sum_{\substack{k=2\\k\neq i,j}}^{K} d_i(t-\tau_i)d_j(t-\tau_j)d_k(t-\tau_k)a_i(t-\tau_i)a_j(t-\tau_j)a_k(t-\tau_k)$$
$$\Big[\cos(\omega_c t+\phi_i+\phi_j-\phi_k)+\cos(\omega_c t+\phi_i-\phi_j+\phi_k)+\cos(\omega_c t-\phi_i+\phi_j+\phi_k)\Big] \tag{4.16}$$

After rearranging, we can now present the LD output as

$$P(t)=P_t\left[\sum_{m=0}^{6} X_m(t)\right] \tag{4.17}$$

where

$$X_0(t)=\left[m_0+\frac{A_3 m_0^3(6K-3)}{4}\right]d_1(t-\tau_1)a_1(t-\tau_1)\cos(\omega_c t+\phi_1) \tag{4.18}$$

$$X_1(t)=\frac{3A_3 m_0^3}{4}\sum_{k=2}^{K} d_1(t-\tau_1)a_1(t-\tau_1)\cos(\omega_c t+2\phi_k-\phi_1) \tag{4.19}$$

$$X_2(t) = \left[m_0 + \frac{A_3 m_0^3(6K-3)}{4}\right] \sum_{k=2}^{K} d_k(t-\tau_k)a_k(t-\tau_k)\cos(\omega_c t + \phi_k) \tag{4.20}$$

$$X_3(t) = \frac{3A_3 m_0^3}{4} \sum_{k=2}^{K} d_k(t-\tau_k)a_k(t-\tau_k)\cos(\omega_c t + 2\phi_1 - \phi_k) \tag{4.21}$$

$$X_4(t) = \frac{3A_3 m_0^3}{4} \sum_{j=2}^{K} \sum_{\substack{k=2 \\ k\neq j}}^{K} d_k(t-\tau_k)a_k(t-\tau_k)\cos(\omega_c t + 2\phi_j - \phi_k) \tag{4.22}$$

$$\begin{aligned} X_5(t) = \frac{3A_3 m_0^3}{4} \sum_{j=2}^{K} \sum_{\substack{k=2 \\ k\neq j}}^{K} & d_1(t-\tau_1)d_j(t-\tau_j)d_k(t-\tau_k)a_1(t-\tau_1)a_j(t-\tau_j)a_k(t-\tau_k) \\ & \left[\cos(\omega_c t + \phi_1 + \phi_j - \phi_k) + \cos(\omega_c t + \phi_1 - \phi_j + \phi_k) + \cos(\omega_c t - \phi_1 + \phi_j + \phi_k)\right] \end{aligned} \tag{4.23}$$

$$\begin{aligned} X_6(t) = \frac{A_3 m_0^3}{4} \sum_{i=2}^{K} \sum_{\substack{j=2 \\ j\neq i}}^{K} \sum_{\substack{k=2 \\ k\neq i,j}}^{K} & d_i(t-\tau_i)d_j(t-\tau_j)d_k(t-\tau_k)a_i(t-\tau_i)a_j(t-\tau_j)a_k(t-\tau_k) \\ & \left[\cos(\omega_c t + \phi_i + \phi_j - \phi_k) + \cos(\omega_c t + \phi_i - \phi_j + \phi_k) + \cos(\omega_c t - \phi_i + \phi_j + \phi_k)\right] \end{aligned} \tag{4.24}$$

At the receiver, the combined desired and interference terms are demodulated as

$$Z_1 = (\eta P_r) \int_{\tau_1}^{T+\tau_1} \sum_{m=0}^{6} X_m(t) a_1(t-\tau_1)\cos(\omega t + \phi_1)dt \tag{4.25}$$

Then, the desired signal is presented as

$$\begin{aligned} D_1 &= d_{1,0}\frac{T}{2}(\eta P_r)\left[m_0 + \frac{A_3 m_0^3(6K-3)}{4}\right] \\ &\cong d_{1,0}\frac{T}{2}(\eta P_r m_0) \end{aligned} \tag{4.26}$$

Calculating the interference of 4.25, the statistical expectations must be computed over all Random Variable (R.V.) parameters in 4.25, which are the phase shifts, time delays and data symbols. These R.V. can be considered as mutually independent. It can be assumed that ϕ_i, ϕ_j and ϕ_k are uniformly distributed on the interval $[0, \pi]$ and τ_i, τ_j and τ_k are independent zero mean random variables that take values +1 or −1 with equal probability. The mean square of the interference, then, can be derived as

$$\left\langle I^2 \right\rangle = (\eta P_r)^2 \left(\sum_{m=1}^{6} \tilde{I}_m \right) \tag{4.27}$$

where

$$\tilde{I}_m = E \left\langle \int_0^T [X_m(t_1)] a_1(t_1) \cos \omega_c t_1 dt_1 \int_0^T [X_m(t_2)] a_1(t_2) \cos \omega_c t_2 dt_2 \right\rangle \tag{4.28}$$

We get

$$\tilde{I}_1 = \left(\frac{A_3 m_0^3}{4} \right)^2 \frac{9T^2}{8} (K-1) \tag{4.29}$$

$$\tilde{I}_2 = \left[m_0 + \frac{A_3 m_0^3 (6K-3)}{4} \right]^2 \frac{T^2}{24N^3} \sum_{k=2}^{K} r_{k,1} \tag{4.30}$$

$$\tilde{I}_3 = \left(\frac{A_3 m_0^3}{4} \right)^2 \frac{3T^2}{8N^3} \sum_{k=2}^{K} r_{k,1} \tag{4.31}$$

$$\tilde{I}_4 = \left(\frac{A_3 m_0^3}{4} \right)^2 \frac{3(K-2)T^2}{8N^3} \sum_{k=2}^{K} r_{k,1} \tag{4.32}$$

where $r_{k,1}$ is the multi-user interference (MUI) which expression is given in Appendix A.

For evaluating $\tilde{I}_5$, it is convenient to consider the following relation

$$q_k(t_1, t_2) = \frac{1}{T} \int_0^T a_k(t_1 - \tau_k) a_k(t_2 - \tau_k) E < d_k(t_1 - \tau_k) d_k(t_2 - \tau_k) > d\tau_k \tag{4.33}$$

with some user k. It has been shown in [50] that $q_k(t_1, t_2)$ is given as

$$q_k(t_1, t_2) = \frac{1}{T}\hat{R}_k(|t_1 - t_2|) \tag{4.34}$$

where $\hat{R}_k(\tau)$ for $0 \leq lT_c \leq \tau \leq (l+1)T_c \leq T$ is the continuous-time partial auto-correlation defined in [51] by

$$\hat{R}_k(\tau) = C_k(l)T_c + [C_k(l+1) - C_k(l)](\tau - lT_c) \tag{4.35}$$

Using (4.34) and average over the phase shifts ϕ_j and ϕ_k, $\tilde{I}_5$ can now be written as

$$\tilde{I}_5 = \left(\frac{A_3 m_0^3}{4}\right)^2 \frac{45}{8T^2} \sum_{j=2}^{K} \sum_{\substack{k=2 \\ k\neq j}}^{K} \int_0^T \int_0^T d_1(t_1)d_1(t_2)\hat{R}_j(|t_1 - t_2|)\hat{R}_k(|t_1 - t_2|)dt_1 dt_2 \tag{4.36}$$

Making a change of variables, $u = t_1 - t_2$ and averaging over data d_1, (4.36) can be found to be

$$\begin{aligned} \tilde{I}_5 &= \left(\frac{A_3 m_0^3}{4}\right)^2 \frac{45}{8T^2} \sum_{j=2}^{K} \sum_{\substack{k=2 \\ k\neq j}}^{K} \int_0^T \int_u^T \hat{R}_j(u)\hat{R}_k(u)dt_1 du \\ &+ \int_{-T}^{0} \int_{-u}^{T} \hat{R}_j(-u)\hat{R}_k(-u)dt_1 du \end{aligned} \tag{4.37}$$

Substituting (4.35) into (4.37), finally, (4.37) can be obtained as

$$\tilde{I}_5 = \left(\frac{A_3 m_0^3}{4}\right)^2 \frac{15T^2}{8N^4} \sum_{j=2}^{K} \sum_{\substack{k=2 \\ k\neq j}}^{K} r_{j,k} \tag{4.38}$$

where

$$r_{j,k} = \sum_{l=1-N}^{N-1} \left(N - l - \frac{1}{2}\right)(C_j(l)C_k(l) + C_j(l+1)C_k(l+1) + C_j(l)C_k(l+1)) \tag{4.39}$$

For random code, it is $r_{j,k} = 2N^2$.

In the same method, $\tilde{I}_6$ can now be presented as

$$\tilde{I}_6 = \left(\frac{A_3 m_0^3}{4}\right)^2 \frac{3T^2}{80N^5} \sum_{i=2}^{K} \sum_{\substack{j=2 \\ j\neq i}}^{K} \sum_{\substack{k=2 \\ k\neq i,j}}^{K} r_{i,j,k} \tag{4.40}$$

where

$$\begin{aligned} r_{i,j,k} &= \sum_{l=1-N}^{N-1} 4C_1(l)C_i(l)C_j(l)C_k(l) + 3C_1(l)C_i(l+1)C_j(l)C_k(l) \\ &+ 2C_1(l)C_i(l+1)C_j(l+1)C_k(l) + C_1(l)C_i(l+1)C_j(l+1)C_k(l+1) \end{aligned} \tag{4.41}$$

For random code, $r_{i,j,k} = 4N^4$.

4.3 The Effect of Imperfect Power Control on CDMA Systems

4.3.1 Near Far Problem

The reverse link of a CDMA system is usually asynchronous, in the sense that the arrival times for each user's code are different. This means that the receiver for each user will observe interference from all other users in the system, since the transmitted codes will not be orthogonal. Hence, the number of users that can be simultaneously accommodated in one cell is interference-limited.

A corollary to the above is that if the power of each user within a cell is not controlled such that they do not appear equal at the base station receiver, then the near-far problem occurs.

The near-far problem occurs when many mobile users share the same channel. In general, the strongest received mobile signal will capture the demodulation at a base station. In CDMA, stronger received signal levels raise the noise floor at the base station demodulators for the weaker signals, thereby decreasing the probability that the weaker signal will be received. To combat the near-far problem, power control is used in most CDMA implementations. Power control is provided by each base station in a cellular system and ensures that each mobile within the base station coverage area provides the same signal level to the base station receiver. This solves the problem of a nearby subscriber overpowering the base station receiver and drowning out the signals of far away subscribers.

Two methods are used for power control

- coarse power control (open loop)- mobile adjusts power based on the power received on the pilot tone.

- fine control (close loop)- base sends commands at the rate of 800 bps to continuously adjust the power, adjusting the power in steps of 1 dB.

The purpose of power control is to ensure that the received signal strengths of all users are equal. However, this cannot be accomplished perfectly with practical systems, resulting in capacity loss due to the nonoptimal performance of the correlation receiver under these circumstances. In what follows, this effect on CDMA system and its influence on the BER taking into account the nonlinearity of the laser diode is studied.

4.3.2 Case of BPSK System

System Model

We consider a DS/SS multiple access system with binary phase shift keying (BPSK) signaling and a correlation receiver based on [52]. There are K users in the system. The k^{th} user that transmits data continuously and asynchronously is represented by the SS signal $s_k(t-\tau_k)$ as

$$\sqrt{2P_k}\, s_k(t-\tau_k) \quad = \quad \sqrt{2P_k}\, d_k(t-\tau_k)a_k(t-\tau_k)\cos(\omega_c t+\phi_k) \tag{4.42}$$

$(k = 1, 2, ..., K)$ and where ω_c is the common center frequency, ϕ_k $(0 \leq \phi_k \leq 2\pi)$ is the phase of the k^{th} carrier, τ_k $(0 \leq \tau_k \leq T)$ is the time delay of the k^{th} user, P_k is the electrical power of the k^{th} user, and T is the bit duration. For this generalised case where the CDMA signal powers are unequal due to the imperfect power control, we introduce the parameter m_k defined as

$$m_k = \frac{\hat{P}_k}{< P >} \tag{4.43}$$

where $\hat{P}_k$ is the amplitude power of the k^{th} user modulating signal. Substituting equation (4.3) into equation (4.43) yields

$$m_k = m_0 \frac{\hat{P}_k}{\hat{P}} = m_0 p_k \tag{4.44}$$

where p_k is a factor proportional to the k^{th} user output optical power $\hat{P}_k$ which in turn is proportional to the modulating electrical current $\sqrt{2P_k}$ of the k^{th} user. Therefore, the optical power output for the generalized case of all users having unequal power is given by

$$P(t) \;=\; P_t\Big(1 + m_0 \sum_{k=1}^{K} p_k s_k(t-\tau_k) + A_3 m_0^3 \Big(\sum_{k=1}^{K} p_k s_k(t-\tau_k)\Big)^3\Big) \qquad (4.45)$$

P_k is assumed to be log-normally distributed according to [53]. This distribution is given by

$$f_{P_k}(P_k) \;=\; \frac{10\log(e)}{\sqrt{2\pi}\sigma_P P_k}\exp\Big(-\frac{(10\log P_k)^2}{2\sigma_P^2}\Big) \qquad (4.46)$$

where σ_P is the standard deviation of the k^{th} power. In the next section, the term induced by the 3^{rd} order intermodulation is derived.

Intermodulation Terms

As has been shown earlier, only the third-order intermodulation is of interest as it is the only term that creates the interference components. The third-order IMD is generated by the cubic term in equation (4.45). This cubic term can be expanded using the formula 4.10.

Noticing that $[d_k(t-\tau_k)]^2 = [a_k(t-\tau_k)]^2 = 1$, eliminating zero, double and triple frequency components, and after algebraic calculations, equation (4.45) yields an expression for the optical power given by

$$P(t) \;=\; P_t\Big(\sum_{m=0}^{6} X_m(t)\Big) \qquad (4.47)$$

where

$$X_0(t) = d_1(t-\tau_1)a_1(t-\tau_1)\cos(\omega t + \phi_1)\Big[\frac{3}{2}A_3 m_0^3 p_1\Big[\sum_{k=2}^{K} p_k^2 + \frac{p_1^2}{2}\Big] + m_0 p_1\Big] \qquad (4.48)$$

$$X_1(t) = \frac{3A_3 m_0^3 p_1}{4} d_1(t-\tau_1)a_1(t-\tau_1)\sum_{k=2}^{K} p_k^2 \cos(\omega_c t + 2\phi_k - \phi_1) \qquad (4.49)$$

$$\begin{aligned} X_2(t) &= \sum_{k=2}^{K} d_k(t-\tau_k)a_k(t-\tau_k)\cos(\omega_c t+\phi_k)\Big(\frac{3}{4}A_3 m_0^3 p_k^3 + m_0 p_k(1+3/2A_3 m_0^2 p_1^2)\Big) \\ &+\frac{3A_3}{2}\sum_{j=2}^{K}\sum_{\substack{k=2\\k\neq j}}^{K} m_0^3 p_j^2 p_k d_k(t-\tau_k)a_k(t-\tau_k)\cos(\omega_c t+\phi_k) \end{aligned} \tag{4.50}$$

$$X_3(t) = \frac{3A_3 m_0^3 p_1^2}{4}\sum_{k=2}^{K} p_k d_k(t-\tau_k)a_k(t-\tau_k)\cos(\omega_c t+2\phi_1-\phi_k) \tag{4.51}$$

$$X_4(t) = \frac{3A_3 m_0^3}{4}\sum_{j=2}^{K}\sum_{\substack{k=2\\k\neq j}}^{K} p_j^2 p_k d_k(t-\tau_k)a_k(t-\tau_k)\cos(\omega_c t+2\phi_j-\phi_k) \tag{4.52}$$

$$\begin{aligned} X_5(t) &= \frac{3A_3}{4}m_0^3 p_1 d_1(t-\tau_1)a_1(t-\tau_1)\sum_{j=2}^{K}\sum_{\substack{k=2\\k\neq j}}^{K} p_j p_k d_j(t-\tau_j)d_k(t-\tau_k)a_j(t-\tau_j)a_k(t-\tau_k) \\ &\Big[\cos(\omega_c t+\phi_1+\phi_j-\phi_k)+\cos(\omega_c t+\phi_1-\phi_j+\phi_k)+\cos(\omega_c t-\phi_1+\phi_j+\phi_k)\Big] \end{aligned} \tag{4.53}$$

$$\begin{aligned} X_6(t) &= \frac{A_3 m_0^3}{4}\sum_{i=2}^{K}\sum_{\substack{j=2\\j\neq i}}^{K}\sum_{\substack{k=2\\k\neq i,j}}^{K} p_i p_j p_k d_i(t-\tau_i)d_j(t-\tau_j)d_k(t-\tau_k)a_i(t-\tau_i)a_j(t-\tau_j)a_k(t-\tau_k) \\ &\Big[\cos(\omega_c t+\phi_i+\phi_j-\phi_k)+\cos(\omega_c t+\phi_i-\phi_j+\phi_k)+\cos(\omega_c t-\phi_i+\phi_j+\phi_k)\Big] \end{aligned} \tag{4.54}$$

At the receiver, the desired and the interference terms are demodulated as

$$Z_1 = \int_{\tau_1}^{T+\tau_1}\Big(\eta P_r\sum_{m=0}^{6} X_m(t)+N_{op}(t)\Big)a_1(t-\tau_1)\cos(\omega t+\phi_1)dt \tag{4.55}$$

where P_r is the average received optical power, η is the photodiode responsivity figure and $N_{op}(t)$ is the optical device noise. Since only relative delays and phase angles are important, we may set $\tau_1=\phi_1=0$. The parameters τ_k and ϕ_k are then the time delay and phase angle for the k^{th} signal relative to the first.

Without loss of generality, the signal from user 1 is assumed to be received and is presented as

$$Z_1 = R_1+\tilde{I}_m+N \tag{4.56}$$

where R_1 is the required term, $\tilde{I}_m$ is the unwanted interference I_m, and N is the noise term.

The random variables, which are the phase shifts, time delays and data symbols, are considered mutually independent. It can be assumed that ϕ_i, ϕ_j and ϕ_k are uniformly distributed in the interval $[0, 2\pi]$, and τ_i, τ_j and τ_k are uniformly distributed in the interval $[0, T]$. Also, all data symbols are independent zero mean random variables that take values +1 or -1 with equal probability. After demodulation at the receiver, and with some algebraic manipulation, the mean-square of the desired signal and the mean square of the interference can be derived in a similar way to [54] and are given respectively by

$$R_1^2 = (\eta P_r)^2 (T m_0)^2/4 \int_0^\infty x^2 p(x)dx \tag{4.57}$$

where $p(x)$ is the probability density function of $\sqrt{P_k}$ which distribution can be derived using the distribution of P_k given by equation (4.46).

The mean-square of the interference can be derived as

$$\langle I^2 \rangle = (\eta P_r)^2 \Big(\sum_{m=1}^{6} \langle \tilde{I}_m^2 \rangle \Big) \tag{4.58}$$

where

$$\begin{aligned}\langle \tilde{I}_m^2 \rangle = {} & E\Big\langle \int_0^T X_m(t_1) a_1(t_1) \cos(\omega_c t_1) dt_1 \\ & \int_0^T X_m(t_2) a_1(t_2) \cos(\omega_c t_2) dt_2 \Big\rangle\end{aligned} \tag{4.59}$$

For the different terms, we get

$$\langle \tilde{I}_1^2 \rangle = (\eta P_r)^2 \frac{1}{2} (K-1) \Big(\frac{3 A_3 m_0^3 T}{8} \Big)^2 \int_0^\infty x^2 p(x)dx \int_0^\infty y^2 p(y)dy \tag{4.60}$$

here $y = x^2$ defines the probability density function of P_k that is given by equation (4.46)

$$\langle \tilde{I}_2^2 \rangle = (\eta P_r)^2 \frac{m_0^2}{8} \frac{2(K-1)T^2}{3N} \Big(\int_0^\infty x^2 p(x)dx + \Big(\frac{3 A_3 m_0^2}{4} \Big)^2 \int_0^\infty z^2 p(z)dz$$

$$
+\frac{3}{2}A_3m_0^2\int_0^\infty y^2p(y)dy+(K-1)3A_3m_0^2\Big(\int_0^\infty x^2p(x)dx\Big)^2
+K(K-1)\frac{9A_3^2m_0^4}{4}\int_0^\infty x^2p(x)dx\int_0^\infty y^2p(y)dy\Big) \tag{4.61}
$$

here $z = x^3$ and p(z) can be derived using $p(z) = p(x)dx/dz$.

$$
\langle \tilde{I}_3^2\rangle = (\eta P_r)^2\frac{3A_3^2m_0^6(K-1)T^2}{64N}\int_0^\infty x^2p(x)dx\int_0^\infty y^2p(y)dy \tag{4.62}
$$

$$
\langle \tilde{I}_4^2\rangle = (\eta P_r)^2\frac{3A_3^2m_0^6(K-1)(K-2)T^2}{64N}\int_0^\infty x^2p(x)dx\int_0^\infty y^2p(y)dy \tag{4.63}
$$

$$
\langle \tilde{I}_5^2\rangle = (\eta P_r)^2\Big(\frac{A_3m_0^3}{4}\Big)^2\frac{15T^2}{4N}(K-1)(K-2)\Big(\int_0^\infty x^2p(x)dx\Big)^3 \tag{4.64}
$$

and

$$
\langle \tilde{I}_6^2\rangle = (\eta P_r)^2\Big(\frac{A_3m_0^3}{4}\Big)^2\frac{3T^2}{20N}(K-1)(K-2)(K-3)\Big(\int_0^\infty x^2p(x)dx\Big)^3 \tag{4.65}
$$

In the following section, the above derived interference terms are used to evaluate the system performance.

System Performance

Beside the nonlinear effect, at the transmitter, the LD output has an intensity fluctuation that is presented by

$$
\langle I_{LD}^2\rangle = RIN(\eta P_r)^2 \tag{4.66}
$$

where RIN accounts for the optical reflections of the system into the LD that causes the output light to fluctuate in amplitude. Multiple access systems are particularly sensitive to it. RIN runs typically between -110 dB/Hz and -150 dB/Hz, depending strongly on how well isolated is the LD. The shot noise variance in a CDMA optical fiber communication system contains the noise components that basically depend on the entire input data sequence, and that is the reason that an optical fiber communication system does not conform to the classical communication model, where the noise is assumed to be stationary and additive. Thus

$$\langle I_{shot}^2 \rangle = 2e\eta P_r \tag{4.67}$$

The variance of thermal noise, assuming that it is flat over the desired bandwidth B is given by

$$\langle I_{th}^2 \rangle = \frac{4kT_t}{R_{PD}} \tag{4.68}$$

where k is the Boltzmann's constant, T_t is the absolute temperature in Kelvin, and R_{PD} is load resistance.

The system performance is evaluated with the aid of BER calculation.

For a given bandwidth B, the BER is given by $BER = \frac{1}{2}\text{erfc}\sqrt{\frac{SNR}{2}}$ where the signal-to-noise ratio (SNR) is given by

$$SNR = \frac{\langle I_{sig}^2 \rangle}{\langle I_{Noise}^2 \rangle} = \frac{\langle R_1^2 \rangle}{\langle I^2 \rangle + \langle N_{op}^2 \rangle} \tag{4.69}$$

For the purpose of calculation, the bandwidth has been taken as $30N$ kHz [54].

The power control mechanism for CDMA cellular systems has been tested via field trials, which have shown that received signal power has a log-normal distribution with a standard deviation in the neighbourhood of 1 dB above the desired power setpoint [55]. Hence, results will be generated for $\sigma_P = 1$ dB as the worst case. Using the derived equations, a system with $N = 127$ has been selected. A 1.3 μm laser diode with a RIN intensity noise of -150 dB/Hz and output power of 2 mW has been chosen. The photodiode responsivity is $\eta = 0.8mA/mW$ and the photodiode thermal noise is $I_{th} = 5pA/\sqrt{Hz}$. Figure 4.4 shows the BER versus the modulation index m_0 for an optical power of -40 dBm for selected number of users, K, for the case with ideal power control contrasted to the practical case with imperfect power control ($\sigma_P = 1$ dB).

For the $K = 8$ case, it can be seen that the BER is degraded when m_0 becomes greater than 0.15 whereas for the other cases it is degraded for values of m_0 greater than 0.1. This is due to the noise domination in the region of low m_0. The interference due to the intermodulation terms is substantial at higher values of m_0. Thus, there exists an optimum value of m_0 for which the BER is maximum. With the increase of the number of users, the effect of the imperfect power control is less important. This can be explained by the fact that the interference become more important than the intermodulation.

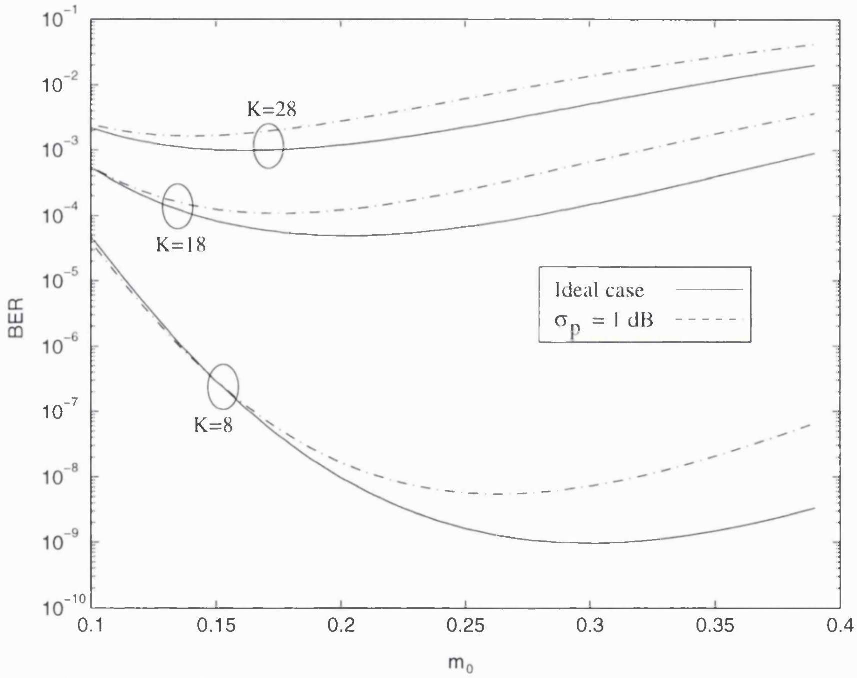

Figure 4.4: Bit-Error-Rate versus the modulation index m_0 for BPSK based systems for different number of users K for the ideal case with perfect power control and the practical case with imperfect power control

Figure 4.5 shows the BER versus the number of users, K, for selected values of the modulation index m_0 for both the ideal case and the case with imperfect power control. It can be easily seen from this figure that when the value of the modulation index is small, e.g. $m_0 = 0.1$, the effect of imperfect power control can yield better results when the number of users is small ($K < 13$). This is because the noise is dominant in this case. For $m_0 = 0.4$, we can see that the BER is less degraded when the number of users increases (values greater than 30).

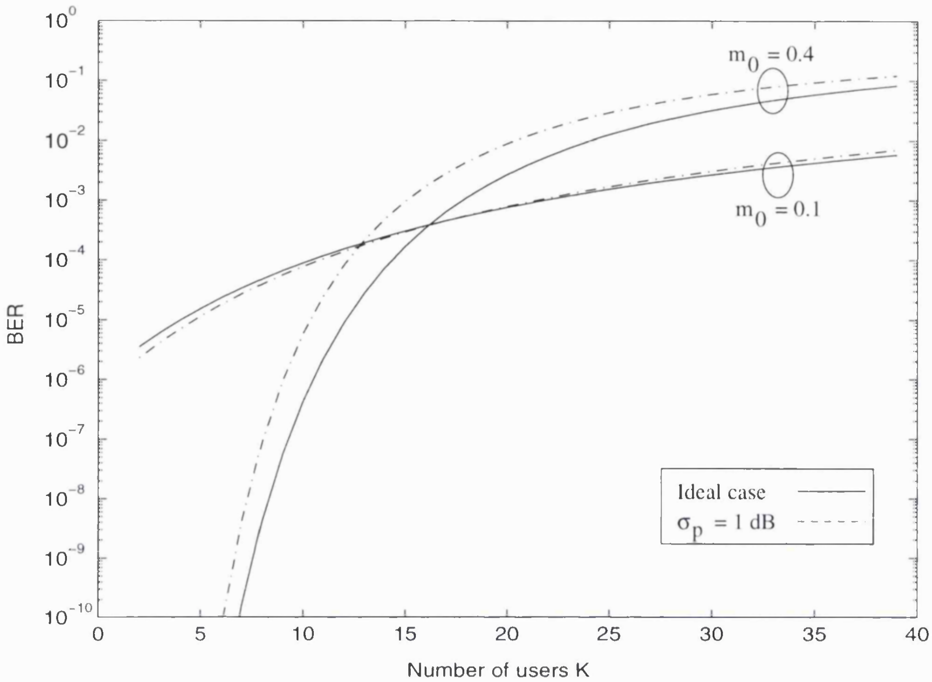

Figure 4.5: Bit-Error-Rate versus the number of users K for BPSK based systems for different values of the modulation index m_0 for the ideal case with perfect power control and the practical case with imperfect power control

4.3.3 Case of QPSK System

Intermodulation Terms

In the case of Quadrature Phase Shift Keying (QPSK), the k^{th} mobile user that transmits data continuously and asynchronously is presented by the Spread-spectrum signal $s_k(t-\tau_k)$ as

$$\begin{aligned} s_k(t-\tau_k) &= \Big(I_k(t-\tau_k)a_{Ik}(t-\tau_k)\cos(\omega_c t+\phi_k) \\ &+ Q_k(t-\tau_k)a_{Qk}(t-\tau_k)\sin(\omega_c t+\phi_k)\Big) \end{aligned} \tag{4.70}$$

with $(k = 1, 2, ..., K)$, $I_k(t)$ and $Q_k(t)$ are baseband bipolar data waveforms representing the in-phase and quadrature data streams respectively, similarly, $a_{Ik}(t)$ and $a_{Qk}(t)$ are two ± 1 sequences occurring at the chip rate and representing spreading codes.

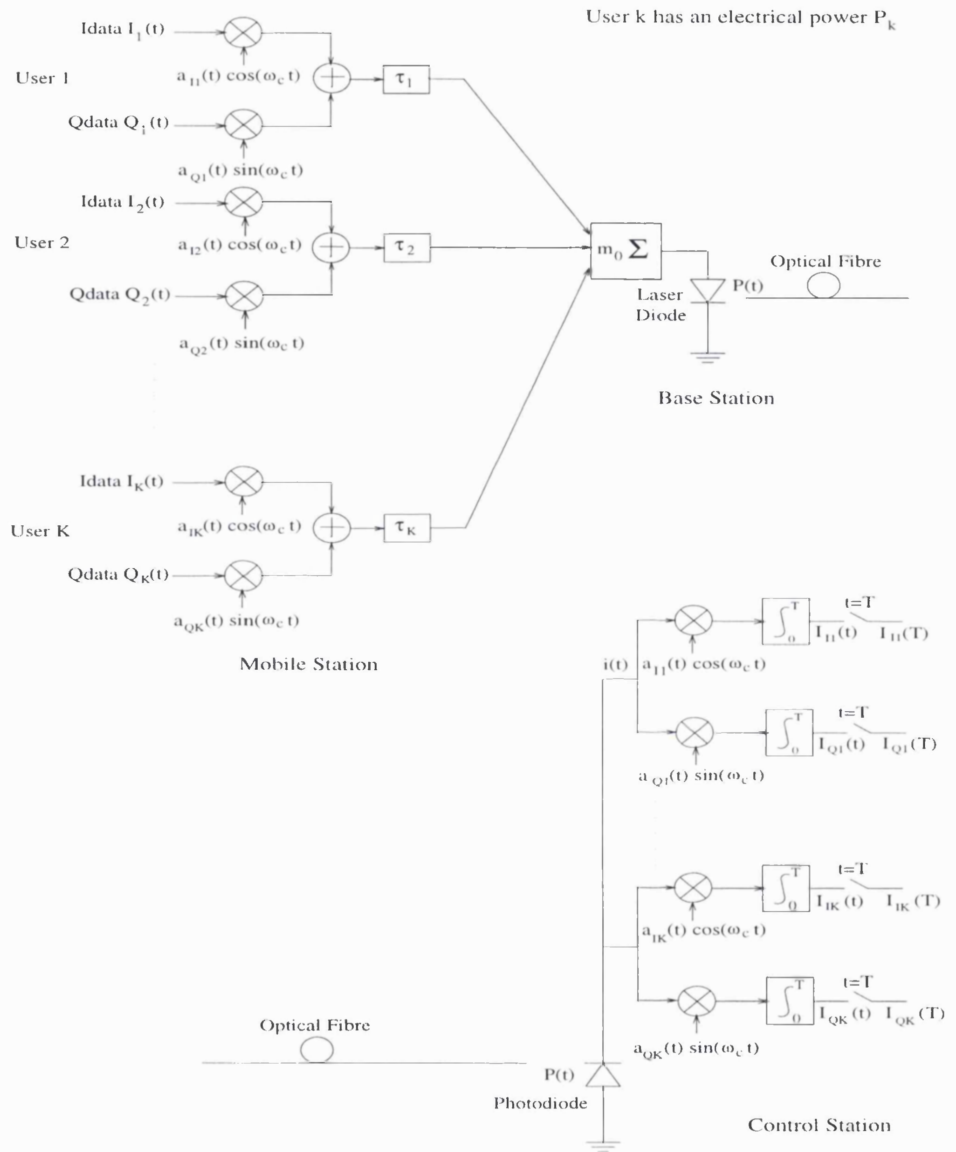

Figure 4.6: QPSK CDMA System Model in Optical Transmission

Because the transmitted signal for a QPSK system can be viewed as the sum of two BPSK signals in quadrature, it is reasonable to expect that demodulation and detection would involve two BPSK receivers or correlators in parallel, one for each quadrature carrier (see Figure 4.6).

The in-phase and quadrature sequences represent alternate bits from the single binary data stream. For the same data rate, the duration of a bit is twice as long in QPSK as it is in BPSK. Therefore, for the same data rate the spreading sequence is double the length of that for BPSK.

In a similar manner to the above BPSK based systems, equations describing the BER for the QPSK based systems have been derived and are presented in Appendix 2.

In the following section, the above derived interference terms are used to evaluate the system performance.

System Performance

Using the derived expressions of the BER of the QPSK based CDMA systems (Appendix 2), Figure 4.7 shows the BER versus the modulation index for the QPSK case with perfect power control, and both BPSK and QPSK cases with imperfect power control for two number of users ($K = 8$ and $K = 18$). For the case $K = 8$, an improvement can be observed for the BER when m_0 becomes greater than 0.2 but in the $K = 18$ case this effect is not present. This is due to the fact that the intermodulation terms become equal in both BPSK and QPSK as the number of users increases.

4.4 CDMA versus FDMA

In a FDMA optical communication system, the laser diode injection current is composed of a dc component plus a number of FM signals occupying separate frequency bands. If the injected current is the sum of equal-amplitude and equal frequency interval FDMA carriers, the optical power output is found and presented exponentially as [2]

$$P(t) = P_t \exp\left(m_0 \sum_{k=1}^{K} \cos\left(\omega_k t + \theta_k(t)\right)\right) \quad (4.71)$$

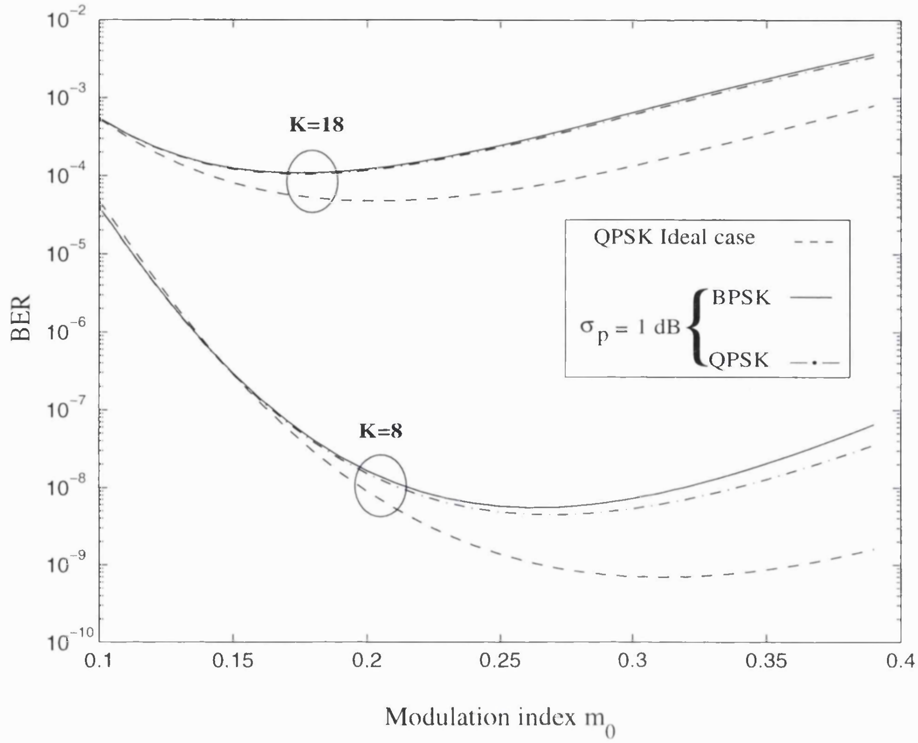

Figure 4.7: Bit-Error-Rate versus the modulation index m_0 for QPSK based systems for different number of users K for the ideal case with perfect power control and the practical case with imperfect power control. The performance of the BPSK case with a standard deviation of 1 dB is also superimposed.

where the average transmitting optical power, P_t and the modulation index, m_0 are determined by the LD parameters and the injected current, $\theta_k(t)$ is the kth channel signal. Expand the exponential function as

$$\exp(x) = 1 + \sum_{m=1}^{\infty} \frac{x^m}{m!} \tag{4.72}$$

Now, using the laser diode rate equation analysis, the value of the distortion coefficients A_2 is estimated to be 1/2 and 1/6 for A_3. Using this in 4.71, the signal power and the IMD can be estimated. It is known that by limiting the transmission band to a single octave the second-order distortion of FDMA system can be ignored and only third-order distortion is of importance. From 4.71, the variance of third-order distortion can be found [49, 2] as

$$\left\langle I_3^2 \right\rangle_{FDMA} = \frac{1}{32} (\eta P_r)^2 m_0^6 N_K(k) \tag{4.73}$$

where $N_K(k)$ is the number of IMD products of the type $\omega_p + \omega_q - \omega_r$ falling on the kth carrier. $N_K(k)$ is given by

$$N_K(k) = \frac{k}{2}(K-k+1) + \frac{1}{4}\left((K-3)^2 - 5\right) - \frac{1}{8}\left(1-(-1)^K\right)(-1)^{K+k} \quad (4.74)$$

Using the results of Section 4.2.3, the variance of the third-order distortion for random sequence CDMA system can be presented by

$$\begin{aligned}\left\langle I_3^2 \right\rangle_{CDMA} &= \frac{(\eta P_r m_0)^2}{2}\left[\frac{A_3 m0^2(2K-1)(K-1)}{4N}\right. \\ &+ \left.\frac{A_3^2 m0^4(K-1)}{64}\left(9+\frac{126K^2+30k-264}{5N}\right)\right] \quad (4.75)\end{aligned}$$

Third-order IMD-to-carrier ratio (IMD/C) of CDMA and FDMA systems is shown as a function of modulation index $m0$ in Figure 4.8.

It is known that the second-order IMD of FDMA is proportional to m_0^4; it is not

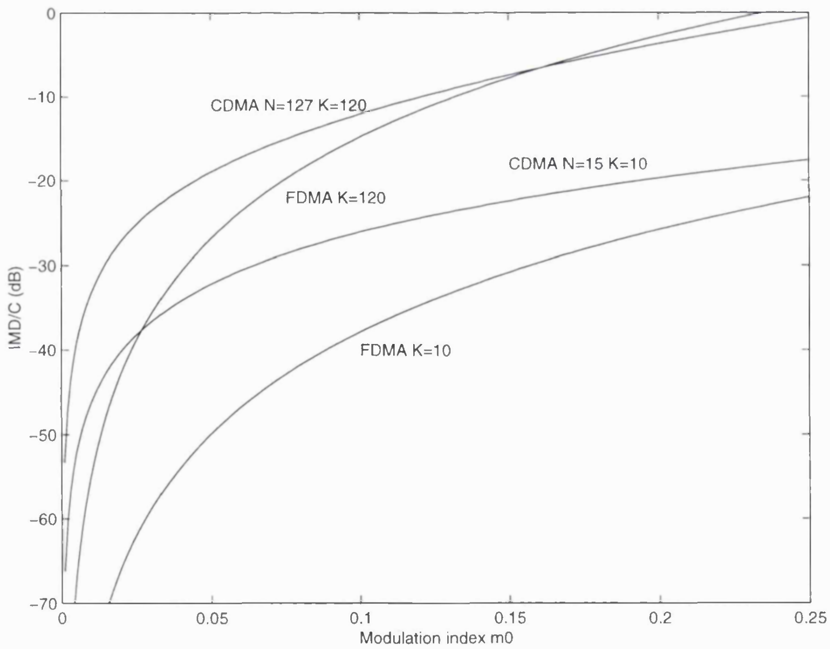

Figure 4.8: IMD/C versus modulation index with the number of users K & code period N as parameters for CDMA and FDMA systems

considered in Figure 4.8. This has been done because there is no second-order IMD when the FDMA transmission band is limited to a single octave in band. In a CDMA system, the second-order IMD does not influence the system performance. However, the correlation components of the MUI and the third-order IMD are proportional to m_0^4, and this is the reason that the third-order IMD of CDMA system is worse than for a FDMA system for the same number of users and the same modulation index.

4.5 Summary

In this chapter, the effect of the intermodulation in DS/CDMA systems with imperfect power control in optical transmission has been presented. A memoryless third-order polynomial has been used to represent the laser diode nonlinearity. The BER is deteriorated by the imperfection in the power control mechanism. With LD nonlinearity it is necessary to select an optimal modulation index that provides better BER. The results achieved are useful for system design and performance analysis.

The next chapter will consider hybrid CDMA/FDMA systems at subcarrier level to suppress the effect of laser nonlinearity. Volterra series expansion will be used to model the laser nonlinearity.

Chapter 5

Laser Nonlinearity on SCM/CDMA Systems: Volterra Analysis

5.1 Introduction

The previous chapters analysed the use of Code Division Multiple Access (CDMA) as a mode of access in mobile radio communications. Some of the advantages of CDMA are asynchronous multiple access, built-in addressing, and ease of implementation. Also, CDMA is robust against interference. However, it is not , for example, as spectrally efficient as frequency division multiple access (FDMA).

Radio Frequency (RF) or microwave SubCarrier Multiplexing (SCM) has recently emerged as a potentially important multiplexing technique for future high-capacity lightwave systems [56, 57]. In SCM systems where a number of RF subcarriers modulate a light beam, nonlinearity of the light source introduces interfering signals that are considered as main contributors to impairments in these systems. Combining CDM and SCM has potential for solving this problem and is very spectrally efficient [58]. This hybrid system becomes robust against interference and is more spectrally efficient than CDMA. Vannucci [59] presents many of the implementation details of a combined CDM/FDMA system. However, this system suffers from intermodulation distortion caused by laser or external modulator nonlinearities [47]

A hybrid SCM/CDMA system at subcarrier level has been proposed to suppress the effect of laser nonlinearity [60]. In this chapter, we present the theoretical model to represent the laser nonlinearity for a SCM/CDMA system. This analysis is based on Volterra functional series[1]. First, we will show that Volterra series can be applied to assess laser nonlinearity. Then the nonlinear transfer functions, which completely characterize the semiconductor laser in the frequency domain, are determined. Finally, we present the method to evaluate the performance of a SCM/CDMA system.

5.2 System Output as a Volterra Expansion

Signal distortion occurs in communication systems when the amplitude $|H(f)|$ and phase $\phi(f)$ of a linear network transfer function $H(f) = |H(f)|e^{i\phi(f)}$ are frequency dependent functions. This type of distortion is called "linear distortion". Besides this type of distortion other deviations can occur if the system possesses nonlinear elements. In this case, the system can not be described by a single transfer function as in the linear case; instead the output, $y(t)$, is often expressed as a nonlinear function of the input $x(t)$, that is, $y(t) = T[x(t)]$. The resulting type of distortion is called "nonlinear distortion".

Volterra series were introduced into nonlinear circuit analysis in 1942 by Wiener. Volterra series are particularly useful in calculating small (but troublesome) distortions in communication systems and have been used to determine the distortion produced in various types of amplifiers [62, 63]. Volterra series have been described as "power series with memory" which express the output of a nonlinear system in "powers" of

[1]This builds further upon research by Dr H. Salgado on applying the Volterra Series to Laser non-linearities

the input $x(t)$.

The semiconductor laser is then viewed as a nonlinear system with memory where the output $p = p_0 + p(t)$, the normalised photon density, related to the input $j = j_0 + j(t)$, the normalised current density, by the functional

$$p(t) \;=\; T[j(t)] \tag{5.1}$$

continuous in all values, where p_0 and j_0 are the corresponding steady-state values. This functional can be represented by its Volterra expansion, which is of the form

$$p(t) \;=\; \sum_{n=1}^{\infty} p_n(t) \tag{5.2}$$

$$p_n(t) \;=\; \int_{-\infty}^{\infty} \cdots \int_{-\infty}^{\infty} h_n(\tau_1, \cdots, \tau_n) \prod_{r=1}^{n} j(t - \tau_r)\, d\tau_r \tag{5.3}$$

This representation is useful when the required number of terms is small and thus is applicable to the small-signal nonlinear case. In equation (5.3) the multidimensional function $h_n(\tau_1, \cdots, \tau_n)$ is the n^{th}-order laser nonlinear impulse response. Just as the linear transfer function is the Fourier transform of $h_1(t)$, the nonlinear transfer function $H_n(f_1, \cdots, f_n)$ is the n-dimensional Fourier transform of $h_n(\tau_1, \cdots, \tau_n)$

$$H_n(f_1, \cdots, f_n) \;=\; \int_{-\infty}^{\infty} \cdots \int_{-\infty}^{\infty} h_n(\tau_1, \cdots, \tau_n) \prod_{r=1}^{n} e^{-i2\pi f_r \tau_r}\, d\tau_r \tag{5.4}$$

The nonlinear impulse responses and nonlinear transfer functions form Fourier transform pairs and so $h_n(\tau_1, \cdots, \tau_n)$ can be obtained from $H_n(f_1, \cdots, f_n)$ by inverse Fourier transformation

$$h_n(\tau_1, \cdots, \tau_n) \;=\; \int_{-\infty}^{\infty} \cdots \int_{-\infty}^{\infty} H_n(f_1, \cdots, f_n) \prod_{r=1}^{n} e^{i2\pi f_r \tau_r}\, df_r \tag{5.5}$$

Taking the conjugate of equation 5.4 the usual Hermitian property is obtained

$$H_n^*(f_1, \cdots, f_n) \;=\; H_n(-f_1, \cdots, -f_n) \tag{5.6}$$

Substituting equation 5.5 into equation 5.3 and carrying out the multiple integrals in $\tau_1, \cdots, \tau_n$ yields

$$p_n(t) = \int_{-\infty}^{\infty} \cdots \int_{-\infty}^{\infty} H_n(f_1, \cdots, f_n) \prod_{r=1}^{n} J(f_r) e^{i2\pi f_r t} \, df_r \tag{5.7}$$

which conveniently expresses the n^{th}-order term of the functional expansion in terms of the input spectrum $J(f)$. The order of each term equals the number of contributing input frequencies when the input signal consists of a sum of individual tones. Note, however, that different order nonlinearities can result in responses at the same frequency and so the frequency of a response is not fully indicative of its order. As an example, the frequency $2f_1 - f_2$ appears to be third-order, that is, $2f_1 - f_2 = f_1 + f_1 - f_2$, but it could also be fifth-order intermodulation product (IMP) $f_1 + f_1 + f_1 - f_1 - f_2$. The input-output spectral relationship is implied by (5.2) and is then

$$P(f) = \sum_{n=1}^{\infty} P_n(f) \tag{5.8}$$

where $P_n(f)$ is obtained by Fourier transform of equation (5.7)

$$P_n(f) = \int_{-\infty}^{\infty} \cdots \int_{-\infty}^{\infty} H_n(f_1, \cdots, f_n) \, \delta(f - f_1 - \cdots - f_n) \prod_{r=1}^{n} J(f_r) df_r \tag{5.9}$$

From (5.3) it can be seen that the output $p_n(t)$ is identical for any permutation of the arguments of $h_n(\tau_1, \cdots, \tau_n)$. In the following discussion it will be assumed that the impulse response $h_n(\tau_1, \cdots, \tau_n)$ and hence the nonlinear transfer functions $H_n(f_1, \cdots, f_n)$ are symmetric with respect to their arguments, i.e., that the order of the arguments can be interchanged. In Reference [65] it is shown that $h_n(\cdot)$ and $H_n(\cdot)$ can always be made symmetric. In order to understand the meaning of equation (5.7) an auxiliary multidimensional time function is defined

$$p_n(t_1, \cdots, t_n) = \int_{-\infty}^{\infty} \cdots \int_{-\infty}^{\infty} H_n(f_1, \cdots, f_n) \prod_{r=1}^{n} J(f_r) e^{i2\pi f_r t_r} \, df_r \tag{5.10}$$

and its n-fold Fourier transform, or multispectral density,

$$P_n(f_1, \cdots, f_n) = \int_{-\infty}^{\infty} \cdots \int_{-\infty}^{\infty} \prod_{r=1}^{n} p_n(t_1, \cdots, t_n)\, e^{-i2\pi f_r t_r} dt_r \tag{5.11}$$

so that

$$p_n(t_1, \cdots, t_n) = \int_{-\infty}^{\infty} \cdots \int_{-\infty}^{\infty} \prod_{r=1}^{n} P_n(f_1, \cdots, f_n)\, e^{i2\pi f_r t_r} df_r \tag{5.12}$$

By comparison of the previous equation with equation (5.7) it follows that

$$P_n(f_1, \cdots, f_n) = H_n(f_1, \cdots, f_n)\, J(f_1) \cdots J(f_n) \tag{5.13}$$

and, in fact (cf 5.3)

$$P_n(f) = \int_{-\infty}^{\infty} \cdots \int_{-\infty}^{\infty} P_n(f_1, \cdots, f_n)\, \delta(f - f_1 - \cdots - f_n)\, df_1 \cdots df_n \tag{5.14}$$

which states that the output spectrum is the integral of the multispectral density $P_n(f_1, \cdots, f_n)$, subject to the constraint $f = f_1 + \cdots + f_n$. This suggests the laser can be represented by the block diagram of Figure 5.1. The representation of the ouput by

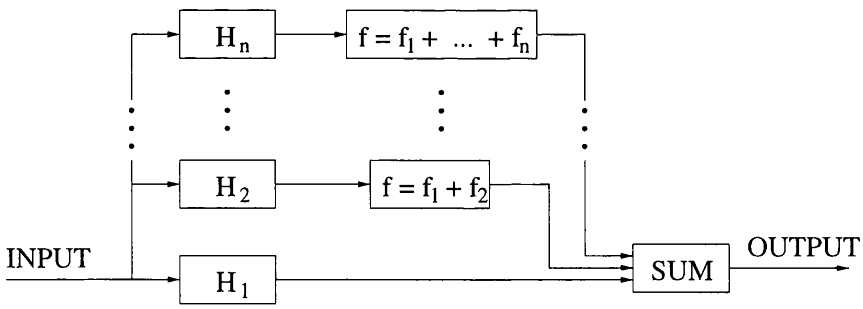

Figure 5.1: Nonlinear Model of the Semiconductor Laser

its Volterra expansion, equation 5.7, requires determination of the nonlinear transfer functions $H_n(f_1, \cdots, f_n)$.

5.3 Determination of Nonlinear Laser Transfer Functions by the Probing Method

5.3.1 The Probing Method

A convenient analysis method for evaluating the nonlinear transfer functions is the so-called "probing" or "harmonic input" method which is considered in this section [65].

Suppose that the input and output of a nonlinear system can be characterized by a relationship T continuous in all values of $p(t)$ so that

$$p(t) = T[j(t)] \tag{5.15}$$

where $j(t)$ is the input and $p(t)$ the output. Suppose further that there exists one, and only one, steady-state solution of this equation. This solution can then be represented by its Volterra expansion which is of the form

$$p(t) = \sum_{n=1}^{\infty} \int_{-\infty}^{\infty} \cdots \int_{-\infty}^{\infty} H_n(\xi_1, \cdots, \xi_n) \prod_{r=1}^{n} J(\xi_r) e^{i2\pi\xi_r t} d\xi_r \tag{5.16}$$

Thus the output of a nonlinear system in the form of (5.16) entails the determination of Volterra kernels $H_n(f_1, \cdots, f_n)$, which we have called the nonlinear transfer functions. Let the input to the system $j(t)$ be a sum of exponentials

$$j(t) = e^{i2\pi f_1 t} + e^{i2\pi f_2 t} + \cdots + e^{i2\pi f_n t} \tag{5.17}$$

where the frequencies f_r, $r = 1, 2, \cdots, n$ are linearly independent, that is, the ratio of all possible pairs of frequencies is not a rational number. The Fourier transform of the input (5.17) is a sum of delta functions

$$J(f) = \sum_{k=1}^{n} \delta(f - f_k) \tag{5.18}$$

This type of input is called a "probing input" or "harmonic input", which accounts for the name of the method. With this input, the n^{th}-order component of the Volterra expansion becomes after substitution into equation 5.7

$$p_n(t) = \int_{-\infty}^{\infty} \cdots \int_{-\infty}^{\infty} H_n(\xi_1, \cdots, \xi_n) \prod_{r=1}^{n} \sum_{k=1}^{\infty} \delta(\xi_r - f_k) e^{i2\pi\xi_r t} d\xi_r \tag{5.19}$$

Expanding the product of the sum and carrying out the multiple integrals yields

$$p_n(t) = \sum_{k_1=1}^{n} \cdots \sum_{k_n=1}^{n} H_n(f_{k1}, \cdots, f_{kn}) e^{i2\pi(f_{k1}+\cdots+f_{kn})t} \tag{5.20}$$

The new frequencies generated, ν, can be written as

$$\nu = m_1 f_1 + \cdots + m_n f_n \tag{5.21}$$

where m_i is the number of times the frequency f_i occurs in generating the intermodulation (IM) frequency. Because exactly n terms are generated by a n^{th}-order nonlinearity the set of values of m_i that defines any IM frequency is subject to the constraint

$$\sum_{r=1}^{n} m_r = n \tag{5.22}$$

In the summations of equation 5.20 it is necessary to determine the number of identical terms at each frequency, except for the permutation of the factors, in order to obtain the correct magnitude of each IM component. For an IM frequency given by equation 5.21 the number of terms is given by the multinomial coefficient

$$\frac{n!}{m_1! \cdots m_n!} \tag{5.23}$$

When the operation in equation 5.20 is carried out and identical terms collected, we get

$$p_n(t) = \sum_{m} \frac{n!}{m_1! \cdots m_n!} H_n(m_1[f_1], \cdots, m_n[f_n]) \prod_{r=1}^{n} e^{i2\pi m_r f_r t} \tag{5.24}$$

where

$$m_r[f_r] = \overbrace{(f_r, \cdots, f_r)}^{m_r \text{ times}} \tag{5.25}$$

that is m_r consecutive arguments in $H_n(\cdot)$ having the same frequency f_r; m under the summation indicates that the sum includes all the distinct sets $\{m_1, \cdots, m_n\}$. In this equation there is a term of order n corresponding to $m_1 = \cdots = m_n = 1$ given by

$$n!\, H_n(f_1, \cdots, f_n)\, e^{i2\pi(f_1+\cdots+f_n)t} \tag{5.26}$$

and there are no more terms associated with $e^{i2\pi(f_1+\cdots+f_n)t}$ than this term because $f_1, \cdots, f_n$ were assumed to be linearly independent. Therefore the n^{th} nonlinear transfer function $H_n(f_1, \cdots, f_n)$ can be determined as the coefficient of $n!e^{i2\pi(f_1+\cdots+f_n)t}$ in the laser output when the input is the sum of exponentials (equation 5.17).

This suggests the use of the perturbation technique to determine all the transfer functions from the single-mode rate equations. The laser is first excited by a single exponential the coefficient of which gives the first-order transfer functions $H_1(f)$ and $G_1(f)$ associated with the photon and electron density, respectively. A sum of two exponentials is then applied yielding $H_2(f_1, f_2)$ and $G_2(f_1, f_2)$ in terms of $H_1(f_1)$ and $G_1(f_1)$. This procedure continues to the required order with one exponential being added at each step. It then follows that the nonlinear transfer function of order n is constructed from all the lower order nonlinear transfer functions.

In the next section, we apply this method to calculate the nonlinear transfer functions of a laser diode.

5.3.2 Nonlinear Laser Transfer Functions

It is assumed here that the laser is described by the single-mode rate equations and these will be the basis for the determination of the laser transfer functions. For simplicity of notation and for computational purposes the normalised rate equations will be used.

We normalize the various quantities in the rate equations (3.1) and (3.2) as follows

$$t \equiv t/\tau_s \tag{5.27}$$

$$p = g_0 \tau_s P \tag{5.28}$$

$$n = g_0 \tau_p N \tag{5.29}$$

$$n_{0m} = g_0 \tau_p N_{0m} \tag{5.30}$$

$$j = g_0 \tau_s \tau_p (J/qd) \tag{5.31}$$

$$\epsilon = \varepsilon/(g_0 tau_s) \tag{5.32}$$

$$\gamma = \tau_s/\tau_p \tag{5.33}$$

We use the same letter t for the time variable but it is supposed to be a normalized variable as given by (5.27) when used in conjunction with the normalized variables n, p and j. Accordingly, equations (3.1) and (3.2) become

$$\frac{dn}{dt} = j - n - (n - n_{0m})(1 - \varepsilon p)p \tag{5.34}$$

$$\frac{dp}{dt} = \gamma[\Gamma(n - n_{0m})(1 - \varepsilon p)p - p + \Gamma\beta n] \tag{5.35}$$

Application of the probing method to the first, second and third-order differential equations for the perturbed electron and photon densities gives, for the n^{th}-order, the following system of equations

$$\begin{aligned} i2\pi(f_1 + \cdots + f_n)G_n(f_1, \cdots, f_n) = -\{&[(1 - \varepsilon p_0)p_0 + 1]G_n(f_1, \cdots, f_n) \\ &+(n_0 - n_{0m})(1 - 2\varepsilon p_0)H_n(f_1, \cdots, f_n) + D_n\} \end{aligned} \tag{5.36}$$

$$i2\pi(f_1 + \cdots + f_n)H_n(f_1, \cdots, f_n) = \gamma\{\Gamma[(1 - \varepsilon p_0)p_0 + \beta]G_n(f_1, \cdots, f_n)$$
$$+[\Gamma(n_0 - n_{0m})(1 - 2\varepsilon p_0) - 1]H_n(f_1, \cdots, f_n) + C_n\} \tag{5.37}$$

where the driving terms C_n and D_n are given in Table 5.1. Solving equations (5.36) and (5.37) for G_n and H_n gives

n	D_n
1	-1
2	$\frac{1}{2}\{(1 - 2\varepsilon p_0)[G_1(f_1)H_1(f_2) + G_1(f_2)H_1(f_1)] - 2(n_0 - n_{0m})\varepsilon H_1(f_1)H_1(f_2)\}$
3	$\frac{1}{3}\{(1 - 2\varepsilon p_0)[H_1(f_1)G_2(f-2, f_3) + H_1(f_2)G_2(f_1, f_3) + H_1(f_3)G_2(f_1, f_2)$ $+G_1(f_1)H(f_2, f_3) + G_1(f_2)H_2(f_1, f_3) + G_1(f_3)H_2(f_1, f_2)]$ $-(n_0 - n_{0m})2\varepsilon[H_1(f_1)H_2(f_2, f_3) + H_1(f_2)H_2(f_1, f_3) + H_1(f_3)H_2(f_1, f_2)]$ $-\varepsilon[G_1(f_1)H_1(f_2)H_1(f_3) + G_1(f_2)H_1(f_1)H_1(f_3) + G_1(f_3)H_1(f_1)H_1(f_2)]\}$

Table 5.1: Driving terms: C_n equals 0 for $n = 1$ and D_n for the other cases.

$$H_n(f_1, \cdots, f_n) = \frac{\gamma\Gamma\{C_n\psi(f_1 + \cdots + f_n) - [(1 - \varepsilon p_0)p_0 + \beta]D_n\}}{\varphi(f_1 + \cdots + f_n)} \tag{5.38}$$

$$G_n(f_1, \cdots, f_n) = -\frac{\gamma\Gamma(n_0 - n_{0m})(1 - 2\varepsilon p_0)C_n + \chi(f_1 + \cdots + f_n)D_n}{\varphi(f_1 + \cdots + f_n)} \tag{5.39}$$

where

$$\psi(f) = i2\pi f + (1 - \varepsilon p_0)p_0 + 1 \tag{5.40}$$

$$\chi(f) = i2\pi f - \gamma\Gamma(n_0 - n_{0m})(1 - 2\varepsilon p_0) + \gamma \tag{5.41}$$

$$\varphi(f) = \psi(f)\chi(f) + \gamma\Gamma[(1 - \varepsilon p_0)p_0 + \beta](n_0 - n_{0m})(1 - 2\varepsilon p_0) \tag{5.42}$$

Equations (5.36) to (5.42) are recursive formulas to calculate H_n as a function of G_{n-1} and H_{n-1}. Note now that the effect of the chip and package parasitics on the laser response can easily be included in the analysis. The result of the laser parasitics is to divert some of the input current from the active region. If $H_p(f)$ is the transfer function of the parasitics, which gives the frequency dependence of the injected current into the active region, the driving term D_1 should be redefined accordingly, that is, $D_1 = -H_p(f)$. This is equivalent to multiplying the first order transfer function of the intrinsic laser by the transfer function $H_p(f)$ of the the parasitics.

5.4 Performance Assessment of SCM/CDMA Systems

5.4.1 Laser Response to a sum of SCM/CDMA Signals

Assuming that the input signal of the laser is bandpass and typically narrow-band compared to the carrier frequency, we denote the sum of K SCM/CDMA signals each centred at ν_k as

$$j(t) = \sum_{k=1}^{K} j_k(t) = \sum_{k=1}^{K} a_k(t) \cos 2\pi\nu_k t \tag{5.43}$$

where $a_k(t)$ is the component of $j_k(t)$. It is convenient to use an equivalent low-pass representation for the bandpass signals by defining the complex envelope $z_k(t)$ of $j_k(t)$

$$z_k(t) = a_k(t) \tag{5.44}$$

With these definitions the input signal can be written as

$$\begin{aligned} j(t) &= \sum_{k=1}^{K} Re\Big\{z_k(t)e^{i2\pi\nu_k t}\Big\} \\ &= \frac{1}{2}\sum_{k=-K}^{K} z_k(t)e^{i2\pi\nu_k t} \end{aligned} \tag{5.45}$$

with $z_0(t) = 0$. Defining $Z_k(f)$ as the Fourier transform of $z_k(t)$ and denoting $Z_{-k}(f)$ and ν_{-k} by $Z_k^*(f)$ and $-\nu_k$, respectively, the spectrum $J_k(f)$ of $j_k(t)$ is

$$\begin{aligned} J_k(f) &= \frac{1}{2}\sum_{k=1}^{K}\Big[Z_k(f-\nu_k) + Z_k^*(-f-\nu_k)\Big] \\ &= \frac{1}{2}\sum_{k=-K}^{K} Z_k(f-\nu_k) \end{aligned} \tag{5.46}$$

After substitution of the above equation into (5.7) and performing the product of the input spectra the photon density becomes

$$p(t) = \sum_{n=1}^{\infty}\sum_{k_1=1}^{K}\cdots\sum_{k_n=1}^{K} 2^{-n}\int_{-\infty}^{\infty}\cdots\int_{-\infty}^{\infty} H_n(f_1,\cdots,f_n)\prod_{r=1}^{n} Z_{kr}(f_r-\nu_{kr})e^{i2\pi f_r t}df_r \tag{5.47}$$

As before there are $n!/(m_{-K}!\cdots m_K!)$ identical integrals for each distinct set $\{k_1,\cdots,k_n\}$ with $k_i = -K,\cdots,K$ where $m_i = 0,\cdots,n$ is the number of times each k_i occurs in the set, so that

$$\sum_{k=-K}^{K} m_k = n \tag{5.48}$$

Collecting those integrals, the nth-order term is

$$p_n(t) = \sum_k \frac{n!}{m_{-K}!\cdots m_K!}\int_{-\infty}^{\infty}\cdots\int_{-\infty}^{\infty} H_n(f_1,\cdots,f_n)\prod_{r=1}^{n} Z_{kr}(f_r-\nu_{kr})e^{i2\pi f_r t}df_r \tag{5.49}$$

in which the summation over k includes all the distinct sets $\{k_1,\cdots,k_n\}$. Each set $\{\nu_{k_1},\cdots,\nu_{k_n}\}$ must have its symmetric $\{-\nu_{k_1},\cdots,-\nu_{k_n}\}$, except in the case of

$$\sum_{k_r=1}^{n} \nu_{kr} = 0 \tag{5.50}$$

The sum of two such terms in (5.49), which are complex conjugates, is designated as

$$\begin{aligned} p_{n\nu}(t) &= Re\Bigg\{\frac{n!2^{-n+1}}{m_{-K}!\cdots m_K!}\Big[\int_{-\infty}^{\infty}\cdots\int_{-\infty}^{\infty} H_n(f_1+\nu_{k1},\cdots,f_n+\nu_{kn}) \\ &\qquad \prod_{r=1}^{n} Z_{kr}(f_r)e^{i2\pi f_r t}df_r\Big]e^{i2\pi\sum_{r=1}^{n}\nu_{k_r}t}\Bigg\} \end{aligned} \tag{5.51}$$

so that

$$p_n(t) = \sum_k p_{n\nu}(t) \tag{5.52}$$

Comparing Equations (5.45) and (5.51) it can be concluded that when the input current consists of a sum of narrow-band signals the laser generates new narrow-band components centred at all carrier intermodulation frequencies. The n-th order output component, $p_{n\nu}$, centred at frequency

$$\nu = \sum_{r=1}^{n} \nu_{kr} = \sum_{k=-K}^{K} m_k \nu_k \tag{5.53}$$

generated by intermodulation of the input signal components centered at $\nu_{k1}, \cdots, \nu_{kn}$ is defined as

$$p_{n\nu}(t) = Re\left\{ q_{n\nu}(t) e^{i2\pi \sum\limits_{r=1}^{n} \nu_{k_r} t} \right\} \tag{5.54}$$

which has a complex envelope $q_{n\nu}(t)$ given by

$$\begin{aligned} q_{n\nu}(t) \quad = \quad & \frac{n! 2^{-n+1}}{m_{-K}! \cdots m_K!} \int_{-\infty}^{\infty} \cdots \int_{-\infty}^{\infty} H_n(f_1 + \nu_{k1}, \cdots, f_n + \nu_{kn}) \\ & \prod_{r=1}^{n} Z_{kr}(f_r) e^{i2\pi f_r t} df_r \end{aligned} \tag{5.55}$$

Hence $p_{n\nu}$ is the intermodulation product due to the input signals with carriers at frequencies $\nu_{k1}, \cdots, \nu_{kn}$. The order of the IMP corresponds to the number of carriers generating this product, with the possibility of n being greater than K and signals intermodulating with themselves. The order of the permutation of the component frequencies $\nu_{k1}, \cdots, \nu_{kn}$ of ν is irrelevant since it does not affect the IM waveform $p_{n\nu}$. Also, any two sets of ν_{ki} are indistinguishable if they differ only by the order of the components within the set. The multinomial coefficient in the integrals (5.51) and (5.55) take into account the number of such indistinguishable sets among all the $(2K)^n$ sets of ν.

In practice there is interest in determining $p_\nu(t)$ the component of $p(t)$ centred on the sum frequency ν

$$p_\nu(t) = Re\left\{ q_\nu(t) e^{i2\pi\nu t} \right\} \tag{5.56}$$

with complex envelope $q_\nu(t)$. Intermodulation of infinity orders and with many different sets of input components $\nu_{k1}, \cdots, \nu_{kn}$, can contribute near a particular frequency. Thus $p_{n\nu}(t)$ and $q_\nu(t)$ is the sum over n and ν of all the $q_{n\nu}(t)$ under the constraint (5.53) that they fall at the same frequency ν

$$q_\nu(t) = \sum_{\nu,n=1}^{\infty} q_{n\nu}(t) \tag{5.57}$$

Next, we present the method to evaluate the performance of the system.

5.4.2 Carrier to Noise Ratio

In order to quantify the effect of the intermodulation noise on the performance of SCM/CDMA systems we define the nth-order Carrier-to-Intermodulation Ratio (CIR) for the rth channel located at frequency ν due to input channels at $f_{k1}, f_{k2}, \cdots, f_{kn}$ as the ratio of the signal power to the nth-order intermodulation power falling in the band (Figure 5.2). CIR is then written as

$$CIR_{nr}(f_{k1}, \cdots, f_{kn}) \quad = \quad \frac{\int_{-1/2T}^{1/2T} G_{p_{1\nu}}(f)df}{\int_{-1/2T}^{1/2T} G_{p_{n\nu_i}}(f)df} \tag{5.58}$$

Since the channel are independent the total nth-order CIR for channel r is obtained

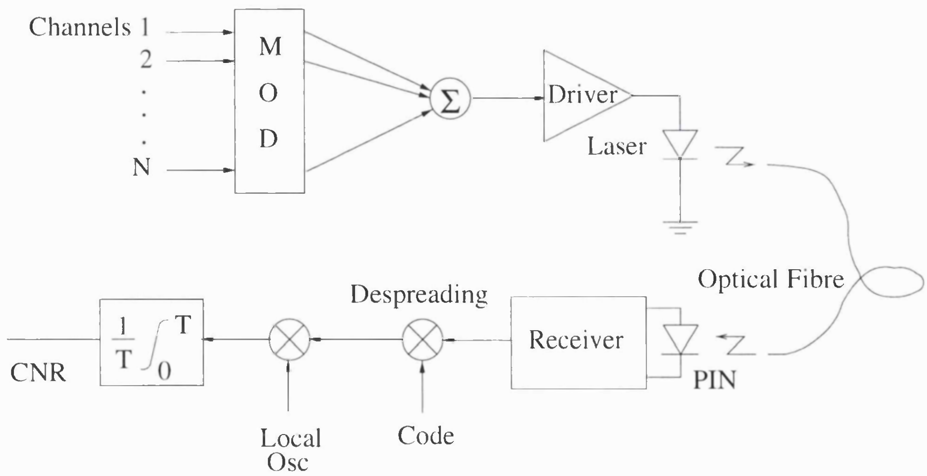

Figure 5.2: Block Diagram of a SCM/CDMA System

by summation of all the IMPs power terms of order n falling at frequency ν_i

$$CIR_{nr} = \frac{\int_{-1/2T}^{1/2T} G_{p_{1\nu}}(f)df}{\sum_k \int_{-1/2T}^{1/2T} G_{p_{n\nu_i}}(f)df} \tag{5.59}$$

where the summation over k includes all the distinct sets $k_1, \cdots, k_n$ such that

$$f_{k_1} + \cdots + f_{k_n} = m_{-N}f_{-N} + \cdots + m_N f_N = \nu_i \tag{5.60}$$

with the signal at frequency ν_i having power falling into the band.

In addition to the intermodulation terms, we have to take into account the interference of the other users. The Carrier-to-Noise Ratio (CNR) is then written as

$$CNR = CIR + CFR \tag{5.61}$$

where CIR is calculated taking into account the second and third-order IMPs only. CFR is the Carrier-to-Interference Ratio defined as

$$CFR = \frac{\int_{-1/2T}^{1/2T} G_{p_{1\nu}}(f)df}{\sum_i \int_{-1/2T}^{1/2T} G_{p_{1\nu_i}}(f)df} \tag{5.62}$$

At the laser output, the amplitudes of the carriers which relate to the per-channel optical modulation depth, m, are given by

$$j_k = \frac{m(f_k)p_0}{H_1(f_k)} \tag{5.63}$$

If the channels have the same amplitude, j_k is given by

$$j_k = \frac{m_0 p_0}{H_1(f_k)} \tag{5.64}$$

5.5 Summary

In this chapter we have presented the Volterra series analysis as a method to predict the nonlinearity introduced by semiconductor lasers. The nonlinear transfer functions characterising the semiconductor laser in the frequency domain have been determined from the single-mode rate equations. Finally, we derived the laser response to a sum of SCM/CDMA signals and present the method to evaluate the system performance. In the next chapter, these expressions will be used to assess the performance of different configurations of SCM/CDMA systems.

Chapter 6

Systems studies

6.1 Introduction

The objective of Personal Communication Systems (PCS) or Personal Communication Networks (PCNs) is to provide ubiquitous wireless communications coverage, enabling users to access the telephone network for different types of communication needs, without regard for the location of the user or the location of the information being accessed. Hence, the mobile and fixed networks will be integrated to provide universal access to the network and its databases. Wireless or hybrid wireless systems based on a radio last drop are a viable choice for these networks.

In this chapter, we introduce two different SCM/CDMA systems using this technique: Wireless Local Loop and Mobile Radio systems. We study the effect of Laser Diode nonlinear distortion on these systems using the theoretical analysis developed in chapter 5. In section 6.2, the downlink channel of a Wireless Local Loop system is considered. Then, two case studies are considered for Mobile Radio systems: the downlink channel of a flexible data rate system is studied in section 6.3, and in section 6.4 we concentrate on the return link of a mobile radio system.

6.2 Wireless Local Loop

6.2.1 Introduction

The history of Wireless Local Loop (WLL), or wireless access to fixed networks as distinct from mobile networks, is relatively short although a niche market has existed for many years in rural areas where radio provided the only cost effective means for providing telephone access to very remote dwellings.

In the last 3-5 years there has been a dramatic rise in interest in WLL stimulated by two new market demands. Firstly there is the need for rapid roll out of telephone services in developing countries in order to stimulate economic growth, and secondly, in the developed world, the move to introduce competition with the established PTTs raised the possibility of competing operators employing radio as the means for providing connection to the subscribers' premises.

Moreover, wireless technology allows developing countries to quickly advance their existing telephone network into the 21st century. A wireless local loop (WLL) system uses radio technology to provide reliable, flexible, and economical local telephone service in place of traditional copper wireline [20, 21]. A WLL is sometimes called a 'fixed cellular system'.

From the service provider's perspective, the key benefits of WLL are low capital costs, fast network deployment, and lower maintenance costs, clearly attractive considerations. Also, the process of building a WLL system does not require precise knowledge of the user's location, adding flexibility to planning and deployment of the system. WLL networks have been proven to have the capability to function as core communications systems in times of disaster; for disaster recovery, service providers have the option of rapidly deploying a WLL system during an emergency. WLL systems can also be used as redundant backup systems for existing wireline networks. This way, communications downtime caused by natural disaster such as floods, earthquakes, hurricanes, and so on can be kept to a minimum.

As seen before, WLL technology is also gaining popularity in the Asian and Latin American countries for providing telephone services in sparsely populated rural areas. A WLL is ideal as a startup telephone system that can be moved around to suit current needs. A WLL eliminates many problems and costs inherent in wireline loop systems. Thus, the WLL market is driven by telecommunications carriers with diverse infrastructure requirements, operating in markets characterised by a wide variety of competitive forces, including

- incumbent or monopoly operators with underdeveloped telecommunications infrastructure are looking at WLL technology as a means of satisfying regulatory or privatisation mandates to install a certain number of main lines per year, to extend telephony service to rural areas, or to reduce waiting lists;
- new operators in developed and developing telecommunications markets view WLL technology as a way to quickly establish market presence and reduce upfront infrastructure costs by building out the network in line with subscriber growth;
- established operators facing new competition are currently examining WLL technologies with a view to matching the speed of deployment and the WLL mobility offerings of their future competitors.

The WLL market is, and will probably remain, fragmented and this is reflected in the wide variety of technical solutions proposed for the air interface. Unlike in the case of GSM, the European standards body ETSI is not attempting to specify a WLL.

Also, current thinking is that WLL will serve only fixed subscriber terminals and hence a number of proprietary systems are assuming the use of directional antennas at the subscriber premises. Arguably this situation may be short lived as WLL operators seek to introduce a level of mobility into their services. In fact this desire is already being expressed by operators wishing to differentiate their offerings from those of fixed (wired) access operators and also wishing to gain a share in the profitable mobile market. Future WLL systems will therefore need to support handheld terminals (with omni-directional antennas) and provide at least low grade, local area mobility [66].

6.2.2 Digital Technologies

Two digital technologies, time-division multiple access (TDMA) and code-division multiple access (CDMA), are emerging as clear choices for a WLL system. TDMA is a narrowband system in which communications per frequency channel are apportioned according to time. For TDMA systems there are two prevalent standards

- North American Telecommunications/Electronics Industry Association (TIA/EIA) IS-136
- European Telecommunications Standards Institute (ETSI) Global System for Mobile Telecommunications (GSM)

CDMA (TIA/EIA/95A) is a direct sequence spread spectrum system where the entire bandwidth is made available to each user. In order to increase the system capacity, we can employ a hybrid system such as a SubCarrier Multiplexing (SCM)/ CDMA system. Furthermore, SCM techniques are very attractive for remote delivery over optical fibre for the provision of flexible customer access connections, offering advantages compared to copper or baseband optical systems. Specifically SCM allows the radio frequency carriers to modulate directly the laser and be transported over the optical fibre without the need for frequency conversion and multiplexing/demultiplexing functions. This will reduce the complexity of the radio distribution point and will facilitate the deployment of remote antennas whilst supporting the required multichannel microwave signal format. A representation of a WLL system is given in Figure 6.1. In this system, the

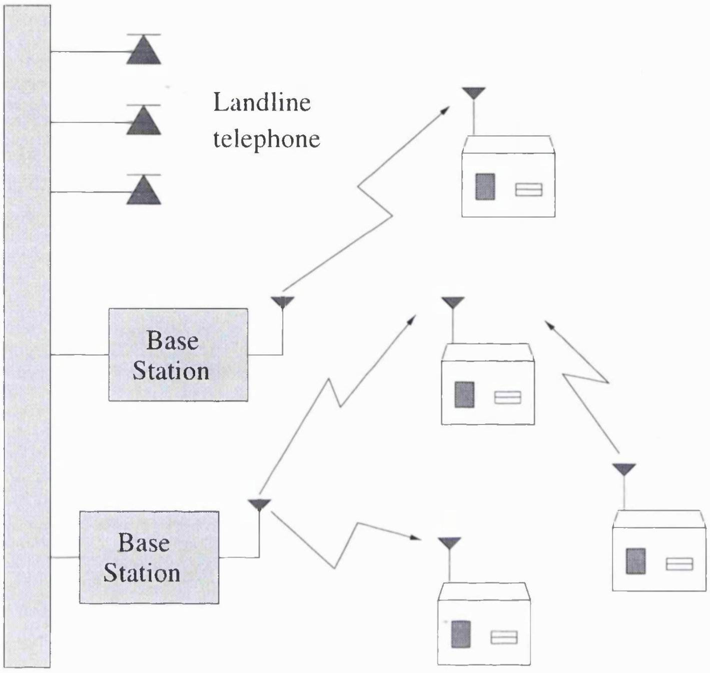

Figure 6.1: Cell sites connected to central office (CO)

users have a direct connection to the wireline network, provided adequate capacity exists on the central office (CO) switch. With this type of application, base stations are connected to the CO and optical fibre is used frequently to perform this connection. In the following, we study the effect of the laser diode nonlinearity in such a system.

6.2.3 Intermodulation Power Spectral Density

For this system, we concentrate on the forward link. The k^{th} signal transmitted to the k^{th} mobile user (see Figure 6.2) is presented by the spread-spectrum signal $s_k(t)(k = 1, 2, ..., K)$ as

$$s_k(t) = d_k(t)c_k(t)\cos(\omega_k t) \tag{6.1}$$

where ω_k is the center frequency of the k^{th} subcarrier. T is the bit duration and the bit data stream of the k^{th} user is given by

$$d_k(t) \;=\; \sum_{\ell=-\infty}^{\infty} d_\ell^{(k)} p_T(t-\ell T); \qquad d_\ell^{(k)} \in \{-1,1\} \tag{6.2}$$

where $d_\ell^{(k)}$ is a bit data value in the interval $[\ell T, (\ell+1)T]$, and $p_T(t) = 1$ for $0 \le t \le T$ and 0 otherwise. Each carrier is phase and amplitude coded by a waveform $c_k(t)$ given by

$$c_k(t) \;=\; \sum_{n=-\infty}^{\infty} c_n^{(k)} p_{T_c}(t-nT_c); \qquad c_n^{(k)} \in \{-1,1\} \tag{6.3}$$

where $c_n^{(k)}$ is a periodic binary sequence. Each bit is assumed to be encoded with N

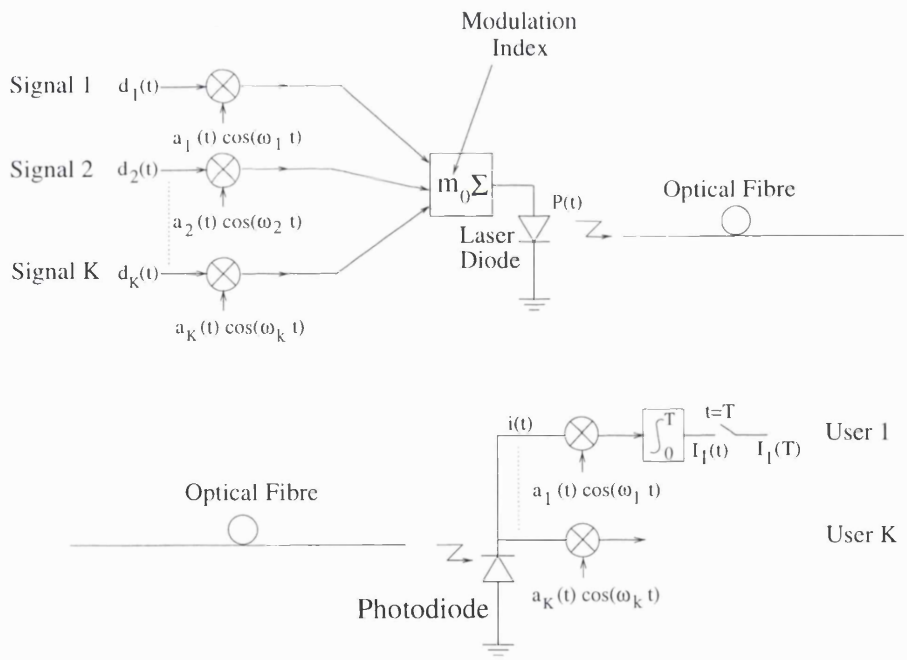

Figure 6.2: Model of synchronous SCM/CDMA system in optical communication

chips ($T = NT_c$).

We represent the input current by

$$j(t) \;=\; \sum_{k=1}^{K} j_k(t) \tag{6.4}$$

$$\begin{aligned} j_k(t) &= \sum_{n=-\infty}^{\infty} \sum_{\ell=-\infty}^{\infty} c_n^{(k)} d_\ell^{(k)} p_{T_c}(t - nT_c) p_T(t - \ell T) \cos(\omega_k t) \\ &= \sum_{n=-\infty}^{\infty} \sum_{\ell=-\infty}^{\infty} c_n^{(k)} d_\ell^{(k)} p_{T_c}(t - nT_c) \cos(\omega_k t) \end{aligned} \tag{6.5}$$

The equivalent low-pass or complex envelope representation of the signal $j_k(t)$ is then written

$$z_k(t) = \sum_{n=-\infty}^{\infty} \sum_{\ell=-\infty}^{\infty} c_n^{(k)} d_\ell^{(k)} p_{T_c}(t - nT_c) \tag{6.6}$$

The complex envelope of the *nth*-order intermodulation falling at frequency ν due to signals centered at $\nu_{k1}, \cdots, \nu_{kn}$ is

$$q_{n\nu}(t) = \frac{n! 2^{-n+1}}{m_{-N}! \cdots m_N!} H_n(\nu) \prod_{k=-N}^{N} [z_k(t)]^{m_k} \tag{6.7}$$

In the case of a CDMA system, the received signal is multiplied by a replica of the code of the desired user signal. The receiver recovers the transmitted data bit by correlating the received signal with the signature sequence of user 1. The signal after this multiplication (or despreading operation) becomes

$$q'_{n\nu}(t) = \frac{n! 2^{-n+1}}{m_{-N}! \cdots m_N!} H_n(\nu) c_1(t) \prod_{k=-N}^{N} [z_k(t)]^{m_k} \tag{6.8}$$

The required signal is given by

$$q'_{\nu}(t) = H_1(\nu) \sum_{\ell=-\infty}^{\infty} d_\ell^{(1)} p_T(t - \ell T) \tag{6.9}$$

Noticing that $d_\ell^{(k)2} = c_n^{(k)2} = 1$, we get for the second order

$$q'_{\nu_1-\nu_i}(t) = H_2(\nu_1 - \nu_i) \sum_{n=-\infty}^{\infty} \sum_{\ell=-\infty}^{\infty} c_n^{(i)} d_\ell^{(1)} d_\ell^{(i)} p_{T_c}(t - nT_c) \tag{6.10}$$

$$q'_{\nu_i-\nu_1}(t) = H_2(\nu_i - \nu_1) \sum_{n=-\infty}^{\infty} \sum_{\ell=-\infty}^{\infty} c_n^{(i)} d_\ell^{(1)} d_\ell^{(i)} p_{T_c}(t - nT_c) \tag{6.11}$$

$$q'_{\nu_i-\nu_j}(t) = H_2(\nu_i - \nu_j) \sum_{n=-\infty}^{\infty} \sum_{\ell=-\infty}^{\infty} c_n^{(1)} c_n^{(i)} d_\ell^{(i)} c_n^{(j)} d_\ell^{(j)} p_{T_c}(t - nT_c) \tag{6.12}$$

For the third-order, we get

$$q'_{2\nu_1-\nu_i}(t) = \frac{3}{4}H_3(2\nu_1-\nu_i)\sum_{n=-\infty}^{\infty}\sum_{\ell=-\infty}^{\infty} c_n^{(1)}c_n^{(i)}d_\ell^{(i)}p_{T_c}(t-nT_c) \tag{6.13}$$

$$q'_{2\nu_i-\nu_1}(t) = \frac{3}{4}H_3(2\nu_i-\nu_1)\sum_{\ell=-\infty}^{\infty} d_\ell^{(1)}p_T(t-\ell T) \tag{6.14}$$

$$q'_{2\nu_i-\nu_j}(t) = \frac{3}{4}H_3(2\nu_i-\nu_j)\sum_{n=-\infty}^{\infty}\sum_{\ell=-\infty}^{\infty} c_n^{(1)}c_n^{(j)}d_\ell^{(j)}p_{T_c}(t-nT_c) \tag{6.15}$$

$$q'_{\nu_1+\nu_i-\nu_j}(t) = \frac{3}{2}H_3(\nu_1+\nu_i-\nu_j)\sum_{n=-\infty}^{\infty}\sum_{\ell=-\infty}^{\infty} d_\ell^{(1)}c_n^{(i)}d_\ell^{(i)}c_n^{(j)}d_\ell^{(j)}p_{T_c}(t-nT_c) \tag{6.16}$$

$$q'_{\nu_j+\nu_i-\nu_1}(t) = \frac{3}{2}H_3(\nu_i+\nu_j-\nu_1)\sum_{n=-\infty}^{\infty}\sum_{\ell=-\infty}^{\infty} d_\ell^{(1)}c_n^{(i)}d_\ell^{(i)}c_n^{(j)}d_\ell^{(j)}p_{T_c}(t-nT_c) \tag{6.17}$$

$$q'_{\nu_i+\nu_j-\nu_k}(t) = \frac{3}{2}H_3(\nu_i+\nu_j-\nu_k)\sum_{n=-\infty}^{\infty}\sum_{\ell=-\infty}^{\infty} c_n^{(1)}c_n^{(i)}d_\ell^{(i)}c_n^{(j)}d_\ell^{(j)}c_n^{(k)}d_\ell^{(k)}p_{T_c}(t-nT_c) \tag{6.18}$$

Next, we calculate the power spectral density of the different intermodulation terms. We start by calculating the Power Spectral Density (PSD) of the desired signal. We need to calculate first the autocorrelation function $R_{q_{n\nu}}(\tau)$ of $q_{n\nu}(t)$ defined as

$$R_{q_{n\nu}}(\tau) = E\{q^*_{n\nu}(t)q_{n\nu}(t+\tau)\} \tag{6.19}$$

which yields the desired PSD after Fourier transformation.

After despreading, the desired signal is a binary random process with values +1 and −1. The autocorrelation function of such a signal is given by

$$R_q(\tau) = \begin{cases} 1-\frac{\tau}{T}, & |\tau| < T \\ 0 & |\tau| \geq T \end{cases} \tag{6.20}$$

Using the Fourier transform of a triangle function, we obtain

$$S_q = T sinc^2(fT) \tag{6.21}$$

From equation (6.38), the PSD of the desired signal is

$$G'_{q_{\nu_1}}(f) \quad = \quad H_1^2(f)Tsinc^2(fT) \tag{6.22}$$

For the intermodulation terms, we get also a binary random process with period T_c instead of T for most of them. Using the same method, the second-intermodulation products give

$$G'_{q_{\nu_1-\nu_i}}(t) \quad = \quad H_2^2(\nu_1-\nu_i)T_c sinc^2(fT_c) \tag{6.23}$$

$$G'_{q_{\nu_i-\nu_1}}(t) \quad = \quad H_2^2(\nu_i-\nu_1)T_c sinc^2(fT_c) \tag{6.24}$$

$$G'_{q_{\nu_i-\nu_j}}(t) \quad = \quad H_2^2(\nu_i-\nu_j)T_c sinc^2(fT_c) \tag{6.25}$$

For the third-intermodulation products, we obtain for the different terms

$$G'_{q_{\nu_i\nu_i\nu_1}}(f) \quad = \quad \frac{9}{16}H_3^2(2\nu_i-\nu_1)Tsinc^2(fT) \tag{6.26}$$

$$G'_{q_{\nu_1\nu_1\nu_i}}(f) = \frac{9}{16}H_3^2(2\nu_1-\nu_i)T_c sinc^2(fT_c) \tag{6.27}$$

$$G'_{q_{\nu_i\nu_i\nu_j}}(f) = \frac{9}{16}H_3^2(2\nu_i-\nu_j)T_c sinc^2(fT_c) \tag{6.28}$$

$$G'_{q_{\nu_1\nu_i\nu_j}}(f) = \frac{9}{4}H_3^2(\nu_1+\nu_i-\nu_j)T_c sinc^2(fT_c) \tag{6.29}$$

$$G'_{q_{\nu_i\nu_j\nu_k}}(f) \quad = \quad \frac{9}{4}H_3^2(\nu_i+\nu_j-\nu_k)T_c sinc^2(fT_c) \tag{6.30}$$

Using these expressions, the performance of the system is assessed in the following section.

6.2.4 System Performance

The characteristics of the system considered here are based on the North American IS-95 standard. Recently, the IS-95 DS-CDMA system (with possible modifications) has been proposed to be used in the Personal Communication Systems (PCS) frequency band of 1850 to 1990 MHz. This standard is specified for reverse link operation in the 1850-1910 MHz and 1930-1990 MHz for the forward link. The forward link (base-to-mobile) is spread at a 1.2288 Mchips/s rate with a maximum user data rate of 9.6 kb/s. The radio spectrum is divided into carriers which are 1,250 kHz (1.25 MHz) wide.
As the band is limited to less than an octave we need to consider only third-order intermodulation because the second-order will produce terms that will fall outside the band.
The laser parameters used, taken from Reference [67], are given in Table 6.1.

Element	Value	Units
V: Active region volume	$0.45\ 10^{-16}$	m^3
g_0: gain slope constant	$2.9\ 10^{-12}$	m^3s^{-1}
ϵ: gain compression factor	$2.5\ 10^{-23}$	m^3
N_{om}: electron density at which net gain is zero	10^{24}	m^{-3}
β: fraction of spon. emission coupled into laser mode	10^{-4}	-
Γ: optical confinement factor	0.25	-
τ_p: photon lifetime	1	ps
τ_s: electron lifetime	1	ns

Table 6.1: Parameter values for a DFB-BH laser

In Figure 6.3, Carrier-to-Intermodulation Ratio (CIR) versus the optical modulation depth per channel (m_0) is given for two bias current of the laser: $I_0 = 40$ mA and

$I_0 = 55$ mA. We have simulated a system with three carriers which are $f_1 = 1958.75$ MHz, $f_2 = 1960$ MHz and $f_3 = 1961.25$ MHz. We have plotted this curve for the middle channel f_2 as it is the most affected by this effect. We see that the system performs better for a higher I_0. This is due to the fact that the third-order laser transfer function is higher for smaller current at frequencies low relative to the resonance frequency. Figure 6.4 plots the CIR as a function of the modulation depth m_0 for systems with three and 5 carriers and $I_0 = 40mA$. The result is also given for the middle channel and the other channels equally spaced from it. We notice an increase of approximately 5 dB of the deterioration of the system performance. With the increase of the number of carriers we increase the number of intermodulation (IMD) terms falling at a particular frequency. Thus, a system with five carriers produces twice the number of IMDs falling on the middle channel compared to a system with three carriers. This phenomenon is observed in the curve of Figure 6.4.

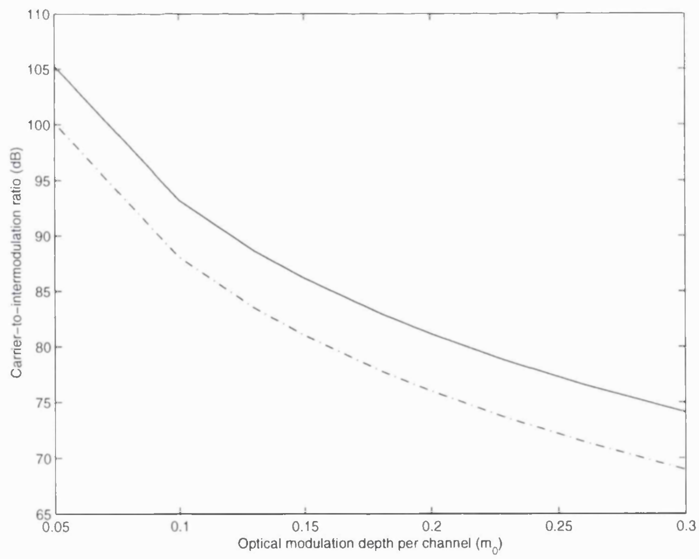

Figure 6.3: Carrier-to-Intermodulation ratio versus Optical modulation depth for three users (-) and five users (-.-)

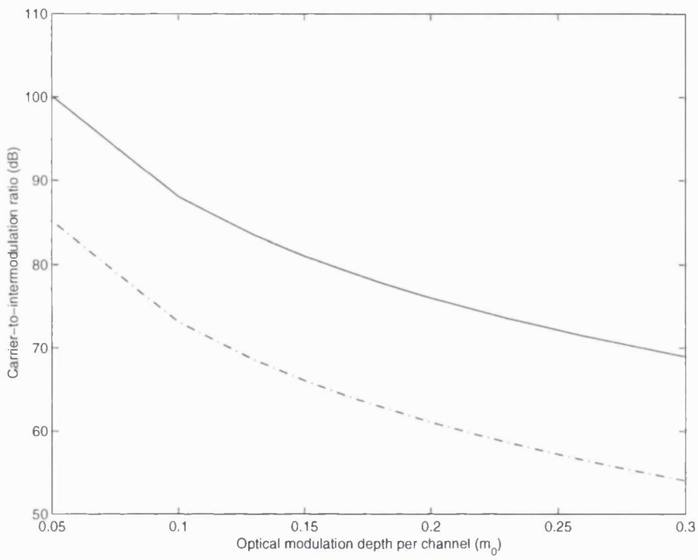

Figure 6.4: Carrier-to-Intermodulation ratio versus Optical modulation depth for bias current $I_0 = 40mA$ (-) and $I_0 = 55mA$ (-.-)

6.3 Fibre Optic Microcellular Radio

6.3.1 System Configuration

Microcellular systems have attracted much attention for fulfilling the rapidly increasing demand for mobile communications [68, 1]. It is well known that the microcellular system, composed of small-size cells with several hundred meter diameter communication range, promises effective frequency spectrum utilisation. However, compared to the conventional cellular systems, the microcellular system requires more base stations (BSs) for the same coverage; for example, more than 5000 base stations would be required in the Tokyo metropolitan area. Therefore, miniaturisation of BS's is an important issue in realising microcellular systems.

To make the BSs compact and cost-effective, it was proposed that fibre-optic feeders be used to transfer all the complicated demultiplexing and signal processing functions to a centralised control station. These considerations led us to envisage the use of microcells wherein the radio signals are radiated and received by many small BSs. Radio signals are transmitted over optical fibers between the BSs and the central station.

6.3.2 Multirate Radio Interface

In Europe, DS/CDMA for the future Universal Mobile Telecommunications System (UMTS) has been studied through the COde DIvision Testbed (CODIT) research project within the framework of the Research in Advanced Communications in Europe (RACE) program.

The overall objective of the COde DIvision Testbed project (RACE 2020) is to explore the potential of code division multiple access (CDMA) for a future high-capacity UMTS.

In fact CDMA has significant advantages in providing users with the bandwidth (bit rate) they need for a particular service. Such 'Bandwidth on Demand' can be achieved simply by varying the spreading factor according to the bit rate required. It is therefore very efficient to slice the total capacity 'cake' (Figure 6.5) in a CDMA system according to a mixed service scenario. The radio interface of third-generation mobile

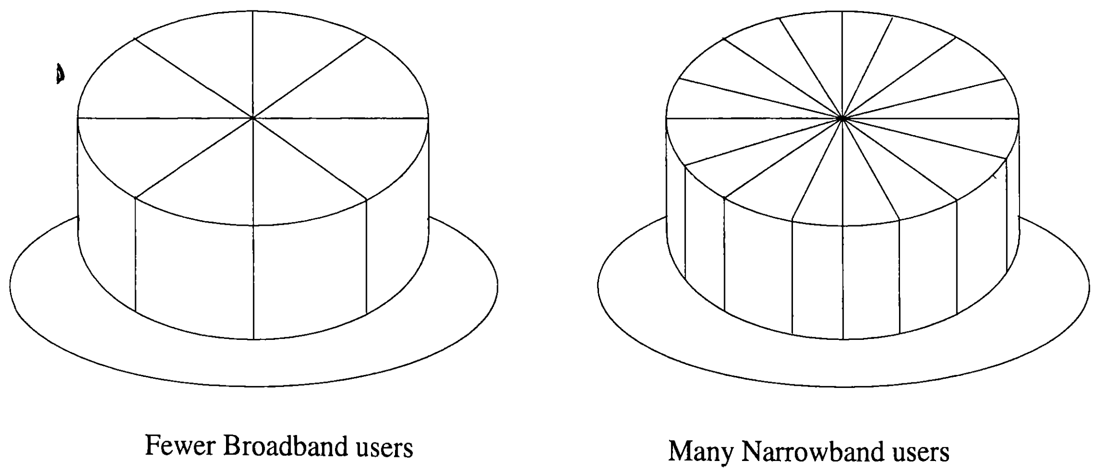

Figure 6.5: Flexibility of Services with CDMA

systems has to be capable of handling a wide selection of services with information bit rates from a few kb/s to as much as 2 Mb/s [16]. DS-CDMA has been shown to be well suited to support variable bit rate services, such as speech, in a spectrum efficient way [69]. Considering the issue of frequency and radio resource management in the light of third-generation multiple operator scenarios, it is obvious that this can hardly be achieved with a single radio frequency (RF) channel bandwidth. This, in particular, holds for CDMA where even moderate spreading factors applied to high information bit rates result in an enormous RF channel bandwidth difficult to provide and handle in cellular radio systems.

Rather than a single-bandwidth system, a CDMA system with multiple RF channel bandwidths seems to be the appropriate way to implement an open and flexible radio interface as required for third-generation systems [70]. In the CODIT project, a direct-sequence (DS) CDMA technique with three different chip rates is investigated [71], R_{c1} = 1.023 Mchip/s, R_{c2} = 5.112 Mchip/s, R_{c3} = 20.46 Mchip/s. The three chip rates correspond to three different RF channel bandwidth of approximately 1, 5, and 20 MHz, which are referred to as narrowband, mediumband, and wideband RF channels, respectively. A user bit rate can be mapped into one of the three chip rates/carrier, depending on the service requested or the RF allocation in operation. Figure 6.6 below shows how a user data bit rate can be mapped into one of the three chip rates. The combination of the three different RF bands enables a high degree of flexibility for an operator. The narrowband channel is suitable for speech and low data rate, which can be provided with a reasonable cell capacity. It also facilitates flexible spectrum allocation, as it only occupies a small portion of spectrum. The medium band channel offers a wider spectrum of services in which low-rate applications can be mixed with medium-rate applications. The wideband channel is mainly used in small cell environments with requirements for high data rates or a large number of users. In general a low rate user employing a large spreading gain can be mixed together with the signal for a high rate user with a lower spreading gain. The concept of multiple

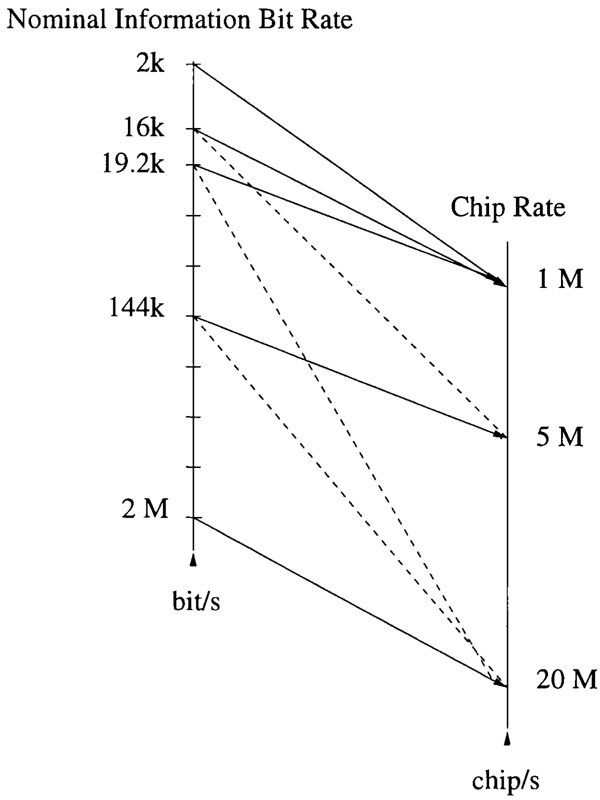

Figure 6.6: Flexible mapping of service bit rates onto chip rates in the CODIT concept

RF bandwidths allows for flexibility in operator spectrum allocations and in ability to mix-and-match services - e.g. a 10 MHz allocation being used for 2×5 MHz bands or 10×1bands.

Following this experience, ETSI has adopted Wideband DS-CDMA for the next generation of mobile communications systems. The RF channel bandwidth is of 5 MHz with an extension to 10 and 20 MHz in the future corresponding to chip rates of 4.096, 8.192 and 16.384 Mchip/s respectively. Obviously, the coding and spreading factor R_c/R_b and, hence, the coding and spreading gain achieved in the proposed transmission scheme varies with the information bit rate. Given a limited RF bandwidth or, equivalently, a fixed maximum chip rate, the system loses its CDMA characteristics more and more if the information bit rate is increased.

6.3.3 System Performance

We study the downlink channel of this system using the derivation of the last section. Different simulations are carried out for various spreading factor, data bit rate and channel spacings.

In Figure 6.7 CIR is plotted versus the optical modulation depth per channel for different services. We use an RF channel bandwidth of 5 MHz and a chip rate of 4.096 Mchip/s. Three different users centred respectively at $f_1 = 2.09$ GHz, $f_2 = 2.14$ GHz and $f_3 = 2.19$ GHz have been chosen. We plot the curves for four services: 32 kbps service with a spreading factor of 128, 64 kbps service with $SF = 32$, 144 kbps service with $SF = 16$ and 384 kbps service with $SF = 4$. We note that the CIR decrease with the increase of the rate service and the decrease of the spreading factor. In particular for the 384 kbps service the CIR is 15 dB lower than for the 32 kbps service. One way to overcome this effect is to increase the bandwidth allocation for each user. Figure 6.8 illustrates this option. Different RF channel bandwidths are considered for the 384 kbps service. Three curves are plotted representing RF channel bandwidths of 5, 10 and 20 MHz and spreading factors of 4, 8 and 16. An average of 6 dB is gained between the case of $SF = 4$ and the case of $SF = 16$. These results show that the allocation of the RF channel bandwidth in a network will depend on the services provided and the bandwidth available.

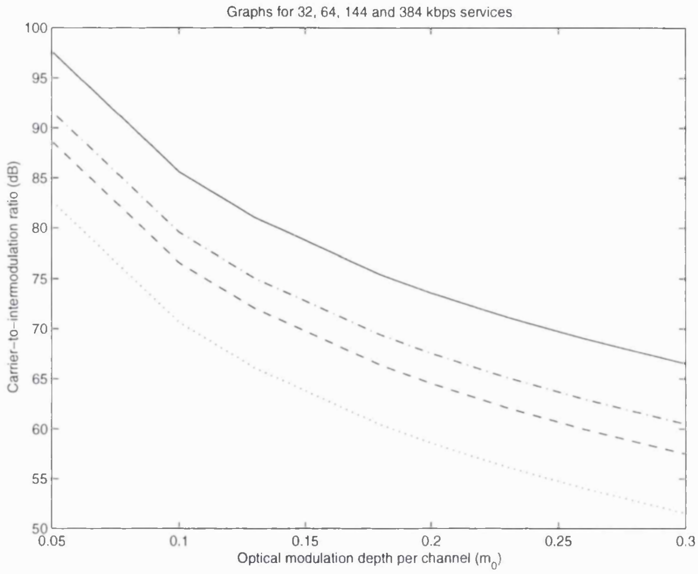

Figure 6.7: Carrier-to-Intermodulation ratio versus Optical modulation depth for four different services: 32 bkps (–), 64 bkps (-.-), 144 bkps (- -) and 384 bkps (...)

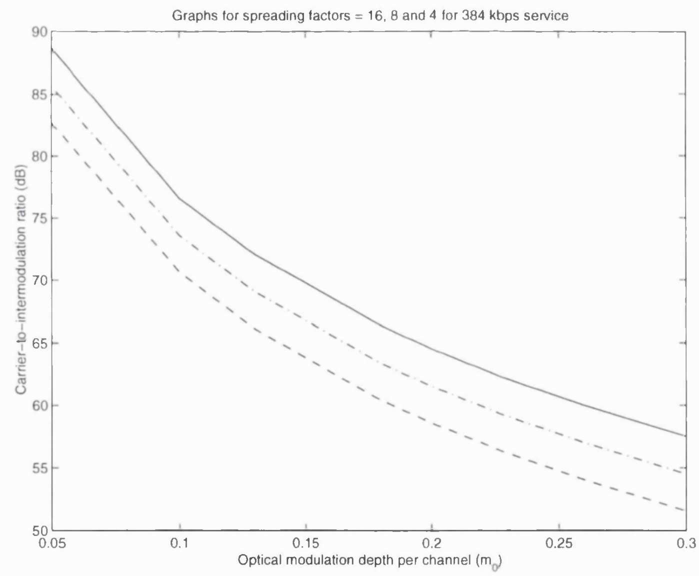

Figure 6.8: Carrier-to-Intermodulation ratio versus Optical modulation depth for 384 kbps service with RF channel bandwidths of 5 (- -), 10 (-.-) and 20 (—)

6.4 SCM/CDMA Fibre Radio return link

In the return optical link, the off-air received signals are used to modulate the laser. Accordingly, the link must be capable of supporting a wide dynamic range of power levels arising from range variations and fading associated with the mobile user. This imposes severe restrictions on laser nonlinearity to ensure that in-band intermodulation products (IMPs), which rapidly increase with the number of channels, are sufficiently suppressed relative to the carrier.

6.4.1 Fibre-Oriented Wireless Access System

While most conventional wireless systems have been constructed on the conception that it is desirable for the radio wave to propagate as far as possible, conversely, future wireless systems will be required to have the ability to confine the radio wave within a small zone, as in microcellular and picocellular systems, thereby enabling support for more channels and/or broadband services. In that sense, an optically-linked microcellular communication system with millimetre wave air interface would be promising in the future [72, 73]. This system shown in Figure 6.9, may be called FTTA (fibre-to-the area) by analogy with FFTH (fibre-to-the home) and FFTC (fibre-to-the curb).

In this FTTA system, radio base stations are connected with optical fibres and millimetre wave is used for radio interface within cells. Furthermore, each base station should be as simple as possible for future flexible deployment of the system. For instance, each radio base station in this system has only E/O and O/E converters, without an RF modulator and demodulator. Namely, the modulated millimetre waves transmitted from subscribers are directly put on the optical fibre without being converted into baseband signals. Instead, the complicated signal processing operations such as modulation, demodulation and frequency allotment, etc. are all done in a con-

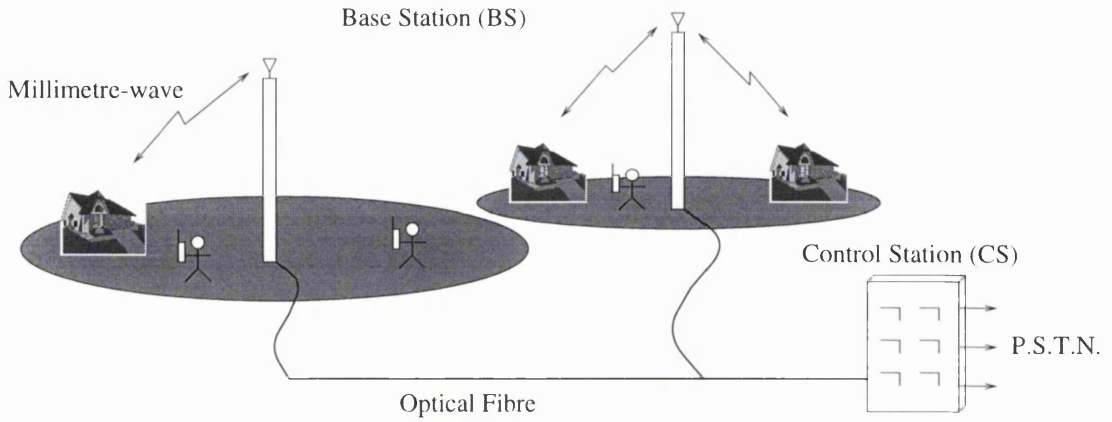

Figure 6.9: Fusion of millimetre wave radio and optical fibre systems

trol station.

In the area of mobile/portable communications, microcell applications - and some commercial systems - have been proposed. The main target of the applications is to deliver radio signals to blind areas such as tunnels and underground areas. Optical fibre links the master antenna located outdoors and the slave antennas located in the blind areas. Although large customers already have direct fibre access, there are requirements also for very cheap installation in the last mile to the residential customer and for user-friendly network termination equipment. Optical technology is very well suited for feeding an existing copper distribution network to form hybrid networks.

6.4.2 Expression of the Intermodulation Products

In this section we calculate the third-order IMPs when the input consists of a sum of N asynchronous channels.

The k^{th} mobile user that transmits data continuously and asynchronously (see Figure 6.10) is presented by the spread-spectrum signal $s_k(t-\tau_k)(k=1,2,...,K)$ as

$$s_k(t-\tau_k) = d_k(t-\tau_k)c_k(t-\tau_k)\cos(\omega_k t+\phi_k) \tag{6.31}$$

where ω_k is the center frequency of the k^{th} subcarrier, $\phi_k = \theta_k - \omega_k \tau_k$ with θ_k the phase of the k^{th} carrier $(0 \leq \theta_k \leq 2\pi)$, τ_k $(0 \leq \tau_k \leq T)$ is the time delay of the k^{th} user, and T is the bit duration. The bit data stream of the k^{th} user is given by

$$d_k(t) = \sum_{\ell=-\infty}^{\infty} d_\ell^{(k)} p_T(t - \ell T); \quad d_\ell^{(k)} \in \{-1, 1\} \tag{6.32}$$

where $d_\ell^{(k)}$ is a bit data value in the interval $[\ell T, (\ell+1)T]$, and $p_T(t) = 1$ for $0 \leq t \leq T$ and 0 otherwise. Each carrier is phase and amplitude coded by a waveform $c_k(t)$ given by

$$c_k(t) = \sum_{n=-\infty}^{\infty} c_n^{(k)} p_{T_c}(t - nT_c); \quad c_n^{(k)} \in \{-1, 1\} \tag{6.33}$$

where $c_n^{(k)}$ is a periodic binary sequence. Each bit is assumed to be encoded with N

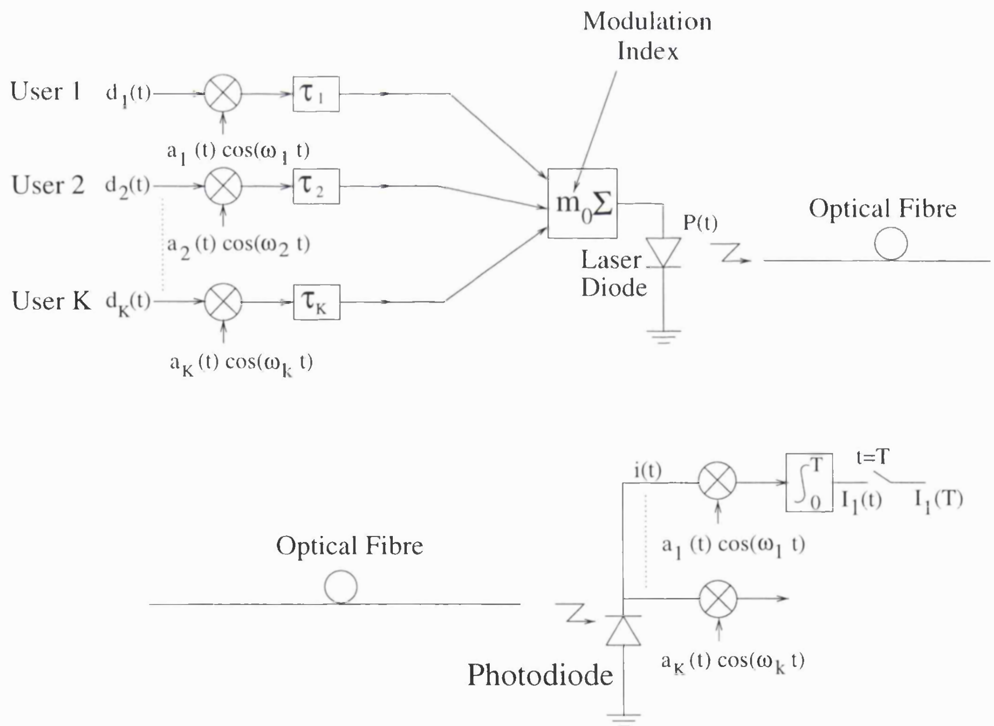

Figure 6.10: Model of SCM/CDMA system in optical communication

chips $(T = NT_c)$.

We represent the input current by

$$\begin{aligned} j(t) &= \sum_{k=1}^{K} j_k(t) \\ &= \sum_{k=1}^{K} d_k(t-\tau_k)c_k(t-\tau_k)\cos(\omega_k t + \phi_k) \\ &= \sum_{k=1}^{K} Re\{z_k(t-\tau_k)e^{(j2\pi\nu_k t)}\} \end{aligned} \tag{6.34}$$

with

$$z_k(t-\tau_k) = d_k(t-\tau_k)c_k(t-\tau_k)e^{j\phi_k} \tag{6.35}$$

The complex envelope of the nth-order intermodulation component falling at frequency ν due to signals centered at $\nu_{k1}, \cdots, \nu_{kn}$ is

$$q_{n\nu}(t) = \frac{n!2^{-n+1}}{m_{-N}! \cdots m_N!} H_n(\nu) \prod_{k=-N}^{N} [z_k(t)]^{m_k} \tag{6.36}$$

In the case of a CDMA system, the received signal is multiplied by a replica of the code of the desired user signal. Without loss of generality, assume that we are trying to receive the signal from user 1 and that $\theta_1 = 0$ and $\tau_1 = 0$. The receiver recovers the transmitted data bit by correlating the received signal with the signature sequence of user 1. The signal after this multiplication (or despreading operation) becomes

$$q'_{n\nu}(t) = \frac{n!2^{-n+1}}{m_{-N}! \cdots m_N!} H_n(\nu)c_1(t) \prod_{k=-N}^{N} [z_k(t-\tau_k)]^{m_k} \tag{6.37}$$

The required signal is given by

$$q'_{\nu}(t) = H_1(\nu)d_1(t) \tag{6.38}$$

Noticing that $d_k^2(t-\tau_k) = c_k^2(t-\tau_k) = 1$, we get for the second order

$$q'_{\nu_1-\nu_i}(t) = H_2(\nu_1-\nu_i)d_1(t)d_i(t-\tau_i)c_i(t-\tau_i)e^{i\phi_i} \tag{6.39}$$

$$q'_{\nu_i-\nu_1}(t) = H_2(\nu_i-\nu_1)d_1(t)d_i(t-\tau_i)c_i(t-\tau_i)e^{i\phi_i} \tag{6.40}$$

$$q'_{\nu_i-\nu_j}(t) = H_2(\nu_i-\nu_j)c_1(t)d_i(t-\tau_i)c_i(t-\tau_i)d_j(t-\tau_j)c_j(t-\tau_j)e^{i(\phi_i\pm\phi_j)} \quad (6.41)$$

For the third-order, we get

$$q'_{2\nu_1-\nu_i}(t) = \frac{3}{4}H_3(2\nu_1-\nu_i)c_1(t)d_i(t-\tau_i)c_i(t-\tau_i)e^{-i\phi_i} \quad (6.42)$$

$$q'_{2\nu_i-\nu_1}(t) = \frac{3}{4}H_3(2\nu_i-\nu_1)d_1(t)e^{i2\phi_i} \quad (6.43)$$

$$q'_{2\nu_i-\nu_j}(t) = \frac{3}{4}H_3(2\nu_i-\nu_j)c_1(t)c_j(t-\tau_j)d_j(t-\tau_j)e^{-i\phi_j} \quad (6.44)$$

$$q'_{\nu_1+\nu_i-\nu_j}(t) = \frac{3}{2}H_3(\nu_1+\nu_i-\nu_j)d_1(t)d_i(t-\tau_i)c_i(t-\tau_i) \\ d_j(t-\tau_j)c_j(t-\tau_j)e^{i(\phi_i-\phi_j)} \quad (6.45)$$

$$q'_{\nu_j+\nu_i-\nu_1}(t) = \frac{3}{2}H_3(\nu_i+\nu_j-\nu_1)d_1(t)d_i(t-\tau_i)e^{i(\phi_i+\phi_j)} \\ c_i(t-\tau_i)d_j(t-\tau_j)c_j(t-\tau_j) \quad (6.46)$$

$$q'_{\nu_i+\nu_j-\nu_k}(t) = \frac{3}{2}[H_3(\nu_i+\nu_j-\nu_k)]c_1(t)d_i(t-\tau_i)c_i(t-\tau_i) \\ d_j(t-\tau_j)c_j(t-\tau_j)d_k(t-\tau_k)c_k(t-\tau_k)e^{i(\phi_i+\phi_j-\phi_k)} \quad (6.47)$$

Next, we calculate the power spectral density of the different intermodulation terms.

6.4.3 Intermodulation Power Spectral Density

We start by calculating the Power Spectral Density (PSD) of the desired signal. We need to calculate first the autocorrelation function $R_{q_{n\nu}}(\tau)$ of $q_{n\nu}(t)$ defined as

$$R_{q_{n\nu}}(\tau) = E\{q^*_{n\nu}(t)q_{n\nu}(t+\tau)\} \quad (6.48)$$

which yields the desired PSD after Fourier transformation.

After despreading, the desired signal is a binary random process with values +1 and

-1. The autocorrelation function of such a signal is given by

$$R_q(\tau) = \begin{cases} 1 - \frac{\tau}{T}, & |\tau| < T \\ 0 & |\tau| \geq T \end{cases} \tag{6.49}$$

Using the Fourier transform of a triangle function, we obtain

$$S_q = T sinc^2(fT) \tag{6.50}$$

From equation (6.38), the PSD of the desired signal is

$$G'_{q_{\nu_1}}(f) = H_1^2(f) T sinc^2(fT) \tag{6.51}$$

For the intermodulation terms, the expression of the autocorrelation functions is more complex. The autocorrelation function can be written as

$$\begin{aligned} R_q(\tau) &= E[q(t)\ q(t+\tau)] \\ &= E\left\{ \sum_{m=-\infty}^{\infty} \sum_{n=-\infty}^{\infty} s_m\ s_{m+n}\ p_{T_c}(t - mT_c)\ p_{T_c}(t + \tau - (m+n)T_c) \right\} \\ &= \sum_{m=-\infty}^{\infty} \sum_{n=-\infty}^{\infty} E\left[s_m\ s_{m+n}\right] E\left\{ p_{T_c}(t - mT_c)\ p_{T_c}(t + \tau - (m+n)T_c) \right\} \\ &= \sum_{m=-\infty}^{\infty} R_m \frac{1}{T_c} \sum_{n=-\infty}^{\infty} \int_0^{T_c} p_{T_c}(t - mT_c)\ p_{T_c}(t + \tau - (m+n)T_c) d\tau \\ &= \sum_{m=-\infty}^{\infty} R_m \frac{1}{T_c} \int_0^{T_c} p_{T_c}(t)\ p_{T_c}(t + \tau - mT_c) d\tau \\ &= \sum_{m=-\infty}^{\infty} R_m\ r(\tau + mT_c) \end{aligned} \tag{6.52}$$

where

$$r(\tau) = \frac{1}{T} \int_{-\infty}^{\infty} p_{T_c}(t)\ p_{T_c}(t+\tau) d\tau \tag{6.53}$$

is the pulse-correlation function.

We start by giving the expression of the PSD of the second-intermodulation products.

For the first two terms, we obtain

$$G_{q_{\nu_1 - \nu_i}}(t) = H_2^2(\nu_1 - \nu_i) T_c sinc^2(fT_c) \tag{6.54}$$

$$G_{q_{\nu_i-\nu_1}}(t) = H_2^2(\nu_i - \nu_1)T_c sinc^2(fT_c) \tag{6.55}$$

For the last term introduced by the second-intermodulation, we present the result as follow

$$G_{q_{\nu_i-\nu_j}}(t) = H_2^2(\nu_i - \nu_j)[\tau_j sinc^2(f\tau_j) + (T_c - \tau_j)sinc^2(f(T_c - \tau_j))] \tag{6.56}$$

where we have assumed $\tau_i < \tau_j$.

For the third-intermodulation products, we are using the same method and we obtain for the different terms

$$G_{q_{\nu_i\nu_i\nu_1}}(f) = \frac{9}{16}H_3^2(2\nu_i - \nu_1)T sinc^2(fT) \tag{6.57}$$

$$G_{q_{\nu_1\nu_1\nu_i}}(f) = \frac{9}{16}H_3^2(2\nu_1 - \nu_i)[\tau_i sinc^2(f\tau_i) + (T_c - \tau_i)sinc^2(f(T_c - \tau_i))] \tag{6.58}$$

$$G_{q_{\nu_i\nu_i\nu_j}}(f) = \frac{9}{16}H_3^2(2\nu_i - \nu_j)[\tau_j sinc^2(f\tau_j) + (T_c - \tau_j)sinc^2(f(T_c - \tau_j))] \tag{6.59}$$

$$\begin{aligned} G_{q_{\nu_1\nu_i\nu_j}}(f) &= \frac{9}{4}H_3^2(\nu_1 + \nu_i - \nu_j)[\tau_i sinc^2(f\tau_i) + (T_j - \tau_i)sinc^2(f(T_j - \tau_i)) \\ &\quad +(T_c - \tau_j)sinc^2(f(T_c - \tau_j))] \end{aligned} \tag{6.60}$$

$$\begin{aligned} G_{q_{\nu_i\nu_j\nu_k}}(f) &= \frac{9}{4}H_3^2(\nu_i + \nu_j - \nu_k)\frac{1}{10N}[\tau_i sinc^2(f\tau_i) + (\tau_j - \tau_i)sinc^2(f(\tau_j - \tau_i)) \\ &\quad +(\tau_k - \tau_j)sinc^2(f(\tau_k - \tau_j)) + (T_c - \tau_k)sinc^2(f(T_c - \tau_k))] \end{aligned} \tag{6.61}$$

6.4.4 System Performance

In this section, we present simulation results based of parameters taken from the WCDMA system of UMTS. The study is done for the return link or the forward link of this system. The frequency band reserve to it is comprises between 2110 and 2170 MHz. In Figure 6.11, a system with three users at frequency centred respectively at

2135, 2140 and 2145 MHz is considered. The CIR is plotted for two different sets of time delays between the users. We can notice that the distribution of the time delays inside the chip duration T_c has an influence around 1.5 dB. In Figure 6.12, the CIR is given for three users with frequencies around 2110 MHz, 2140 MHz, and 2170 MHz. We see that the CIR decreases with the increase of the frequencies. A comparison with curve of 32 kbps service of Figure 6.7 shows that the gain of a synchronous system relative to an asynchronous one is about 2 dB.

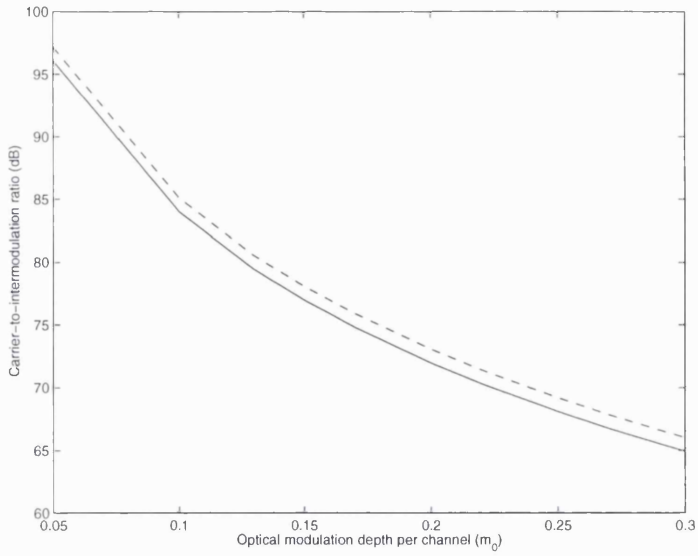

Figure 6.11: Carrier-to-Intermodulation ratio versus Optical modulation depth for two different sets of time delays: $\tau_i = 1/4\ T_c$, $\tau_j = 1/2\ T_c$ and $\tau_k = 3/4\ T_c$ (–); $\tau_i = 1/40\ T_c$, $\tau_j = 1/30\ T_c$, $\tau_k = 1/20\ T_c$ (- -).

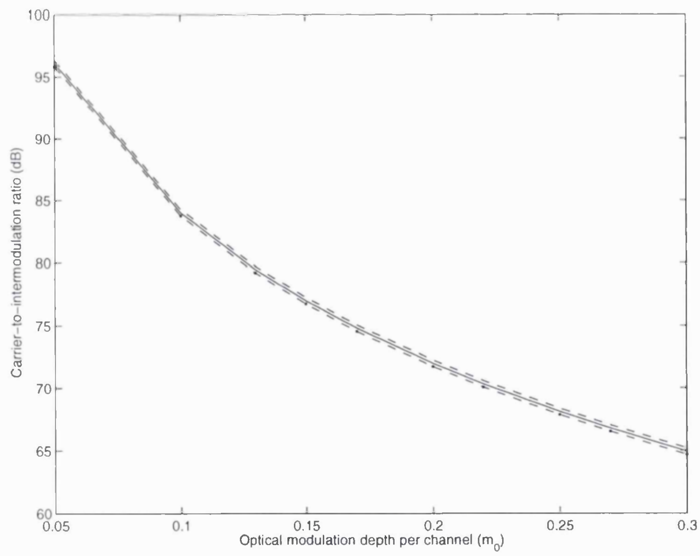

Figure 6.12: Carrier-to-Intermodulation ratio versus Optical modulation depth for frequencies taken for three different bands: 2110 MHz (- -), 2140 MHz (–) and 2170 MHz (- .-).

6.5 Summary

In this chapter, we have used the method described in chapter 5 to assess the effect of laser diode nonlinearity in two SCM/CDMA case studies. In the case of flexible multirate system, we see that there is a trade-off between the spreading factor used and the bandwidth allocated. From this consideration, it can be said that the choice of the network infrastructure has impact on the system capacity.

For the return (or forward) link of Fibre-Optic microcellular system, we have shown that the CIR is affected by the distribution of the time delays between the users and the frequency band chosen.

Chapter 7

Concluding Remarks

Wireless communications is in the process of revolutionising telecommunications services and the way people use them. Future wireless systems will have the ability to support more channels and/or broadband services than present day system. The introduction of the fibre-radio technology in such a system provide flexible and cost effective networks. Code Division Multiple Access (CDMA) is a promising Spread Spectrum technique for radio access in future cellular and personal communications systems. Therefore, the aim of this thesis has been to assess the impact of laser diode intermodulation products on CDMA signals via optical fibre.

Chapter 2 began by presenting a review of the different standards used in the first and second generation wireless communications systems. We then presented the current status of the third generation standard and the new generation of wireless communications based on fibre-radio technologies. We also described the multiple access methods employed in wireless systems.

In chapter 3 we introduced the Spread Spectrum technology and its applications. Special attention was given to the most commonly deployed technique called either Direct Sequence (DS) or CDMA. Following this presentation, a fibre-optic CDMA system has been assessed using Alta's Signal Processing Worksystem (SPW) simulation framework. From simulation results we noted that the performance of the system was deteriorated because of the intermodulation terms introduced by the laser diode used for the electrical-to- optical conversion.

In chapter 4 we addressed the impact of laser diode nonlinearity on system performance. This nonlinearity is modeled initially by a memoryless third-order polynomial. From this theory we derived the expression of the intermodulations terms for an asynchronous CDMA system with unequal power transmission. From the evaluation of the system performance, we noticed that there exists an optimal modulation index providing better BER.

A detailed analytic model based on the Volterra series method of nonlinear systems theory is developed in chapter 5 for the case of SubCarrier Multiplexing (SCM) CDMA systems. Following the presentation of the method, the nonlinear transfer functions of the laser diode are determined and used to derive performance results for SCM/CDMA systems.

The results of chapter 5 are used in chapter 6 to assess the performance of different configurations of SCM/CDMA systems. The downlink channel of a wireless local loop system is first considered. We then separated the study of mobile radio systems into two cases: the downlink channel of a flexible data rate system and the forward link of a system based on the Universal Mobile Telecommunications System.

The research summarised above suggests several possible directions for future investigations. Firstly, it is clear that there is considerable scope for employing 'radio over fibre' techniques to support a variety of wireless system applications, but that careful modelling and study of laser non-linearities is imperative. The general methods and ideas introduced and explored in this thesis may be developed further for other such specific applications. As just three examples of specific topics deserving investigation, the following are suggested:

- Using the method described in Chapter 4, the effect of imperfect power control on SCM/CDMA systems could be derived.

- Effect of the Laser Diode Nonlinearity on Frequency Hopping CDMA systems deserves examination.

- An assessment is required of the effect of the Laser Diode Nonlinearity on SCM/CDMA systems using Orthogonal Optical Codes.

It should be emphasised, though, that radio over fibre exploiting CDMA or other 'multi-path tolerant' wideband modulation schemes (such as orthogonal frequency division multiplexing (OFDM) combined with CDMA) is a powerful new arrangment which it is considered deserving new serious consideration for wireless system applications. It is hoped that this thesis has contributed usefully and pointed a direction for such further studies.

Appendix A

Multi-User Interference

Here, we calculate the multi-user interference for binary signature sequences in an asynchronous spread spectrum multiple access communication system.

For asynchronous systems the received signal $r(t)$ at the receiver is given by

$$r(t) = \sum_{k=1}^{K} a_k(t-\tau)d_k(t-\tau)\cos(\omega_c t + \phi_k) \tag{A.1}$$

where $\phi_k = \theta_k - \omega_c\tau_k$.

Since we are concerned with relative shifts modulo 2π and relative time delays modulo T, there is no loss in generality in assuming $\theta_i = 0$ and $\tau_i = 0$ and considering only $0 \le \tau_k < T$ and $0 \le \theta_k < 2\pi$ for $k \neq i$.

If the received signal $r(t)$ is the input to a correlation receiver matched to $s_i(t)$, the output is

$$Z_i = \int_0^T r(t)a_i(t)\cos(\omega_c t)dt \tag{A.2}$$

The output of the correlation receiver at $t = T$ is given by

$$Z_i = b_{i,0}T + \sum_{\substack{k=1,\\ k\neq i}}^{K} [b_{k,-1}R_{k,i}(\tau_k) + b_{k,0}\hat{R}_{k,i}(\tau_k)]\cos\phi_k \tag{A.3}$$

where $R_{k,i}$ and $\hat{R}_{k,i}$ are the continuous-time partial cross-correlation functions defined by

$$R_{k,i}(\tau) = \int_0^\tau a_k(t-\tau)a_i(t)dt \tag{A.4}$$

$$\hat{R}_{k,i}(\tau) = \int_\tau^T a_k(t-\tau)a_i(t)dt \tag{A.5}$$

for $0 \leq \tau \leq T$. It is easy to see that for $0 \leq lT_c \leq \tau \leq (l+1)T_c \leq T$, these two cross-correlation functions can be written as

$$R_{k,i}(\tau) = C_{k,i}(l-N)T_c + \Big[C_{k,i}(l+1-N) - C_{k,i}(l-N)\Big](\tau - lT_c) \tag{A.6}$$

and

$$\hat{R}_{k,i}(\tau) = C_{k,i}(l)T_c + \Big[C_{k,i}(l+1) - C_{k,i}(l)\Big](\tau - lT_c) \tag{A.7}$$

where the discrete aperiodic cross-correlation function $C_{k,i}$ for the sequences $(a_j^{(k)})$ and $(a_j^{(i)})$ is defined by

$$C_{k,i}(l) = \begin{cases} \sum_{j=0}^{N-1-l} a_j^{(k)} a_{j+l}^{(i)}, & 0 \leq l \leq N-1 \\ \sum_{j=0}^{N-1-l} a_{j-l}^{(k)} a_j^{(i)}, & 1-N \leq l \leq 0 \\ 0, & |l| \geq N \end{cases} \tag{A.8}$$

The periodic cross-correlation function $\theta_{k,i}$ is given by

$$\theta_{k,i}(l) = \sum_{j=0}^{N-1} a_j^{(k)} a_{j+l}^{(i)} \tag{A.9}$$

for any integer l. Notice that $\theta_{k,i}(l) = C_{k,i}(l) + C_{k,i}(l-N)$ for $0 \leq l < N$. We also define $\hat{\theta}_{k,i}(l) = C_{k,i}(l) - C_{k,i}(l-N)$ for $0 \leq l < N$. The function $\hat{\theta}_{k,i}$ is called the odd cross-correlation function by Massey and Uhran since it has the property $\hat{\theta}_{k,i}(l) = -\hat{\theta}_{k,i}(N-l)$ whereas the periodic (or even) cross-correlation function satisfies $\theta_{k,i}(l) = \theta_{k,i}(N-l)$.

Both of these relationships follow from the observation that $C_{k,i}(l) = C_{k,i}(-l)$.

The variance of the interference component of Z_i is

$$\begin{aligned} Var\{Z_i\} &= \frac{1}{T}\sum_{\substack{k=1,\\k\neq i}}^{K}\int_0^T [R_{k,i}^2(\tau) + \hat{R}_{k,i}^2(\tau_k)]d\tau \\ &= \frac{1}{T}\sum_{\substack{k=1,\\k\neq i}}^{K}\sum_{l=0}^{N-1}\int_{lT_c}^{(l+1)T_c}[R_{k,i}^2(\tau) + \hat{R}_{k,i}(\tau_k)]d\tau \end{aligned} \quad (A.10)$$

We next substitute for $R_{k,i}(\tau)$ and $\hat{R}_{k,i}(\tau_k)$ from (A.6) and (A.7) into (A.10). Upon evaluating the resulting integral we find that

$$Var\{Z_i\} = \frac{T^2}{3N^3}\sum_{\substack{k=1,\\k\neq i}}^{K} r_{k,i} \quad (A.11)$$

where

$$\begin{aligned} r_{k,i} = \sum_{l=0}^{N-1}\{C_{k,i}^2(l-N) + C_{k,i}(l-N)C_{k,i}(l-N+1) + C_{k,i}^2(l-N+1) \\ + C_{k,i}^2(l) + C_{k,i}(l)C_{k,i}(l+1) + C_{k,i}^2(l+1)\} \end{aligned} \quad (A.12)$$

This last expression can be written in terms of the cross-correlation parameters $\mu_{k,i}(n)$ which are defined by

$$\mu_{k,i}(n) = \sum_{l=1-N}^{N-1} C_{k,i}(l)C_{k,i}(l+n) \quad (A.13)$$

Notice that

$$\begin{aligned} \mu_{k,i}(0) = \sum_{l=1-N}^{N-1} C_{k,i}^2(l) &= \sum_{l=0}^{N-1} C_{k,i}^2(l-N) + C_{k,i}^2(l) \\ &= \sum_{l=0}^{N-1} C_{k,i}^2(l-N+1) + C_{k,i}^2(l+1) \end{aligned} \quad (A.14)$$

and

$$\begin{aligned} \mu_{k,i}(1) &= \sum_{l=1-N}^{N-1} C_{k,i}(l)C_{k,i}(l+1) \\ &= \sum_{l=0}^{N-1} C_{k,i}(l-N)C_{k,i}(l-N+1) + C_{k,i}(l)C_{k,i}(l+1) \end{aligned} \quad (A.15)$$

Therefore

$$r_{k,i} = 2\mu_{k,i}(0)1) + \mu_{k,i}(1) \tag{A.16}$$

For binary sequences, we consider the special case $k = i$ and obtain

$$\sum_{l=1-N}^{N-1} C_{k,i}(l)C_{k,i}(l+n) = \sum_{l=1-N}^{N-1} C_k(l)C_i(l+n) \tag{A.17}$$

In particular

$$\mu_{k,i}(0) = \sum_{l=1-N}^{N-1} C_{k,i}^2(l) = N^2 + 2\sum_{l=1}^{N-1} C_k(l)C_i(l) \tag{A.18}$$

since $C_k(0) = C_i(0) = N$. The corresponding bounds based on the Cauchy inequality become

$$N^2 - 2\{S_k S_i\}^{1/2} \leq \mu_{k,i}(0) \leq N^2 + 2\{S_k S_i\}^{1/2} \tag{A.19}$$

where

$$S_k = \sum_{l=1}^{N-1} C_k^2(l), S_i = \sum_{l=1}^{N-1} C_i^2(l) \tag{A.20}$$

From (A.16), it is easy to see that

$$r_{k,i} = 2N^2 + 4\sum_{l=1}^{N-1} C_k(l)C_i(l) + \sum_{l=1-N}^{N-1} C_k(l)C_i(l+1) \tag{A.21}$$

Using the Cauchy inequality, one can obtain $4N^2 + 6\{S_k S_i\}^{1/2}$ as an upper bound on $r_{k,i}$. Fot most applications, however, the approximation $r_{k,i} = 2\mu_{k,i}(0)$ is quite satisfactory even for moderate values of N, and the upper bound on $r_{k,i}$ is a gross overestimate.

For our derivations, we use the result $r_{k,i} = 2N^2$ for the multi-user interference.

Appendix B

Derivation of the Third-Order-Intermodulation Terms for CDMA Systems with QPSK Modulation

In this appendix, we derive the expression of the third-order intermodulation terms for QPSK case system.

The k^{th} mobile user that transmits data continuously and asynchronously is presented by the Spread-spectrum signal $s_k(t-\tau_k)(k=1,2,...,K)$ as (see Figure 4.6)

$$s_k(t) = \Big(d_{1k}(t-\tau_k)a_{1k}(t-\tau_k)\cos(\omega_c t+\phi_k) \\ +d_{2k}(t-\tau_k)a_{2k}(t-\tau_k)\sin(\omega_c t+\phi_k)\Big) \tag{B.1}$$

where ω_c is the common centre frequency, ϕ_k is the phase of the k^{th} carrier, τ_k is the time delay of the k^{th} user and T is a bit duration.

The third-order IMD is generated by the X^3 term for the K mobile users sum of the signal B.1. Using the following relation

$$\begin{aligned}\left[\sum_{k=1}^{K} x_k\right]^3 &= \sum_{k=1}^{K} x_k^3 + 3x_1^2 \sum_{k=2}^{K} x_k + 3x_1 \sum_{k=2}^{K} x_k^2 \\ &\quad +3\sum_{j=2}^{K}\sum_{\substack{k=2\\k\neq j}}^{K} x_j^2 x_k + 3x_1 \sum_{j=2}^{K}\sum_{\substack{k=2\\k\neq j}}^{K} x_j x_k + \sum_{i=2}^{K}\sum_{\substack{j=2\\j\neq i}}^{K}\sum_{\substack{k=2\\k\neq i,j}}^{K} x_i x_j x_k \qquad \text{(B.2)}\end{aligned}$$

For the different terms, we get

$$\begin{aligned}\sum_{k=1}^{K} s_k^3 = \frac{3}{2} m_0^3 \sum_{k=1}^{K} p_k^3 \Big(& d_{1k}(t-\tau_k) a_{1k}(t-\tau_k)\cos(\omega_c t + \phi_k) \\ &+ d_{2k}(t-\tau_k) a_{2k}(t-\tau_k)\sin(\omega_c t + \phi_k)\Big) \qquad \text{(B.3)}\end{aligned}$$

$$\begin{aligned}3s_1^2 \sum_{k=2}^{K} s_k = 3m_0^3 p_1^2 \sum_{k=2}^{K} p_k \Bigg[&\Big(d_{1k}(t-\tau_k) a_{1k}(t-\tau_k)\cos(\omega_c t + \phi_k) \\ &+ d_{2k}(t-\tau_k) a_{2k}(t-\tau_k)\sin(\omega_c t + \phi_k)\Big) \\ &+\frac{1}{2} d_{11}(t) a_{11}(t) d_{21}(t) a_{21}(t)\Big(d_{1k}(t-\tau_k) a_{1k}(t-\tau_k)\sin(\omega_c t - \phi_k) \\ &+ d_{2k}(t-\tau_k) a_{2k}(t-\tau_k)\cos(\omega_c t - \phi_k)\Big)\Bigg] \qquad \text{(B.4)}\end{aligned}$$

$$\begin{aligned}3s_1 \sum_{k=2}^{K} s_k^2 = 3m_0^3 p_1 \sum_{k=2}^{K} p_k^2 \Bigg[&\Big(d_{11}(t) a_{11}(t)\cos(\omega_c t) + d_{21}(t) a_{21}(t)\sin(\omega_c t)\Big) \\ &+\frac{1}{2} d_{1k}(t-\tau_k) a_{1k}(t-\tau_k) d_{2k}(t-\tau_k) a_{2k}(t-\tau_k)\Big(d_{11}(t) a_{11}(t)\sin(\omega_c t + 2\phi_k) \\ &+ d_{21}(t) a_{21}(t)\cos(\omega_c t + 2\phi_k)\Big)\Bigg] \qquad \text{(B.5)}\end{aligned}$$

$$\begin{aligned}3\sum_{j=2}^{K}\sum_{\substack{k=2\\k\neq j}}^{K} s_j^2 s_k = 3m_0^3 \sum_{j=2}^{K}\sum_{\substack{k=2\\k\neq j}}^{K} p_j^2 p_k \Bigg[&\Big(d_{1k}(t-\tau_k) a_{1k}(t-\tau_k)\cos(\omega_c t + \phi_k) \\ &+ d_{2k}(t-\tau_k) a_{2k}(t-\tau_k)\sin(\omega_c t + \phi_k)\Big) \\ &+\frac{1}{2} d_{1j}(t-\tau_j) a_{1j}(t-\tau_j) d_{2j}(t-\tau_j) a_{2j}(t-\tau_j) \\ &\Big(d_{1k}(t-\tau_k) a_{1k}(t-\tau_k)\sin(\omega_c t + 2\phi_j - \phi_k) \\ &+ d_{2k}(t-\tau_k) a_{2k}(t-\tau_k)\cos(\omega_c t + 2\phi_j - \phi_k)\Big)\Bigg] \qquad \text{(B.6)}\end{aligned}$$

The term $3s_1 \sum\limits_{j=2}^{K} \sum\limits_{\substack{k=2 \\ k\neq j}}^{K} s_j s_k$ gives

$$
\begin{aligned}
&\frac{3}{4} m_0^3 p_1 \sum_{j=2}^{K} \sum_{\substack{k=2 \\ k\neq j}}^{K} p_j p_k \\
&\qquad \Big[\Big(a_{1j}(t-\tau_j) a_{1k}(t-\tau_k) a_{11}(t-\tau_1) d_{1j}(t-\tau_j) d_{1k}(t-\tau_k) d_{11}(t-\tau_1) \\
&\qquad + a_{11}(t-\tau_1) a_{2j}(t-\tau_j) a_{2k}(t-\tau_k) d_{11}(t-\tau_1) d_{2j}(t-\tau_j) d_{2k}(t-\tau_k) \\
&\qquad + a_{1k}(t-\tau_k) a_{2j}(t-\tau_j) a_{21}(t-\tau_1) d_{1k}(t-\tau_k) d_{2j}(t-\tau_j) d_{21}(t-\tau_1) \\
&\qquad - a_{1j}(t-\tau_j) a_{2k}(t-\tau_k) a_{21}(t-\tau_1) d_{1j}(t-\tau_j) d_{2k}(t-\tau_k) d_{21}(t-\tau_1) \Big) \\
&\qquad \cos(\omega_c t + \phi_1 - \phi_j + \phi_k) \\
&\qquad + \Big(a_{1j}(t-\tau_j) a_{1k}(t-\tau_k) a_{11}(t-\tau_1) d_{1j}(t-\tau_j) d_{1k}(t-\tau_k) d_{11}(t-\tau_1) \\
&\qquad - a_{11}(t-\tau_1) a_{2j}(t-\tau_j) a_{2k}(t-\tau_k) d_{11}(t-\tau_1) d_{2j}(t-\tau_j) d_{2k}(t-\tau_k) \\
&\qquad + a_{1k}(t-\tau_k) a_{2j}(t-\tau_j) a_{21}(t-\tau_1) d_{1k}(t-\tau_k) d_{2j}(t-\tau_j) d_{21}(t-\tau_1) \\
&\qquad + a_{1j}(t-\tau_j) a_{2k}(t-\tau_k) a_{21}(t-\tau_1) d_{1j}(t-\tau_j) d_{2k}(t-\tau_k) d_{21}(t-\tau_1) \Big) \\
&\qquad \cos(\omega_c t - \phi_1 + \phi_j + \phi_k) \\
&\qquad + \Big(a_{1j}(t-\tau_j) a_{1k}(t-\tau_k) a_{11}(t-\tau_1) d_{1j}(t-\tau_j) d_{1k}(t-\tau_k) d_{11}(t-\tau_1) \\
&\qquad + a_{11}(t-\tau_1) a_{2j}(t-\tau_j) a_{2k}(t-\tau_k) d_{11}(t-\tau_1) d_{2j}(t-\tau_j) d_{2k}(t-\tau_k) \\
&\qquad - a_{1k}(t-\tau_k) a_{2j}(t-\tau_j) a_{21}(t-\tau_1) d_{1k}(t-\tau_k) d_{2j}(t-\tau_j) d_{21}(t-\tau_1) \\
&\qquad + a_{1j}(t-\tau_j) a_{2k}(t-\tau_k) a_{21}(t-\tau_1) d_{1j}(t-\tau_j) d_{2k}(t-\tau_k) d_{21}(t-\tau_1) \Big) \\
&\qquad \cos(\omega_c t + \phi_1 + \phi_j - \phi_k) \\
&\qquad - \Big(a_{1k}(t-\tau_k) a_{11}(t-\tau_1) a_{2j}(t-\tau_j) d_{1k}(t-\tau_k) d_{11}(t-\tau_1) d_{2j}(t-\tau_j) \\
&\qquad - a_{1j}(t-\tau_j) a_{11}(t-\tau_1) a_{2k}(t-\tau_k) d_{1j}(t-\tau_j) d_{11}(t-\tau_1) d_{2k}(t-\tau_k) \\
&\qquad - a_{1j}(t-\tau_j) a_{1k}(t-\tau_k) a_{21}(t-\tau_1) d_{1j}(t-\tau_j) d_{1k}(t-\tau_k) d_{21}(t-\tau_1) \\
&\qquad - a_{2j}(t-\tau_j) a_{2k}(t-\tau_k) a_{21}(t-\tau_1) d_{2j}(t-\tau_j) d_{2k}(t-\tau_k) d_{21}(t-\tau_1) \Big) \\
&\qquad \sin(\omega_c t + \phi_1 - \phi_j + \phi_k)
\end{aligned}
$$

$$+\Big(a_{1k}(t-\tau_k)a_{11}(t-\tau_1)a_{2j}(t-\tau_j)d_{1k}(t-\tau_k)d_{11}(t-\tau_1)d_{2j}(t-\tau_j)$$
$$+a_{1j}(t-\tau_j)a_{11}(t-\tau_1)a_{2k}(t-\tau_k)d_{1j}(t-\tau_j)d_{11}(t-\tau_1)d_{2k}(t-\tau_k)$$
$$-a_{1j}(t-\tau_j)a_{1k}(t-\tau_k)a_{21}(t-\tau_1)d_{1j}(t-\tau_j)d_{1k}(t-\tau_k)d_{21}(t-\tau_1)$$
$$+a_{2j}(t-\tau_j)a_{2k}(t-\tau_k)a_{21}(t-\tau_1)d_{2j}(t-\tau_j)d_{2k}(t-\tau_k)d_{21}(t-\tau_1)\Big)$$
$$\sin(\omega_c t-\phi_1+\phi_j+\phi_k)$$
$$+\Big(a_{1k}(t-\tau_k)a_{11}(t-\tau_1)a_{2j}(t-\tau_j)d_{1k}(t-\tau_k)d_{11}(t-\tau_1)d_{2j}(t-\tau_j)$$
$$-a_{1j}(t-\tau_j)a_{11}(t-\tau_1)a_{2k}(t-\tau_k)d_{1j}(t-\tau_j)d_{11}(t-\tau_1)d_{2k}(t-\tau_k)$$
$$+a_{1j}(t-\tau_j)a_{1k}(t-\tau_k)a_{21}(t-\tau_1)d_{1j}(t-\tau_j)d_{1k}(t-\tau_k)d_{21}(t-\tau_1)$$
$$+a_{2j}(t-\tau_j)a_{2k}(t-\tau_k)a_{21}(t-\tau_1)d_{2j}(t-\tau_j)d_{2k}(t-\tau_k)d_{21}(t-\tau_1)\Big)$$
$$\sin(\omega_c t+\phi_1+\phi_j-\phi_k)\Big] \quad \text{(B.7)}$$

The term $\sum_{i=2}^{K}\sum_{\substack{j=2\\ j\neq i}}^{K}\sum_{\substack{k=2\\ k\neq i,j}}^{K} S_iS_jS_k$ gives

$$\frac{1}{4}m_0^3\sum_{i=2}^{K}\sum_{\substack{j=2\\ j\neq i}}^{K}\sum_{\substack{k=2\\ k\neq i,j}}^{K} p_ip_jp_k$$
$$\Big[\Big(a_{1j}(t-\tau_j)a_{1k}(t-\tau_k)a_{1i}(t-\tau_i)d_{1j}(t-\tau_j)d_{1k}(t-\tau_k)d_{1i}(t-\tau_i)$$
$$+a_{1i}(t-\tau_i)a_{2j}(t-\tau_j)a_{2k}(t-\tau_k)d_{1i}(t-\tau_i)d_{2j}(t-\tau_j)d_{2k}(t-\tau_k)$$
$$+a_{1k}(t-\tau_k)a_{2j}(t-\tau_j)a_{2i}(t-\tau_i)d_{1k}(t-\tau_k)d_{2j}(t-\tau_j)d_{2i}(t-\tau_i)$$
$$-a_{1j}(t-\tau_j)a_{2k}(t-\tau_k)a_{2i}(t-\tau_i)d_{1j}(t-\tau_j)d_{2k}(t-\tau_k)d_{2i}(t-\tau_i)\Big)$$
$$\cos(\omega_c t+\phi_i-\phi_j+\phi_k)$$
$$+\Big(a_{1j}(t-\tau_j)a_{1k}(t-\tau_k)a_{1i}(t-\tau_i)d_{1j}(t-\tau_j)d_{1k}(t-\tau_k)d_{1i}(t-\tau_i)$$
$$-a_{1i}(t-\tau_i)a_{2j}(t-\tau_j)a_{2k}(t-\tau_k)d_{1i}(t-\tau_i)d_{2j}(t-\tau_j)d_{2k}(t-\tau_k)$$
$$+a_{1k}(t-\tau_k)a_{2j}(t-\tau_j)a_{2i}(t-\tau_i)d_{1k}(t-\tau_k)d_{2j}(t-\tau_j)d_{2i}(t-\tau_i)$$
$$+a_{1j}(t-\tau_j)a_{2k}(t-\tau_k)a_{2i}(t-\tau_i)d_{1j}(t-\tau_j)d_{2k}(t-\tau_k)d_{2i}(t-\tau_i)\Big)$$
$$\cos(\omega_c t-\phi_i+\phi_j+\phi_k)$$

$$
\begin{aligned}
&+\Big(a_{1j}(t-\tau_j)a_{1k}(t-\tau_k)a_{1i}(t-\tau_i)d_{1j}(t-\tau_j)d_{1k}(t-\tau_k)d_{1i}(t-\tau_i)\\
&\quad +a_{1i}(t-\tau_i)a_{2j}(t-\tau_j)a_{2k}(t-\tau_k)d_{1i}(t-\tau_i)d_{2j}(t-\tau_j)d_{2k}(t-\tau_k)\\
&\quad -a_{1k}(t-\tau_k)a_{2j}(t-\tau_j)a_{2i}(t-\tau_i)d_{1k}(t-\tau_k)d_{2j}(t-\tau_j)d_{2i}(t-\tau_i)\\
&+a_{1j}(t-\tau_j)a_{2k}(t-\tau_k)a_{2i}(t-\tau_i)d_{1j}(t-\tau_j)d_{2k}(t-\tau_k)d_{2i}(t-\tau_i)\Big)\\
&\hfill \cos(\omega_c t+\phi_i+\phi_j-\phi_k)\\
&-\Big(a_{1k}(t-\tau_k)a_{1i}(t-\tau_i)a_{2j}(t-\tau_j)d_{1k}(t-\tau_k)d_{1i}(t-\tau_i)d_{2j}(t-\tau_j)\\
&\quad -a_{1j}(t-\tau_j)a_{1i}(t-\tau_i)a_{2k}(t-\tau_k)d_{1j}(t-\tau_j)d_{1i}(t-\tau_i)d_{2k}(t-\tau_k)\\
&\quad -a_{1j}(t-\tau_j)a_{1k}(t-\tau_k)a_{2i}(t-\tau_i)d_{1j}(t-\tau_j)d_{1k}(t-\tau_k)d_{2i}(t-\tau_i)\\
&-a_{2j}(t-\tau_j)a_{2k}(t-\tau_k)a_{2i}(t-\tau_i)d_{2j}(t-\tau_j)d_{2k}(t-\tau_k)d_{2i}(t-\tau_i)\Big)\\
&\hfill \sin(\omega_c t+\phi_i-\phi_j+\phi_k)\\
&+\Big(a_{1k}(t-\tau_k)a_{1i}(t-\tau_i)a_{2j}(t-\tau_j)d_{1k}(t-\tau_k)d_{1i}(t-\tau_i)d_{2j}(t-\tau_j)\\
&\quad +a_{1j}(t-\tau_j)a_{1i}(t-\tau_i)a_{2k}(t-\tau_k)d_{1j}(t-\tau_j)d_{1i}(t-\tau_i)d_{2k}(t-\tau_k)\\
&\quad -a_{1j}(t-\tau_j)a_{1k}(t-\tau_k)a_{2i}(t-\tau_i)d_{1j}(t-\tau_j)d_{1k}(t-\tau_k)d_{2i}(t-\tau_i)\\
&+a_{2j}(t-\tau_j)a_{2k}(t-\tau_k)a_{2i}(t-\tau_i)d_{2j}(t-\tau_j)d_{2k}(t-\tau_k)d_{2i}(t-\tau_i)\Big)\\
&\hfill \sin(\omega_c t-\phi_i+\phi_j+\phi_k)\\
&+\Big(a_{1k}(t-\tau_k)a_{1i}(t-\tau_i)a_{2j}(t-\tau_j)d_{1k}(t-\tau_k)d_{1i}(t-\tau_i)d_{2j}(t-\tau_j)\\
&\quad -a_{1j}(t-\tau_j)a_{1i}(t-\tau_i)a_{2k}(t-\tau_k)d_{1j}(t-\tau_j)d_{1i}(t-\tau_i)d_{2k}(t-\tau_k)\\
&\quad +a_{1j}(t-\tau_j)a_{1k}(t-\tau_k)a_{2i}(t-\tau_i)d_{1j}(t-\tau_j)d_{1k}(t-\tau_k)d_{2i}(t-\tau_i)\\
&+a_{2j}(t-\tau_j)a_{2k}(t-\tau_k)a_{2i}(t-\tau_i)d_{2j}(t-\tau_j)d_{2k}(t-\tau_k)d_{2i}(t-\tau_i)\Big)\\
&\hfill \sin(\omega_c t+\phi_i+\phi_j-\phi_k)\Big]
\end{aligned}
\tag{B.8}
$$

After rearranging, we get

$$
X_0(t)=d_{11}(t-\tau_1)a_{11}(t-\tau_1)\cos(\omega_c t+\phi_1)\Big[3A_3m_0^3p_1\Big[\sum_{k=2}^{K}p_k^2+\frac{p_1^2}{2}\Big]+m_0p_1\Big]
$$

$$+d_{21}(t-\tau_1)a_{21}(t-\tau_1)\sin(\omega_c t+\phi_1)\left[3A_3 m_0^3 p_1\Big[\sum_{k=2}^{K} p_k^2+\frac{p_1^2}{2}\Big]+m_0 p_1\right] \quad \text{(B.9)}$$

$$X_1(t) = \frac{3A_3m_0^3p_1}{2}\sum_{k=2}^{K}p_k^2d_{1k}(t-\tau_k)a_{1k}(t-\tau_k)d_{2k}(t-\tau_k)a_{2k}(t-\tau_k)$$
$$\Big(d_{11}(t-\tau_1)a_{11}(t-\tau_1)\sin(\omega_ct+2\phi_k-\phi_1)$$
$$+d_{21}(t-\tau_1)a_{21}(t-\tau_1)\cos(\omega_ct+2\phi_k-\phi_1)\Big) \quad \text{(B.10)}$$

$$X_2(t) = m_0\sum_{k=2}^{K}p_k\Big(d_{1k}(t-\tau_k)a_{1k}(t-\tau_k)\cos(\omega_ct+\phi_k)$$
$$+d_{2k}(t-\tau_k)a_{2k}(t-\tau_k)\sin(\omega_ct+\phi_k)\Big)$$
$$+3m_0^3A_3p_1^2\sum_{k=2}^{K}p_k\Big(d_{1k}(t-\tau_k)a_{1k}(t-\tau_k)\cos(\omega_ct+\phi_k)$$
$$+d_{2k}(t-\tau_k)a_{2k}(t-\tau_k)\sin(\omega_ct+\phi_k)\Big)$$
$$+\frac{3}{2}m_0^3A_3\sum_{k=2}^{K}p_k^3\Big(d_{1k}(t-\tau_k)a_{1k}(t-\tau_k)\cos(\omega_ct+\phi_k)$$
$$+d_{2k}(t-\tau_k)a_{2k}(t-\tau_k)\sin(\omega_ct+\phi_k)\Big)$$
$$+3m_0^3A_3\sum_{j=2}^{K}\sum_{\substack{k=2\\k\neq j}}^{K}p_j^2p_k\Big(d_{1k}(t-\tau_k)a_{1k}(t-\tau_k)\cos(\omega_ct+\phi_k)$$
$$+d_{2k}(t-\tau_k)a_{2k}(t-\tau_k)\sin(\omega_ct+\phi_k)\Big) \quad \text{(B.11)}$$

$$X_3(t) = \frac{3A_3m_0^3p_1^2}{2}\sum_{k=2}^{K}p_kd_{11}(t-\tau_1)a_{11}(t-\tau_1)d_{21}(t-\tau_1)a_{21}(t-\tau_1)$$
$$\Big(d_{1k}(t-\tau_k)a_{1k}(t-\tau_k)\sin(\omega_ct+2\phi_1-\phi_k)$$
$$+d_{2k}(t-\tau_k)a_{2k}(t-\tau_k)\cos(\omega_ct+2\phi_1-\phi_k)\Big) \quad \text{(B.12)}$$

$$X_4(t) = \frac{3A_3m_0^3}{2}\sum_{j=2}^{K}\sum_{\substack{k=2\\k\neq j}}^{K}p_j^2p_kd_{1j}(t-\tau_j)a_{1j}(t-\tau_j)d_{2j}(t-\tau_j)a_{2j}(t-\tau_j)$$
$$\Big(d_{1k}(t-\tau_k)a_{1k}(t-\tau_k)\sin(\omega_ct+2\phi_j-\phi_k)$$
$$+d_{2k}(t-\tau_k)a_{2k}(t-\tau_k)\cos(\omega_ct+2\phi_j-\phi_k)\Big) \quad \text{(B.13)}$$

$$
\begin{aligned}
X_5(t) = \frac{3}{4} m_0^3 A_3 p_1 \sum_{j=2}^{K} \sum_{\substack{k=2\\k\neq j}}^{K} p_j p_k \\
\Big[\Big(& a_{1j}(t-\tau_j) a_{1k}(t-\tau_k) a_{11}(t-\tau_1) d_{1j}(t-\tau_j) d_{1k}(t-\tau_k) d_{11}(t-\tau_1) \\
& + a_{11}(t-\tau_1) a_{2j}(t-\tau_j) a_{2k}(t-\tau_k) d_{11}(t-\tau_1) d_{2j}(t-\tau_j) d_{2k}(t-\tau_k) \\
& + a_{1k}(t-\tau_k) a_{2j}(t-\tau_j) a_{21}(t-\tau_1) d_{1k}(t-\tau_k) d_{2j}(t-\tau_j) d_{21}(t-\tau_1) \\
& - a_{1j}(t-\tau_j) a_{2k}(t-\tau_k) a_{21}(t-\tau_1) d_{1j}(t-\tau_j) d_{2k}(t-\tau_k) d_{21}(t-\tau_1) \Big) \\
& \cos(\omega_c t + \phi_1 - \phi_j + \phi_k) \\
+ \Big(& a_{1j}(t-\tau_j) a_{1k}(t-\tau_k) a_{11}(t-\tau_1) d_{1j}(t-\tau_j) d_{1k}(t-\tau_k) d_{11}(t-\tau_1) \\
& - a_{11}(t-\tau_1) a_{2j}(t-\tau_j) a_{2k}(t-\tau_k) d_{11}(t-\tau_1) d_{2j}(t-\tau_j) d_{2k}(t-\tau_k) \\
& + a_{1k}(t-\tau_k) a_{2j}(t-\tau_j) a_{21}(t-\tau_1) d_{1k}(t-\tau_k) d_{2j}(t-\tau_j) d_{21}(t-\tau_1) \\
& + a_{1j}(t-\tau_j) a_{2k}(t-\tau_k) a_{21}(t-\tau_1) d_{1j}(t-\tau_j) d_{2k}(t-\tau_k) d_{21}(t-\tau_1) \Big) \\
& \cos(\omega_c t - \phi_1 + \phi_j + \phi_k) \\
+ \Big(& a_{1j}(t-\tau_j) a_{1k}(t-\tau_k) a_{11}(t-\tau_1) d_{1j}(t-\tau_j) d_{1k}(t-\tau_k) d_{11}(t-\tau_1) \\
& + a_{11}(t-\tau_1) a_{2j}(t-\tau_j) a_{2k}(t-\tau_k) d_{11}(t-\tau_1) d_{2j}(t-\tau_j) d_{2k}(t-\tau_k) \\
& - a_{1k}(t-\tau_k) a_{2j}(t-\tau_j) a_{21}(t-\tau_1) d_{1k}(t-\tau_k) d_{2j}(t-\tau_j) d_{21}(t-\tau_1) \\
& + a_{1j}(t-\tau_j) a_{2k}(t-\tau_k) a_{21}(t-\tau_1) d_{1j}(t-\tau_j) d_{2k}(t-\tau_k) d_{21}(t-\tau_1) \Big) \\
& \cos(\omega_c t + \phi_1 + \phi_j - \phi_k) \\
- \Big(& a_{1k}(t-\tau_k) a_{11}(t-\tau_1) a_{2j}(t-\tau_j) d_{1k}(t-\tau_k) d_{11}(t-\tau_1) d_{2j}(t-\tau_j) \\
& - a_{1j}(t-\tau_j) a_{11}(t-\tau_1) a_{2k}(t-\tau_k) d_{1j}(t-\tau_j) d_{11}(t-\tau_1) d_{2k}(t-\tau_k) \\
& - a_{1j}(t-\tau_j) a_{1k}(t-\tau_k) a_{21}(t-\tau_1) d_{1j}(t-\tau_j) d_{1k}(t-\tau_k) d_{21}(t-\tau_1) \\
& - a_{2j}(t-\tau_j) a_{2k}(t-\tau_k) a_{21}(t-\tau_1) d_{2j}(t-\tau_j) d_{2k}(t-\tau_k) d_{21}(t-\tau_1) \Big) \\
& \sin(\omega_c t + \phi_1 - \phi_j + \phi_k) \\
+ \Big(& a_{1k}(t-\tau_k) a_{11}(t-\tau_1) a_{2j}(t-\tau_j) d_{1k}(t-\tau_k) d_{11}(t-\tau_1) d_{2j}(t-\tau_j)
\end{aligned}
$$

$$+a_{1j}(t-\tau_j)a_{11}(t-\tau_1)a_{2k}(t-\tau_k)d_{1j}(t-\tau_j)d_{11}(t-\tau_1)d_{2k}(t-\tau_k)$$

$$-a_{1j}(t-\tau_j)a_{1k}(t-\tau_k)a_{21}(t-\tau_1)d_{1j}(t-\tau_j)d_{1k}(t-\tau_k)d_{21}(t-\tau_1)$$

$$+a_{2j}(t-\tau_j)a_{2k}(t-\tau_k)a_{21}(t-\tau_1)d_{2j}(t-\tau_j)d_{2k}(t-\tau_k)d_{21}(t-\tau_1)\Big)$$

$$\sin(\omega_c t-\phi_1+\phi_j+\phi_k)$$

$$+\Big(a_{1k}(t-\tau_k)a_{11}(t-\tau_1)a_{2j}(t-\tau_j)d_{1k}(t-\tau_k)d_{11}(t-\tau_1)d_{2j}(t-\tau_j)$$

$$-a_{1j}(t-\tau_j)a_{11}(t-\tau_1)a_{2k}(t-\tau_k)d_{1j}(t-\tau_j)d_{11}(t-\tau_1)d_{2k}(t-\tau_k)$$

$$+a_{1j}(t-\tau_j)a_{1k}(t-\tau_k)a_{21}(t-\tau_1)d_{1j}(t-\tau_j)d_{1k}(t-\tau_k)d_{21}(t-\tau_1)$$

$$+a_{2j}(t-\tau_j)a_{2k}(t-\tau_k)a_{21}(t-\tau_1)d_{2j}(t-\tau_j)d_{2k}(t-\tau_k)d_{21}(t-\tau_1)\Big)$$

$$\sin(\omega_c t+\phi_1+\phi_j-\phi_k)\Big] \quad \text{(B.14)}$$

$$X_6(t)=\frac{1}{4}A_3 m_0^3\sum_{i=2}^{K}\sum_{\substack{j=2\\ j\neq i}}^{K}\sum_{\substack{k=2\\ k\neq i,j}}^{K} p_i p_j p_k$$

$$\Big[\Big(a_{1j}(t-\tau_j)a_{1k}(t-\tau_k)a_{1i}(t-\tau_i)d_{1j}(t-\tau_j)d_{1k}(t-\tau_k)d_{1i}(t-\tau_i)$$

$$+a_{1i}(t-\tau_i)a_{2j}(t-\tau_j)a_{2k}(t-\tau_k)d_{1i}(t-\tau_i)d_{2j}(t-\tau_j)d_{2k}(t-\tau_k)$$

$$+a_{1k}(t-\tau_k)a_{2j}(t-\tau_j)a_{2i}(t-\tau_i)d_{1k}(t-\tau_k)d_{2j}(t-\tau_j)d_{2i}(t-\tau_i)$$

$$-a_{1j}(t-\tau_j)a_{2k}(t-\tau_k)a_{2i}(t-\tau_i)d_{1j}(t-\tau_j)d_{2k}(t-\tau_k)d_{2i}(t-\tau_i)\Big)$$

$$\cos(\omega_c t+\phi_i-\phi_j+\phi_k)$$

$$+\Big(a_{1j}(t-\tau_j)a_{1k}(t-\tau_k)a_{1i}(t-\tau_i)d_{1j}(t-\tau_j)d_{1k}(t-\tau_k)d_{1i}(t-\tau_i)$$

$$-a_{1i}(t-\tau_i)a_{2j}(t-\tau_j)a_{2k}(t-\tau_k)d_{1i}(t-\tau_i)d_{2j}(t-\tau_j)d_{2k}(t-\tau_k)$$

$$+a_{1k}(t-\tau_k)a_{2j}(t-\tau_j)a_{2i}(t-\tau_i)d_{1k}(t-\tau_k)d_{2j}(t-\tau_j)d_{2i}(t-\tau_i)$$

$$+a_{1j}(t-\tau_j)a_{2k}(t-\tau_k)a_{2i}(t-\tau_i)d_{1j}(t-\tau_j)d_{2k}(t-\tau_k)d_{2i}(t-\tau_i)\Big)$$

$$\cos(\omega_c t-\phi_i+\phi_j+\phi_k)$$

$$+\Big(a_{1j}(t-\tau_j)a_{1k}(t-\tau_k)a_{1i}(t-\tau_i)d_{1j}(t-\tau_j)d_{1k}(t-\tau_k)d_{1i}(t-\tau_i)$$

$$+a_{1i}(t-\tau_i)a_{2j}(t-\tau_j)a_{2k}(t-\tau_k)d_{1i}(t-\tau_i)d_{2j}(t-\tau_j)d_{2k}(t-\tau_k)$$

$$-a_{1k}(t-\tau_k)a_{2j}(t-\tau_j)a_{2i}(t-\tau_i)d_{1k}(t-\tau_k)d_{2j}(t-\tau_j)d_{2i}(t-\tau_i)$$

$$+a_{1j}(t-\tau_j)a_{2k}(t-\tau_k)a_{2i}(t-\tau_i)d_{1j}(t-\tau_j)d_{2k}(t-\tau_k)d_{2i}(t-\tau_i)\Big)$$

$$\cos(\omega_c t+\phi_i+\phi_j-\phi_k)$$

$$-\Big(a_{1k}(t-\tau_k)a_{1i}(t-\tau_i)a_{2j}(t-\tau_j)d_{1k}(t-\tau_k)d_{1i}(t-\tau_i)d_{2j}(t-\tau_j)$$

$$-a_{1j}(t-\tau_j)a_{1i}(t-\tau_i)a_{2k}(t-\tau_k)d_{1j}(t-\tau_j)d_{1i}(t-\tau_i)d_{2k}(t-\tau_k)$$

$$-a_{1j}(t-\tau_j)a_{1k}(t-\tau_k)a_{2i}(t-\tau_i)d_{1j}(t-\tau_j)d_{1k}(t-\tau_k)d_{2i}(t-\tau_i)$$

$$-a_{2j}(t-\tau_j)a_{2k}(t-\tau_k)a_{2i}(t-\tau_i)d_{2j}(t-\tau_j)d_{2k}(t-\tau_k)d_{2i}(t-\tau_i)\Big)$$

$$\sin(\omega_c t+\phi_i-\phi_j+\phi_k)$$

$$+\Big(a_{1k}(t-\tau_k)a_{1i}(t-\tau_i)a_{2j}(t-\tau_j)d_{1k}(t-\tau_k)d_{1i}(t-\tau_i)d_{2j}(t-\tau_j)$$

$$+a_{1j}(t-\tau_j)a_{1i}(t-\tau_i)a_{2k}(t-\tau_k)d_{1j}(t-\tau_j)d_{1i}(t-\tau_i)d_{2k}(t-\tau_k)$$

$$-a_{1j}(t-\tau_j)a_{1k}(t-\tau_k)a_{2i}(t-\tau_i)d_{1j}(t-\tau_j)d_{1k}(t-\tau_k)d_{2i}(t-\tau_i)$$

$$+a_{2j}(t-\tau_j)a_{2k}(t-\tau_k)a_{2i}(t-\tau_i)d_{2j}(t-\tau_j)d_{2k}(t-\tau_k)d_{2i}(t-\tau_i)\Big)$$

$$\sin(\omega_c t-\phi_i+\phi_j+\phi_k)$$

$$+\Big(a_{1k}(t-\tau_k)a_{1i}(t-\tau_i)a_{2j}(t-\tau_j)d_{1k}(t-\tau_k)d_{1i}(t-\tau_i)d_{2j}(t-\tau_j)$$

$$-a_{1j}(t-\tau_j)a_{1i}(t-\tau_i)a_{2k}(t-\tau_k)d_{1j}(t-\tau_j)d_{1i}(t-\tau_i)d_{2k}(t-\tau_k)$$

$$+a_{1j}(t-\tau_j)a_{1k}(t-\tau_k)a_{2i}(t-\tau_i)d_{1j}(t-\tau_j)d_{1k}(t-\tau_k)d_{2i}(t-\tau_i)$$

$$+a_{2j}(t-\tau_j)a_{2k}(t-\tau_k)a_{2i}(t-\tau_i)d_{2j}(t-\tau_j)d_{2k}(t-\tau_k)d_{2i}(t-\tau_i)\Big)$$

$$\sin(\omega_c t+\phi_i+\phi_j-\phi_k)\Bigg] \quad \text{(B.15)}$$

At the receiver, the desired and the interference terms are demodulated as

$$Z_{11} = \eta P_r \int_{\tau_1}^{T+\tau_1} \sum_{m=0}^{6} X_m(t)a_{11}(t-\tau_1)\cos(\omega_c t+\phi_1)dt \quad \text{(B.16)}$$

Since only relative delays and phase angles are important, we may set $\tau_1 = \phi_1 = 0$. The parameters τ_k and ϕ_k are then the time delay and phase angle for the k^{th} signal relative to the first.

Then, the desired signal is presented as

$$D_{11} = \eta P_r m_0 d_{11,0}\frac{T}{2}\Big[3A_3 m_0^3 p_1\big[\sum_{k=2}^{K} p_k^2 + \frac{p_1^2}{2}\big] + p_1 m_0\Big] \tag{B.17}$$

$$\int_0^T X_1(t)a_{11}(t)\cos(\omega_c t)dt = \frac{3A_3 m_0^3 p_1}{4} T \sum_{k=2}^{K} p_k^2 d_{1k}(t-\tau_k)a_{1k}(t-\tau_k)$$
$$d_{2k}(t-\tau_k)a_{2k}(t-\tau_k)\Big(d_{11,0}\sin(2\phi_k) + d_{21,0}a_{11}(t)a_{21}(t)\cos(2\phi_k)\Big) \tag{B.18}$$

$$\begin{aligned}\int_0^T X_2(t)a_{11}(t)\cos(\omega_c t)dt = {}& \frac{m_0 T}{2}\sum_{k=2}^{K} p_k\Big(d_{1k}(t-\tau_k)a_{1k}(t-\tau_k)a_{11}(t)\cos\phi_k \\ & + d_{2k}(t-\tau_k)a_{2k}(t-\tau_k)a_{11}(t)\sin\phi_k\Big) \\ & + \frac{3m_0^3 A_3}{2} p_1^2 \sum_{k=2}^{K} p_k\Big(d_{1k}(t-\tau_k)a_{1k}(t-\tau_k)a_{11}(t)\cos\phi_k \\ & + d_{2k}(t-\tau_k)a_{2k}(t-\tau_k)a_{11}(t)\sin\phi_k\Big) \\ & + \frac{3}{4} m_0^3 A_3 \sum_{k=2}^{K} p_k^3\Big(d_{1k}(t-\tau_k)a_{1k}(t-\tau_k)a_{11}(t)\cos\phi_k \\ & + d_{2k}(t-\tau_k)a_{2k}(t-\tau_k)a_{11}(t)\sin\phi_k\Big) \\ & + \frac{3m_0^3 A_3}{2}\sum_{j=2}^{K}\sum_{\substack{k=2 \\ k\neq j}}^{K} p_j^2 p_k\Big(d_{1k}(t-\tau_k)a_{1k}(t-\tau_k)a_{11}(t)\cos\phi_k \\ & + d_{2k}(t-\tau_k)a_{2k}(t-\tau_k)a_{11}(t)\sin\phi_k\Big)\end{aligned} \tag{B.19}$$

with

$$R_{k,i}(\tau) = \int_0^{\tau} a_k(t-\tau)a_i(t)dt \tag{B.20}$$

$$\hat{R}_{k,i}(\tau) = \int_{\tau}^{T} a_k(t-\tau)a_i(t)dt \tag{B.21}$$

$$\begin{aligned}\int_0^T X_3(t)a_{11}(t)\cos(\omega_c t)dt = {}& \frac{3A_3 m_0^3 p_1^2 T}{4}\sum_{k=2}^{K} p_k d_{11,0}d_{21,0}a_{21}(t) \\ & \Big(-d_{1k}(t-\tau_k)a_{1k}(t-\tau_k)\sin\phi_k \\ & + d_{2k}(t-\tau_k)a_{2k}(t-\tau_k)\cos\phi_k\Big)\end{aligned} \tag{B.22}$$

$$\int_0^T X_4(t)a_{11}(t)\cos(\omega_c t)dt = \frac{3A_3m_0^3T}{4}\sum_{j=2}^{K}\sum_{\substack{k=2\\k\neq j}}^{K} p_j^2p_kd_{1j}(t-\tau_j)d_{2j}(t-\tau_j)$$
$$a_{1j}(t-\tau_j)a_{2j}(t-\tau_j)a_{11}(t)\Big(d_{1k}(t-\tau_k)a_{1k}(t-\tau_k)\sin(2\phi_j-\phi_k)$$
$$+d_{2k}(t-\tau_k)a_{2k}(t-\tau_k)\cos(2\phi_j-\phi_k)\Big) \qquad \text{(B.23)}$$

$$Z_{21} = \eta P_r\int_{\tau_1}^{T+\tau_1}\sum_{m=0}^{6} X_m(t)a_{21}(t-\tau_1)\sin(\omega_c t+\phi_1)dt \qquad \text{(B.24)}$$

Since only relative delays and phase angles are important, we may set $\tau_1 = \phi_1 = 0$. The parameters τ_k and ϕ_k are then the time delay and phase angle for the k^{th} signal relative to the first. Then, the desired signal is presented as

$$D_{11} = \eta P_r m_0\frac{T}{2}\left[3A_3m_0^3p_1\Big[\sum_{k=2}^{K}p_k^2+\frac{p_1^2}{2}\Big]+p_1m_0\right] \qquad \text{(B.25)}$$

$$\int_0^T X_1(t)a_{21}(t)\sin(\omega_c t)dt = \frac{3A_3m_0^3p_1}{4}T\sum_{k=2}^{K}p_k^2d_{1k}(t-\tau_k)a_{1k}(t-\tau_k)$$
$$d_{2k}(t-\tau_k)a_{2k}(t-\tau_k)\Big(d_{11,0}a_{11}(t)a_{21}(t)\cos(2\phi_k)-d_{21,0}\sin(2\phi_k)\Big) \qquad \text{(B.26)}$$

$$\int_0^T X_2(t)a_{21}(t)\sin(\omega_c t)dt = \frac{Tm_0}{2}\sum_{k=2}^{K}p_k\Big(-d_{1k}(t-\tau_k)a_{1k}(t-\tau_k)a_{21}(t)\sin\phi_k$$
$$+d_{2k}(t-\tau_k)a_{2k}(t-\tau_k)a_{11}(t)\cos(\phi_k)\Big)$$
$$+\frac{3m_0^3A_3}{2}p_1^2\sum_{k=2}^{K}p_k\Big(-d_{1k}(t-\tau_k)a_{1k}(t-\tau_k)a_{21}(t)\sin\phi_k$$
$$+d_{2k}(t-\tau_k)a_{2k}(t-\tau_k)a_{11}(t)\cos(\phi_k)\Big)$$
$$+\frac{3}{4}m_0^3A_3\sum_{k=2}^{K}p_k^3\Big(-d_{1k}(t-\tau_k)a_{1k}(t-\tau_k)a_{21}(t)\sin\phi_k$$
$$+d_{2k}(t-\tau_k)a_{2k}(t-\tau_k)a_{11}(t)\cos\phi_k\Big)$$
$$+\frac{3m_0^3A_3}{2}\sum_{j=2}^{K}\sum_{\substack{k=2\\k\neq j}}^{K}p_j^2p_k\Big(-d_{1k}(t-\tau_k)a_{1k}(t-\tau_k)a_{21}(t)\sin\phi_k$$
$$+d_{2k}(t-\tau_k)a_{2k}(t-\tau_k)a_{11}(t)\cos\phi_k\Big) \qquad \text{(B.27)}$$

$$\int_0^T X_3(t)a_{21}(t)\sin(\omega_c t)dt = \frac{3A_3m_0^3Tp_1^2}{4}\sum_{k=2}^{K}p_kd_{11,0}d_{21,0}a_{11}(t)\Big(d_{1k}(t-\tau_k)a_{1k}(t-\tau_k)$$
$$\cos(2\phi_1-\phi_k)-d_{2k}(t-\tau_k)a_{2k}(t-\tau_k)\cos(2\phi_1-\phi_k)\Big) \qquad \text{(B.28)}$$

$$\int_0^T X_4(t)a_{21}(t)\sin(\omega_c t)dt = \frac{3A_3m_0^3T}{4}\sum_{j=2}^{K}\sum_{\substack{k=2\\k\neq j}}^{K} p_j^2 p_k d_{1j}(t-\tau_j)d_{2j}(t-\tau_j)a_{1j}(t-\tau_j)$$

$$a_{2j}(t-\tau_j)a_{21}(t)\Big(d_{1k}(t-\tau_k)a_{1k}(t-\tau_k)\cos(2\phi_j-\phi_k)$$

$$-d_{2k}(t-\tau_k)a_{2k}(t-\tau_k)\sin(2\phi_j-\phi_k)\Big) \quad \text{(B.29)}$$

$$\int_0^T X_5(t)a_1(t)\cos(\omega_c t)dt = \frac{3A_3m_0^3p_1}{8}d_{1,0}\sum_{j=2}^{K}\sum_{\substack{k=2\\k\neq j}}^{K} p_j p_k d_{1j}(t)d_{2j}(t)a_{1j}(t)a_{2j}(t)$$

$$\Big(d_{1k}(t-\tau_k)a_{1k}(t-\tau_k)\sin(2\phi_1-\phi_k)+d_{2k}(t-\tau_k)a_{2k}(t-\tau_k)\cos(2\phi_1-\phi_k)\Big) \quad \text{(B.30)}$$

with

$$R_{j,k}(0,\tau_j) \quad = \quad \int_0^{\tau_j} a_j(t-\tau_j)a_k(t-\tau_k)dt \quad \text{(B.31)}$$

$$\int_0^T X_6(t)a_1(t)\cos(\omega_c t)dt = \frac{A_3m_0^3}{8}\sum_{i=2}^{K}\sum_{\substack{j=2\\j\neq i}}^{K}\sum_{\substack{k=2\\k\neq i,j}}^{K} p_i p_j p_k\Big[d_{i,-1}d_{j,-1}d_{k,-1}R_{i,j,k}(0,\tau_i)$$

$$+d_{i,0}d_{j,-1}d_{k,-1}R_{i,j,k}(\tau_i,\tau_j)+d_{i,0}d_{j,0}d_{k,-1}R_{i,j,k}(\tau_j,\tau_k)+d_{i,0}d_{j,0}d_{k,0}R_{i,j,k}(\tau_k,T)\Big]$$

$$\Big[\cos(\phi_i+\phi_j-\phi_k)+\cos(\phi_i-\phi_j+\phi_k)+\cos(-\phi_i+\phi_j+\phi_k)\Big] \quad \text{(B.32)}$$

with

$$R_{i,j,k}(0,\tau_i) \quad = \quad \int_0^{\tau_i} a_i(t-\tau_i)a_j(t-\tau_j)a_k(t-\tau_k)a_1(t)dt \quad \text{(B.33)}$$

Noise

Beside the nonlinear effect, at the transmitter, the effect of LD output fluctuation results in

$$\langle I_{PD}^2 \rangle = RIN(\eta P_r)^2 \tag{B.34}$$

where RIN is relative intensity noise density for the LD output. Typical RIN value is less than -150dB/Hz. Also, at the receiver, there are shot noise and thermal circuit noise being presented, respectively, as

$$\langle I_{shot}^2 \rangle = 2e\eta P_r \tag{B.35}$$

$$\langle I_{th}^2 \rangle = \frac{4kT_tNF}{R_PD} \tag{B.36}$$

where k is the Boltzmann constant, T_t is the absolute temperature, NF is the noise factor and R_{PD} is load impedance.

We define N_0 as the sum of RIN, shot noise and thermal circuit noise.

Bit Error Rate

$$< I^2 > = (\eta P_r)^2 \sum_{m=1}^{6} I_m \tag{B.37}$$

The desired signal can be presented as

$$I_{10} = (\eta P_r)^2 (Tm_0)^2/4 \int x^2 p(x) dx \tag{B.38}$$

where $y = x^2$ and p(x) is log-normal.

For X_1, we get

$$I_{11} = (\eta P_r)^2 \frac{(K-1)}{12N}\Big(\frac{3A_3 m_0^3 T}{4}\Big)^2\Big(1+(17/N)^2\Big)\int_0^\infty x^2 p(x)dx \int_0^\infty y^2 p(y)dy \quad \text{(B.39)}$$

where $z = x^4$.

$$\sum_{k=2}^{K} var(R_k) = \frac{T^2}{3N^3}(K-1)*2N^2 = \frac{2(K-1)T^2}{3N} \quad \text{(B.40)}$$

For X_3, we get the following term

$$I_{13} = (\eta P_r)^2 \frac{3A_3^2 m_0^6 (K-1)T^2}{128N}\int x^2 p(x)dx \int y^2 p(y)dy \quad \text{(B.41)}$$

For X_4, we get the following term

$$I_{14} = (\eta P_r)^2 \frac{3A_3^2 m_0^6 (K-2)T^2}{64N^3}\int x^2 p(x)dx \int y^2 p(y)dy \quad \text{(B.42)}$$

For X_2, we get the following term

$$\begin{aligned} I_2 &= (\eta P_r)^2 \Big\langle \sum_{k=2}^{K}\Big(\frac{m_0}{R}_k \cos(\phi_k)\big(p_k + \frac{3A_3 m_0^2 p_k^3}{4} + (K-1)\frac{3A_3 m_0^2}{2} p_k p_1^2\big)\Big) \\ &\quad \sum_{k=2}^{K}\Big(\frac{m_0}{R}_k \cos(\phi_k)\big(p_k + \frac{3A_3 m_0^2 p_k^3}{4} + (K-1)\frac{3A_3 m_0^2}{2} p_k p_1^2\big)\Big)\Big\rangle \\ &= (\eta P_r)^2 \frac{m_0^2 (K-1)T^2}{3N}\Big(\int x^2 p(x)dx + \big(3A_3 m_0^2\big)^2 \int z^2 p(z)dz \\ &\quad +(K-1)^2 9A_3^2 m_0^4 \int x^2 p(x)dx \int y^2 p(y)dy + 6A_3 m_0^2 \int z^2 p(z)dz \\ &\quad +(K-1)12A_3 m_0^2\Big(\int x^2 p(x)dx\Big)^2 + (K-1)9A_3^2 m_0^4 \int y^2 p(y)dy \int x^2 p(x)dx\Big) \end{aligned} \quad \text{(B.43)}$$

where $z = x^3$. The log-normal distribution for $x = p_k$ is given by:

$$p(x) = \frac{10\log e}{\sigma_P \sqrt{2\pi} x} e^{-(10\log x)^2/(2\sigma_p^2)} \quad \text{(B.44)}$$

Now for $y = x^2$, we have $x = \sqrt{(y)}$ and

$$p(y) \quad = \quad p(x)\frac{dx}{dy} = \frac{5\log e}{\sigma_P\sqrt{2\pi y}} e^{-(5\log y)^2/(2\sigma_p^2)} \tag{B.45}$$

Now for $z = x^3$, we have $x = (z)^{1/3}$ and

$$p(z) \quad = \quad p(x)\frac{dx}{dz} = \frac{10\log e}{3\sigma_P\sqrt{2\pi z}} e^{-(10/3\log z)^2/(2\sigma_p^2)} \tag{B.46}$$

Bibliography

[1] S. Komaki, K. Tukamoto, S. Hara, and N. Morinaga, "Proposal of fiber and radio extension link for future personal communications", *IEEE Microwave and Optical Tech. Letters, VOL. 6, NO. 1, pp. 55-60*, Jan. 1993.

[2] M. T. Abuelma'atti, "Carrier-to-intermodulation performance of multiple FM/FDM carriers through a GaAlAs heterojunction laser diode", *IEEE Trans. On Communications, VOL. COM-33, N0. 3, pp. 246-248*, March 1985.

[3] K. Stubkjaer, and M. Danielsen, "Nonlinearities of GaAlAs lasers - Harmonic distortion", *IEEE J. Quantum Electron. , Vol. QE-16, pp. 531-537*, May 1980.

[4] T. Magedanz, "Integration and Evolution of Existing Mobile Telecommunications Systems towards UMTS", *IEEE Commun. Mag., Vol. 34, N0. 9, pp. 90-96*, Sep. 1996.

[5] W. R. Young, "Advanced Mobile Phone Service: Introduction, Background, and Objectives", *Bell Systems Technical Journal, VOL. 58, pp. 1-14*, Jan. 1979.

[6] R. S. Swaim, "Cordless Communication in the UK", *British Telecom Technol. J., VOL. 3, NO. 2, pp. 32-38*, April 1985.

[7] ETSI, "Radio Equipment and Systems- Technical characteristics, test conditions and methods of measurement for radio aspects of cordless telephones CT1."

[8] M. Mouly, and M. B. Pautet, "The GSM System for Mobile Communication", *ISBN: 2-9507190-0-7*, 1992.

[9] C. Dechaux, and R. Scheller, "What are GSM and DECT", *Electrical Communication, pp. 118-127*, 2nd quarter 1993.

[10] K. Raith, and J. Uddenfeldt, "Capacity of Digital Cellular TDMA Systems" *IEEE Transactions on Vehicular Technology, VOL. 40, N0. 2, pp. 323-331*, May 1991.

[11] Gilhousen, et al., "On the Capacity of Cellular CDMA System", *IEEE Transactions on Vehicular Technology, Vol. 40, N0. 2, pp. 303-311*, May 1991.

[12] D. Moralee, "CT2 a New Generation of Cordless Phones", *IEE Review, pp. 177-180*, May 1989.

[13] J. S. Dasilva, B. Arroyo, B. Barani and D. Ikonomou, "European Third Generation Mobile Systems", *IEEE Commun. Mag., VOL. 33, NO. 1, pp. 28-42*, Janv. 1995.

[14] Raymond Steele, "The Evolution of Personal Communications", *IEEE Personal Communications, pp. 6-11*, Second Quarter 1994.

[15] R. Pandya, "Emerging Mobile and Personal Communication Systems", *IEEE Commun. Mag., Vol. 33, N0 6, pp.*, June 1995.

[16] "Objectives and framework of the UMTS", *Draft ETSI Tech. Rep. SMG-50101, Version 0.7.0*, Jan. 1993.

[17] A. Plattner, "Recent European development programmes for volume applications of millimetre waves IC's", *Eumc 1994, p. 144*, 1994.

[18] M. Chelouche, and A. Plattner, "Mobile broadband system (MBS): Trends and impact on 60 GHz band MMIC development", *Electronics & Communication Engineering Journal*, June 1993.

[19] J. T. Zubrzycki, "MBS- A wireless network for digital video", *International Broadcasting Convention, IEE 397*, Sept. 1994.

[20] D. C. Cox, "Portable digital radio communications- an approach to tetherless access", *IEEE Commun. Mag., VOL. 27, NO. 7, pp. 30-40*, July 1989.

[21] T. R. Rowbotham, "Local loop development in the U.K.", *IEEE Commun. Mag., VOL. 29, NO. 3, pp. 50-59*, Mar. 1991.

[22] T. Hattori, H. Sekiguchi, K. Kohiyama, and H. Yamamoto, "Personal communications- concept and architecture", *Proc. ICC'90, pp. 1351-1357*, June 1990.

[23] J. E. Padgett, C. G. Gunther, and T. Hattori, "Overview of Wireless Personal Communications", *IEEE Commun. Mag., VOL. 33, NO. 1, pp. 28-42*, Janv. 1995.

[24] B. Fabianek, K. Fitchew, S. Myken, and A. Houghton, "Optical Network Research and Development in European Community Programs: From RACE to ACTS", *IEEE Commun. Mag., pp. 50-56*, April 1997.

[25] R. Steele, "Mobile Radio Communications", *John Wiley and IEEE Press*, 1992.

[26] P. W. Baier, "CDMA or TDMA? CDMA for GSM", *PIMRC'94, pp. 1280-1284*, Sep. 1994.

[27] R. Dixon, "Why Spread Spectrum", *IEEE Commun. Soc. Mag., VOL. 13, 21*, 1975.

[28] R. A. Scholtz, "The spread spectrum concept", *IEEE Trans. on Communications, VOL. 25, NO. 8*, 1977.

[29] R. A. Scholtz, "The origins of Spread-Spectrum communications", *IEEE Trans. on Communications, VOL. COM-30, NO. 5, pp. 822-854*, May 1982.

[30] H. J. Kochevar, "Spread spectrum multiple access communication experiment through a satellite", *IEEE Trans. on Communications, VOL. 27, pp. 853-856*, Aug. 1979.

[31] D. L. Schilling, L. B. Milstein, R. L. Pickholtz, M. Kullback, and F. Miller, "Spread spectrum for commercial communications", *IEEE Commun. Mag., VOL. 29, NO. 4, pp. 66-79*, April 1991.

[32] J. K. Omura, "Spread spectrum radios for commercial wireless communications", 7^{th} *Mediterranean Electrotechnical Conference, ch. 343, p. I-16*, 1994.

[33] D. T. Magill, F. D. Natali, and G. P. Edwards, "Spread-Spectrum Technology for Commercial Applications", *Proceeding of the IEEE, VOL. 82, NO. 4, pp. 572-584*, April 1994.

[34] R. Dixon, "Spread Spectrum Systems", *Wiley Interscience Publication.*

[35] S. W. Kim, "Frequency-hopping multiple-access communications with concatenated diversity/ Reed-Solomon coding", *IEE Proceedings, VOl. 136, Pt. I, NO. 1, pp. 81-86*, February 1989.

[36] D. V. Sarwate, and M. B. Pursley, "Cross-correlation properties of pseudorandom and related sequences", *Proc. IEEE, VOL. 68, pp. 593-619*, 1980.

[37] A. Alexandridis, et al "Use of synchronous code division multiple access techniques with short coding sequences in the development of a local communication network", *International Journal of Electronics, VOL. 68, NO. 6, pp. 939-956*, 1990.

[38] R. Gold, "Optimal binary sequences for spread spectrum multiplexing", *IEEE Trans. on Inform. Theory, VOL. IT-13, pp. 619-621*, 1967.

[39] J. A. Saheli, "Code Division Multiple-Access Techniques in Optical Fiber Networks- Part I: Fundamental Principles", *IEEE Trans. On Communications, VOL. 37, NO. 8, pp. 824-842*, August 1989.

[40] G. P. Agrawal and N. K. Dutta, "Long-Wavelength Semiconductor Lasers", *New York: Van Nostrand Reinhold Company*, 1986.

[41] R. Gross and R. Olshansky, "Multichannel coherent FSK experiments using subcarrier multiplexing techniques", *J. Lightwave Technol., VOL. 8, pp. 406-415*, March 1990.

[42] K. Konnerth, and C. Lanza, "Delay between current pulse and light emission of a Gallium Arsenide injection laser", *Appl. Phys. Lett, VOL. 4, NO. 2, pp. 120-121*, April 1964.

[43] F. Simpson and J. M. Holtzman, "Direct Sequence CDMA Power Control, Interleaving, and Coding", *IEEE Journal on Selected Areas in Communications, VOL. 11, N0. 7, pp. 1085-1095*, September 1993.

[44] Rick Cameron and Brain Woerner, "Performance Analysis of CDMA with Imperfect Power Control", *IEEE transactions on Communications, VOL. 44, NO. 7, pp. 777-781*, July 1996.

[45] R. Pervez and M. Nakagawa, "Semiconductor Laser's Nonlinearity Compensation for DS-CDMA Transmission System by Post Nonlinearity recovery Block", *IEICE Trans. on Commun., VOL. E79-B, NO. 3, pp. 424-430*, March 1996.

[46] K. Y. Lau, and A. Yariv, "Intermodulation distortion in a directly modulated semiconductor injection laser", *Appl. Phys. Lett. , Vol. 45, pp. 1034-1036*, 15 November 1984.

[47] T. E. Darcie, R. S. Tucker, and G. J. Sullivan, "Intermodulation and harmonic distortion in InGaAsP lasers", *Electron. Lett. , VOL. 21, pp. 665-666*, 1985.

[48] B. Arnold "Third order intermodulation products in a CATV system", *IEEE Trans. Cable TV, VOL. CATV-2, pp. 67-80*, Apr. 77.

[49] J. C. Daly, "Fiber Optic Intermodulation Distortion", IEEE Transactions on Communications, VOL. 30, No. 8, pp. 1954-1958, August 1982.

[50] D. E. Borth and M. B. Pursley, "Analysis of direct-sequence sspread-spectrum multiple-access communication over Rician fading channels", *IEEE Trans. On Communications, VOL. COM-27, N0. 10, pp. 1566-1577*, October 1979.

[51] M. B. Pursley, "Performance evaluation for phase-coded spread-spectrum multiple-access communication- Part I: System analysis", *IEEE Trans. On Communications, VOL. COM-25, N0. 8, pp. 795-799*, August 1977.

[52] M. B. Pursley, "Spread spectrum multiple access communications", *in Multi-User Communication Systems. New York: Springer-Verlag, pp139-199*, 1981.

[53] W. C. Lee, "Mobile Communications Design Fundamentals", *New York, Wiley*, 1993.

[54] Wei Huang and Masao Nakagawa, "Nonlinear Effect of Direct-Sequence CDMA in Optical Transmission", 1994 IEEE Globecom'94, pp. 1185-1189.

[55] A. J. Viterbi, A. M. Viterbi, and E. Zehavi, "Performance of Power-Controlled Wideband Terrestrial Digital Communications" IEEE Transactions on Communications, Vol. 41, No. 4, pp. 559-569, April 1993.

[56] R. Olshansky et al, "Subcarrier multiplexed lightwave systems for broad-band distribution" *J. Lightwave Technol., VOL. LT-6, pp. 100-108*, 1988.

[57] Kojiro Araki and Hiroyuki Ohtsuka, "Fiber-Oriented Wireless Systems for Intelligent Networks", *IEICE Trans. Commun., VOL. E79-B, NO. 3, pp. 222-238*, Mar.1996.

[58] Farideh Khaleghi, and Mohsen Kavehrad , "A Subcarrier Multiplexed CDM Optical Local Area Network, Theory and Experiment", *Trans. on Commun., VOL. 43 , NO. 1, pp. 75-87*, Jan. 1995.

[59] G. Vannucci, "Combining frequency-division and code-division multiplexing in a high capacity optical network", *IEEE Network, pp. 21-30*, Mar.1989.

[60] M. Kavehrad, F. Khaleghi and G. Bodeep, "An Experiment on a CDM Subcarrier Multiplexed Optical-Fiber Local Area Network", *IEEE Photonics Technology Letters, VOL. 4, N0. 7, pp. 793-796*, July 1992

[61] N. Wiener, "Nonlinear Problems in Random Theory", *Cambridga MAss.: Technology Press and New York; Wiley*, 1958.

[62] S. Narayanan, "Transistor distortion analysis using Volterra series representation", *Bell Syst. Tech. Jour., VOL. 46, pp. 991-1023*, 1967.

[63] A. Mircea, and H. Sinnreich, "Distortion noise in frequency-dependent nonlinear networks", *Proc. Inst. Elec. Ing., VOL. 116, pp. 1644-1648*, 1969.

[64] Edwards Bedrosian, and Stephen O. Rice, "The Output Properties of Volterra Systems (Nonlinear System with Memory) driven by Harmonic and Gaussian Inputs", *Proceedings of the IEEE., VOL. 59, NO. 12, pp. 1688-1707*, DEc. 1971.

[65] J. J. Bussgang, L. Ehrman and J. W. Graham, "Analysis of nonlinear systems with multiple inputs", *Proc. IEEE, VOl. 62, pp. 1088-1119*, Aug. 1974.

[66] M. P. Fucute, Y. J. Guo, S. K. Barton, and T. A. Wilkinson, "Direct sequence spread spectrum radio LANs", *IEE Colloquium Digest, NO. 171, pp. 4*, 1995.

[67] R. S. vodhanel, A. F. Elrefaie, R. E. Wagner, M. Z. Iqbal, J. L. Gimlett, and S. Tsuji, "10-to-20 Gbit/s modulation perfromance of 1.5 μm distributed feedback lasers for frequency-shift-keying systems" *J. Lightwave Technol., VOL. 10, pp. 235-243*, Fev. 1992.

[68] T. S. Chu, and M. J. Gans, "Fiber optic microcellular radio" , *IEEE Trans. Veh. Technol., VOL. 40, pp. 599-606*, 1991.

[69] A. Baier, "Open multi-rate radio interface architecture based on CDMA" *Proc. 2nd Int. Conf. Universal Personal Commun., Ottawa, Canada*, Oct. 1993.

[70] A. H. Aghvami, "Future CDMA cellular mobile systems supporting multi-service option", *PIMRC'94, pp. 1276-1279*, Sep. 1994.

[71] A. Baier, "Multi-rate DS-CDMA: A promising access technique for third-generation mobile radio systems" *Proc. 4th Int. Symp. Personal, Indoor and Mobile Radio Commun., Yokohama, Japan*, Sept. 1993.

[72] H. Ogawa, D. Polifko, and S. Banba "Millimeter-wave fiber optics systems for personal radio communications", *IEEE Trans. Microwave Theory & Tech. , VOL. MTT-40, NO. 12, pp. 2285-2293*, Dec. 1992.

[73] H. Ogawa "Microwave and millimeter-wave fiber optic technologies for subcarrier transmission systems", *IEICE Trans. Commun., VOL. E76-B, NO. 9, pp. 1978-1990*, Sep. 1993.